Naturally Occurring Radioactive Material in Two Mine Waste Sites in Finland

Master's Thesis
Topi Suominen

Master's Programme in
Chemistry and Molecular
Sciences
University of Helsinki
June 2020

HELSINGIN YLIOPISTO
HELSINGFORS UNIVERSITET
UNIVERSITY OF HELSINKI
MATEMAATTIS-LUONNONTIETEELLINEN TIEDEKUNTA
MATEMATISK-NATURVETENSKAPLIGA FAKULTETEN
FACULTY OF SCIENCE

Tiedekunta – Fakultet – Faculty Faculty of Science	Koulutusohjelma – Utbildningsprogram – Degree programme Master's Programme in Chemistry and Molecular Sciences
Opintosuunta – Studieinrikting – Study track Radiochemistry	
Tekijä – Författare – Author Topi Juhani Suominen	
Työn nimi – Arbetets titel – Title Naturally Occurring Radioactive Material in Two Mine Waste Sites in Finland	

Työn laji – Arbetets art – Level	Aika – Datum – Month and year	Sivumäärä – Sidoantal – Number of pages
Master's Thesis	06/2020	111

Tiivistelmä – Referat – Abstract

Naturally occurring radioactive material (NORM) is defined by the IAEA as "Radioactive material containing no significant amounts of radionuclides other than naturally occurring radionuclides". In the EC directive 2013/58/Euratom several industry sectors are listed that are known to often deal with NORM, either in residues, wastes, by-products, or products, the mining industry is one of these. The risk posed by NORM is defined by exposure potential and concentration. In the wastes created by the mining industry these are tied to the management of wastes and concentration of radionuclides in the exploited mineral resource.

Wastes created by the mining industry are often of environmental concern as they are in many cases piled on the mining site after closure. The tailings of a mine may contain pyrite, which when oxidized creates acid mine drainage. The acidic waters in such sites can enhance the mobility of radionuclides and other harmful elements.

In this thesis two mine waste sites were selected for study, which were known to have had issues with natural radioactivity. These two sites were the old Zn, Pb, Cu mine of Vihanti and the Pb, REE mine of Korsnäs. The current state of these two sites was studied. Possible transport of radionuclides or other harmful elements and the dose to a member of the public on the sites was also studied. Soil, waste, sediment, and water samples were collected from both sites and analyzed. Solid samples were analyzed using gamma spectrometry and the radionuclides of interest were: ^{238}U, ^{226}Ra, ^{210}Pb, ^{232}Th, ^{228}Th, ^{228}Ra. Water samples were analyzed with ICP-MS and the elements measured with this method were: Al, Si, P, V, Cr, Mn, Fe, Co, Ni, Cu, Zn, As, Se, Mo, Cd, Pb and U. In addition, some mine waste samples were studied further using XRF and SR-XRPD methods.

The results of this thesis indicate that in Vihanti, the wastes have been adequately covered, reducing the external radiation dose to near background levels. The gamma spectrometry results showed no concerning activity concentrations in soil, sediment or waste samples. Two locations were found where the ICP-MS analyses yielded high concentrations of nearly all measured elements, the pH of these sites was low as well. Signs of acid mine drainage were found in these locations, but the effects seem to be localized and no evidence of large-scale transport of contaminants through waterways was found.

In Korsnäs the wastes are split into two piles, one containing tailings, and the other enriched lanthanide that was never sold. The results indicate that the lanthanide pile has been adequately covered and the external radiation dose around the pile is near background levels. While the tailings have not been covered like the lanthanide pile has, the results showed that a member of the public is unlikely to receive a dose exceeding 0.1 mSv/a from spending time on the site. Activity concentrations exceeding 1 Bq/g were detected in samples collected from the lanthanide pile, with some evidence of uranium mobilization also seen. In addition, uranium concentrations in the waters of the old open pit mine were relatively high.

Avainsanat – Nyckelord – Keywords
Naturally occurring radioactive material, NORM, Uranium, Radium, Mining, Tailings, Mine wastes, Natural radioactivity, Vihanti, Korsnäs, Gamma spectrometry, ICP-MS, XRF, SR-XRPD

Säilytyspaikka – Förvaringställe – Where deposited
E-thesis

Muita tietoja – Övriga uppgifter – Additional information

Table of Contents

Abbreviations 1
1 Overview 2
Part I: Introduction 3
2 Naturally occurring radioactive material 3
3 Natural radionuclides 3
3.1 Uranium 4
3.2 Thorium 5
3.3 Radium 5
3.4 Lead 6
4 Soil chemistry of radionuclides 6
4.1 Soil organic matter and humic substances 8
5 Industries 9
5.1 Increased concentration and exposure potential 9
5.2 Mining and mineral processing 11
5.2.1 Mining and comminution of ores 11
5.2.2 Physical separation of minerals 12
5.2.3 Wet chemical separation 12
5.2.4 Thermal processes 13
6 Residues and wastes 13
6.1 Waste rocks and tailings 13
6.1.1 Uranium mill tailings 15
7 Acid mine drainage 16
7.1 Pyrite oxidation 16
7.2 Secondary minerals 17
7.3 Signs of acid mine drainage 17
Part II: Experimental 18
8 Site descriptions 18
8.1 Korsnäs 18
8.1.1 Geology 18
8.1.2 History 19
8.1.3 Waste 19
8.1.4 Environmental impact 19
8.1.5 Remediation 20

8.2 Vihanti 20
8.2.1 Geology 20
8.2.2 History 20
8.2.3 Waste 21
8.2.4 Environmental impact 21
8.2.5 Remediation 22
9 Sampling 22
9.1 Soil sampling 23
9.2 Water sampling 24
9.2.1 Surface water 25
9.2.2 Porewater 26
9.2.3 Groundwater 27
9.2.4 Field measurements 27
9.3 Sediment sampling 27
9.4 Mine waste sampling 28
9.5 Core samples 28
10 Pretreatment of samples 29
10.1 Pretreatment of soils 29
10.2 Pretreatment of waters 29
10.3 Pretreatment of sediments 30
10.4 Pretreatment of mine wastes 30
10.5 Pretreatment of core samples 30
10.6 Pretreatment of SR-XRPD and XRF samples 30
11 pH measurements of solid samples 31
12 Methods 31
12.1 Inductively coupled plasma mass spectrometry 31
12.2 X-ray fluorescence 33
12.3 Synchrotron radiation X-ray powder diffraction 33
12.4 Gamma spectrometry 34
12.4.1 Calculation of results 35
12.4.2 Self-attenuation of ^{210}Pb 37
13 Results and discussion 37
13.1 Characterization of wastes 37
13.1.1 Tailings from Vihanti 37
13.1.2 Tailings from Korsnäs 39
13.1.3 Enriched lanthanide from Korsnäs 40
13.2 Water quality 40

13.3 pH of solid samples 43
13.4 ICP-MS results 44
13.4.1 Surface water 44
13.4.2 Groundwater 54
13.4.3 Evaluation of Data 58
13.5 Gamma spectrometry results 59
13.5.1 Soil samples of Vihanti 59
13.5.2 Soil Samples of Korsnäs 62
13.5.3 Sediment samples of Vihanti 65
13.5.4 Sediment samples of Korsnäs 66
13.5.5 Core samples from Vihanti 67
13.5.6 Core samples from Korsnäs 70
14 Dose assessment 74
14.1 Vihanti 74
14.2 Korsnäs 76
15 Conclusions 77
15.1 Vihanti 77
15.2 Korsnäs 78
16 References 80
17 Appendix 85

Abbreviations

AMD – Acid Mine Drainage

EC – European Council

ELY – The Finnish Centre for Economic Development, Transport and the Environment

EQS – Environmental Quality Standard

GTK – Geological Survey of Finland

IAEA – International Atomic Energy Agency

ICP-MS – Inductively Coupled Plasma Mass Spectrometry

MDA – Minimum Detectable Activity

NORM – Naturally occurring radioactive material

SR-XRPD – Synchrotron Radiation X-ray Powder Diffraction

STM – The Finnish Ministry of social affairs and health

STUK – The Finnish radiation and nuclear safety authority

UNSCEAR – United Nations Scientific Committee on the Effects of Atomic Radiation

XRF – X-ray Fluorescence

1 Overview

This thesis consists of two parts, first a literature review of naturally occurring radioactive material in the mining industry is presented with an emphasis on the radionuclides studied in this work, followed by an experimental section. The experimental section focuses on two mine waste sites known to have had issues with natural radioactivity in the past, and contains descriptions of the waste sites, and sampling and analysis methods. The results and discussion and the conclusions are in this section as well.

The aims of this thesis are to gain new and up-to-date information on the current state of the wastes on the sites, to briefly assess the effectiveness of the remediation of the waste sites, and to estimate the dose a member of the public might receive while spending time on the waste sites. The current state of these waste sites was studied by finding out what is the activity concentration of the waste and its surroundings, are the wastes contained (is there transport of contaminants or signs of acid mine drainage) and is the radiation dose under 0.1 mSv/a for a member of the public spending time on the sites. The effectiveness of remediation is tied to all of these factors.

To accomplish the objectives described above, sampling was conducted on the two waste sites and field measurements were conducted. Sample matrices collected included water, sediment, soil, and mine waste. All solid samples were analyzed using gamma spectrometry and water samples were analyzed using inductively coupled plasma mass spectrometry. Additionally, select waste samples were analyzed with X-ray fluorescence and X-ray powder diffraction techniques.

This work was done as a part of ongoing co-operation between the Finnish Radiation and Nuclear Safety Authority (STUK) and the University of Helsinki. This thesis was made as a part of STUK's larger 'FINNORM' project and most of the work was done at STUK.

Part I: Introduction

2 Naturally occurring radioactive material

Currently, there are multiple definitions for naturally occurring radioactive material (NORM) used by different agencies. However, in this thesis NORM shall be defined as in the IAEA Safety Glossary: "Radioactive material containing no significant amounts of radionuclides other than naturally occurring radionuclides" (IAEA, 2007). As is stated in the IAEA Safety Glossary, "significant amounts" is a regulatory decision. Additionally, it should be noted that the definition above makes no distinction between NORM in its natural state and NORM that has had its activity concentration or exposure potential altered by a process (e.g. mining). In this thesis, these are both considered to be naturally occurring radioactive material.

When assessing the potential risk caused by NORM, it is important to define when the derived risk is significant from a radiation protection standpoint. The mere presence of NORM does not automatically justify the level of regulation present in, for example, the uranium mining industry. The general principles of risk assessment can also be applied to NORM. A hazard exists in the form of radiation, but a hazard does not automatically create a risk, a pathway for exposure is also needed (Michalik, 2008).

3 Natural radionuclides

Natural radionuclides found on earth can be divided into two categories: cosmogenic radionuclides and primordial radionuclides. Unlike cosmogenic radionuclides, no new primordial radionuclides are formed naturally on earth. These radionuclides have been on earth since its formation (UNSCEAR, 2008). They have very long half-lives, occurring as singly occurring radionuclides or in decay chains. Of the singly occurring radionuclides ^{40}K is the most significant one, as it is found alongside stable potassium in the human body and in the environment (Kathren, 1998). It causes an annual effective dose of around 0.17 mSv, over half of the 0.29 mSv annual effective dose (global average) received through inhalation and ingestion of radionuclides, excluding radon (UNSCEAR, 2008).

There are three decay chains, or decay series, found in nature. These are the uranium series, the thorium series and the actinium series, which are headed by ^{238}U, ^{232}Th, and ^{235}U, respectively. All of the series end in different stable isotopes of lead (Kathren, 1998). The chains are host to a number of important radionuclides, some of which are discussed in more detail in sections 3.1 through 3.4.

An important measure of the conditions a decay chain has experienced is the relationship between the activity of a long-lived nuclide and its short-lived daughter. In an undisturbed state the activity of the short-lived daughter will be the same as the long-lived parents. Due to the difference in chemistry between radionuclides in a series, the series can be in disequilibrium. This means that the activities of the radionuclides are no longer the same.

3.1 Uranium

Two decay chains are headed by uranium isotopes: the uranium series, which is headed by ^{238}U and the actinium series, which is headed by ^{235}U. A third uranium isotope is also present in nature, ^{234}U, and it is found as a part of the uranium series (Kathren, 1998). In Finland, the average concentration of uranium in the bedrock is 2.0 ppm. The global average concentration in the Earth's upper crust is 2.7 ppm (Lauri et al., 2010). Of the many uranium minerals, only a few are found as ores. The most important of these ores is uraninite, where uranium is found in the ideal oxidation sate IV+ as UO_2 (Lehto and Hou, 2011).

Behavior of uranium is strongly dependent on the redox conditions of the surrounding media. In typical geological conditions uranium is found in either the oxidation state IV+ as UO_2 or in the oxidation state VI+ as UO_2^{2+} (uranyl). Other possible forms are uranyl complexes with fluoride, phosphate, or carbonate. Of these, the uranyl fluoride complex is found in acidic oxidizing waters alongside uranyl ions, but in waters that are near neutral and oxidizing (or if sulfuric acid is used as a leaching agent) the phosphate complexes are of importance. In alkaline oxidizing conditions, the carbonate complexes are the predominant species (Landa, 2007).

In solution uranium can exist in oxidation states ranging from III+ to VI+, of these the IV+ and VI+ states are the most stable. The V+ state, however, tends to disproportionate to the IV+ and VI+ states, as can be seen in equation 1.

$$2\,UO_2^+ + 4\,H^+ \rightleftarrows U^{4+} + UO_2^{2+} + 2\,H_2O \qquad 1$$

As with all actinides the pentavalent and hexavalent cations do not exist in solution as free cations and are found as hydrolyzed species UO_2^+ and UO_2^{2+} (Lehto and Hou, 2011).

3.2 Thorium

Thorium is found in nature as both a daughter in a decay chain and as the head of one. By mass almost all of natural thorium is ^{232}Th, even though it is found as six different isotopes (Lehto and Hou, 2011; Kathren, 1998). The global average concentration of thorium is 10.5 ppm in the Earth's upper crust and in Finland the concentration in the bedrock is 8.9 ppm (Lauri et al., 2010). Thorium is commonly found in monazite minerals, which are often used as a raw material in production of thorium (IAEA, 2006).

The chemistry of thorium is somewhat more straightforward than that of uranium. This is because the speciation of thorium is dominated by Th(IV) over a broad pH and eH range. Thorium also has low solubility and tends to adsorb strongly onto surfaces. These properties lead to the low concentrations of thorium observed in natural waters. However, solubility of thorium can be increased by the presence of carbonate, as thorium forms moderately strong complexes with it. Other complexes formed by thorium include fluoride-, sulfate- and phosphate-complexes (Lehto and Hou, 2011).

3.3 Radium

Radium is found in all the natural decay chains and is present as four different isotopes. Of these the most significant are the ^{226}Ra and ^{228}Ra isotopes. The mobility of radium is enhanced by the recoil a radium atom experiences as it is formed in the decay of thorium. As thorium decays radium and an alpha particle are formed. The radium nucleus experiences some recoil as the alpha particle is ejected. If this event takes place on the surface of minerals the recoil may in fact push the radium away from the surface and help transfer it into the water phase (Lehto and Hou, 2011).

Since radium is an alkaline earth metal, it is found only in the oxidation state of II+, exhibiting similar chemistry as barium. The salts formed by radium with Cl^-, Br^- and $NO_3^-$are water-soluble. The sulfate salt, however, is relatively insoluble. While radium does not form minerals, it can be found coprecipitated along certain minerals, including some calcium and barium minerals (Landa, 2007).

In biological systems radium acts like calcium making it an important part in the transfer of NORM into the biosphere. In humans, radium is stored in the skeleton where the majority of the dose form radium is received. It has been shown that most plants experience enhanced radium uptake in the absence of calcium (Kathren, 1998).

3.4 Lead

Lead is found in all the natural decay chains as the final stable isotope of the chain. These stable isotopes are not interesting from a radiochemical point of view. However, since the radioactive and stable isotopes of a single element behave the same way chemically, with the niche exception of radiation chemistry, involving for example radiolysis, stable lead can affect the chemistry of radiolead, by for example allowing for solubility constants to be exceeded. Arguably the most important radioactive isotope of lead is ^{210}Pb since it has a relatively long half-life. Another factor that makes ^{210}Pb more important is that it follows ^{222}Rn in the uranium series. The mobility of Rn of course then affects the occurrence of ^{210}Pb.

Lead has two oxidation states, II+ and IV+. Of these two the II+ state is the most common, while the IV+ state can only be formed in very oxidizing conditions. Most compounds of lead are sparingly soluble in water, but a few water-soluble lead compounds exist. These include acetate, nitrate, chlorate and perchlorate. Some of the sparingly soluble lead compounds, for example lead sulfate, can be dissolved with the help of complexation. Lead forms complexes with excess acetate and hydroxide and above pH 13 lead exists as a plumbite ion, $Pb(OH)_4^{2-}$ (Lehto and Hou, 2011).

Radioactive lead has been found to be associated with humic acids and different oxides of iron, aluminum and manganese. Unsurprisingly radioactive lead has been shown to follow stable lead in soils. The cation exchange capacity of soil also affects the concentration of lead, and indeed a positive correlation between the two has previously been seen in boreal soils (Vaaramaa et al., 2010).

4 Soil chemistry of radionuclides

The mobility of radionuclides is heavily affected by certain key soil parameters. These are: the overall composition of the soil solution (pH, redox potential, inorganic ions and organic substances), physical and chemical properties of the soil (clay minerals, oxides, organic matter, surface charge and particle size), micro-organisms and fungi, and temperature (Strebl et al., 2009).

pH and redox potential affect the mobility of radionuclides by facilitating changes in their oxidation states, an example of such behavior would be uranium and its two common oxidation states (IV+ and VI+), out of these two the VI+ oxidation state is the more mobile one. So, if the pH and redox potential in the soil solution are favorable for the formation of the VI+ oxidation state, then the mobility of uranium in this type of soil can be expected to be higher. Inorganic ions, in turn, can affect the mobility of radionuclides by competing with them for ion exchange sites, while organic substances

can form complexes with some radionuclides. The mobility of the complexed radionuclide can be either increased or decreased, depending on the mobility of the complexing agent.

The physical and chemical properties of soil strongly affect the sorption of radionuclides in the soil. Different minerals, particularly clay minerals, can act as natural ion exchangers for radionuclides. Since clay minerals typically have a negative net charge, many cations are effectively retained by them (Strawn et al., 2015). Surface charge of a mineral plays a role in the retention of radionuclides by enabling ion exchange. Typically, the functional groups of ion exchange materials are weak acids or bases that can be protonated or deprotonated depending on the pH. If the functional group is charged, ion exchange is possible and depending on the charge either cations or anions can be retained. The pH, at which an ion exchanger is neutral is called the point of zero charge, denoted by pH_{pzc}.

Two types of ion exchange interactions can be found in soils, these are inner sphere and outer-sphere complexation. In inner-sphere complexation a radionuclide bonds with a mineral's functional groups, which interact with the radionuclide directly leading to the formation of an ionic or covalent bond. The hydration sphere surrounding the ion is at least partially lost in this type of interaction. In outer sphere complexation, however, the radionuclide does not lose its hydration sphere while interacting with the mineral surface, leaving at least one water molecule in between the ion and the surface. Sorption is not limited to just ion exchange interactions, however, and it can happen, for example, by an ion being bound to a surface by formation of chemical bonds, formation of distinct surface precipitates, hydrophobic partitioning of organic molecules or absorption (Strawn et al, 2015).

Ions that have large hydrated ionic radii and low charge tend to interact by outer-sphere complexation, alkaline metals and alkaline earth metals exhibit these properties. Meanwhile, transition metal cations, Al^{3+}, Be^{2+}, Pb^{2+}, lanthanides and actinides show properties that favor inner-sphere complexation. The most important properties for inner-sphere complexation are water solubility of the ion, ionization energy and the ability of the ion to form covalent bonds (Strawn et al., 2015). So, the only important radionuclide in NORM that falls into the category of elements that prefer outer-sphere complexation would be radium, as it is and alkaline earth metal.

An important parameter in soil sorption studies is the cation exchange capacity of a material. It describes the total number of cations the soil matrix can retain, which, on the other hand, is equal to the net negative charge of the soil. Clays and soil organic matter give soils most of their cation exchange capacity (Strawn et al., 2015).

4.1 Soil organic matter and humic substances

Organic matter is found in soils in many different forms. It comprises of simple molecules, more complex biomolecules, microbial and plant cellular residues, parts of plants and even living organisms. Colloidal organic particles that are associated with minerals and microbes are referred to as humus. This type of soil organic matter is very abundant in soils (Strawn et al., 2015).

Humic substances are another type of soil organic matter, which comprise of fulvic acids, humic acids and humin. All these substances are formed similarly from decomposition products of plants as they decompose even further in oxic conditions. The differences between the types of humic substances are in molecular weight and solubility. Humins are the largest of these substances and the least soluble, they dissolve in neither acidic nor alkaline solutions. Fulvic acids, on the other hand, are the smallest and most soluble, dissolving in both acidic and alkaline solutions. Humic acids, in turn, fall in between fulvic acids and humin. They are of intermediate molecular weight and dissolve in alkaline solutions (Strawn et al., 2015; Lehto and Hou, 2011).

Humic substances cannot be described with discreet molecular formulas as they are large polymers with many different functional groups. Many metals can sorb onto the functional groups of humic substances. Carboxyl groups and free electron pairs of oxygen and nitrogen atoms serve as possible sites for sorption. Because of this Humic substances contribute significantly to the ion exchange capacity of soils (Lehto and Hou, 2011).

Both humic and fulvic acids form complexes with tetravalent and hexavalent actinides, and fulvic acids play an important role in the transportation of metals by complexing them, as fulvic acids are quite soluble can transport the complexed compound deeper into the soil with them. Eventually the complexed element is released into the soil’s enrichment layer as the fulvic acid breaks down (Lehto and Hou, 2011).

5 Industries

Several industry sectors have been identified that deal with NORM to such an extent that some form of regulation may be required. These industry sectors, as listed in the EC directive 2013/58/Euratom (EC, 2013), are:

- Extraction of rare earths from monazite
- Production of thorium compounds and manufacture of thorium-containing products
- Processing of niobium/tantalum ore
- Oil and gas production
- Geothermal energy production
- TiO2 pigment production
- Thermal phosphorus production
- Zircon and zirconium industry
- Production of phosphate fertilizers
- Cement production, maintenance of clinker ovens
- Coal-fired power plants, maintenance of boilers
- Phosphoric acid production
- Primary iron production
- Tin/lead/copper smelting
- Groundwater filtration facilities
- Mining of ores other than uranium ore

While doses from NORM sources are typically low (some μSv) it has been stated that some critical groups may receive doses in the ranges of millisieverts (UNSCEAR, 2008). So, in some cases the doses received from NORM may in fact be unacceptable from a regulatory standpoint.

5.1 Increased concentration and exposure potential

The exposure and therefore possible detrimental effects caused by NORM are defined by the scale of the NORM occurrence and the amount of material accumulated on site (e.g. tailings). These factors are independent from the origin of the NORM. Significant factors also affecting environmental contamination are the possible chemical and physical processes that might disturb the state of NORM. If one is assessing the possible negative effects for the environment caused by NORM, one should perform a multistage evaluation, simplified in Figure 1, covering at least some of the following areas: radionuclide inventory; radionuclide availability and mobility; biota exposure to external radiation; radionuclide transfer factors into biota and committed dose evaluation; and radiation effects on biota (Michalik, 2008).

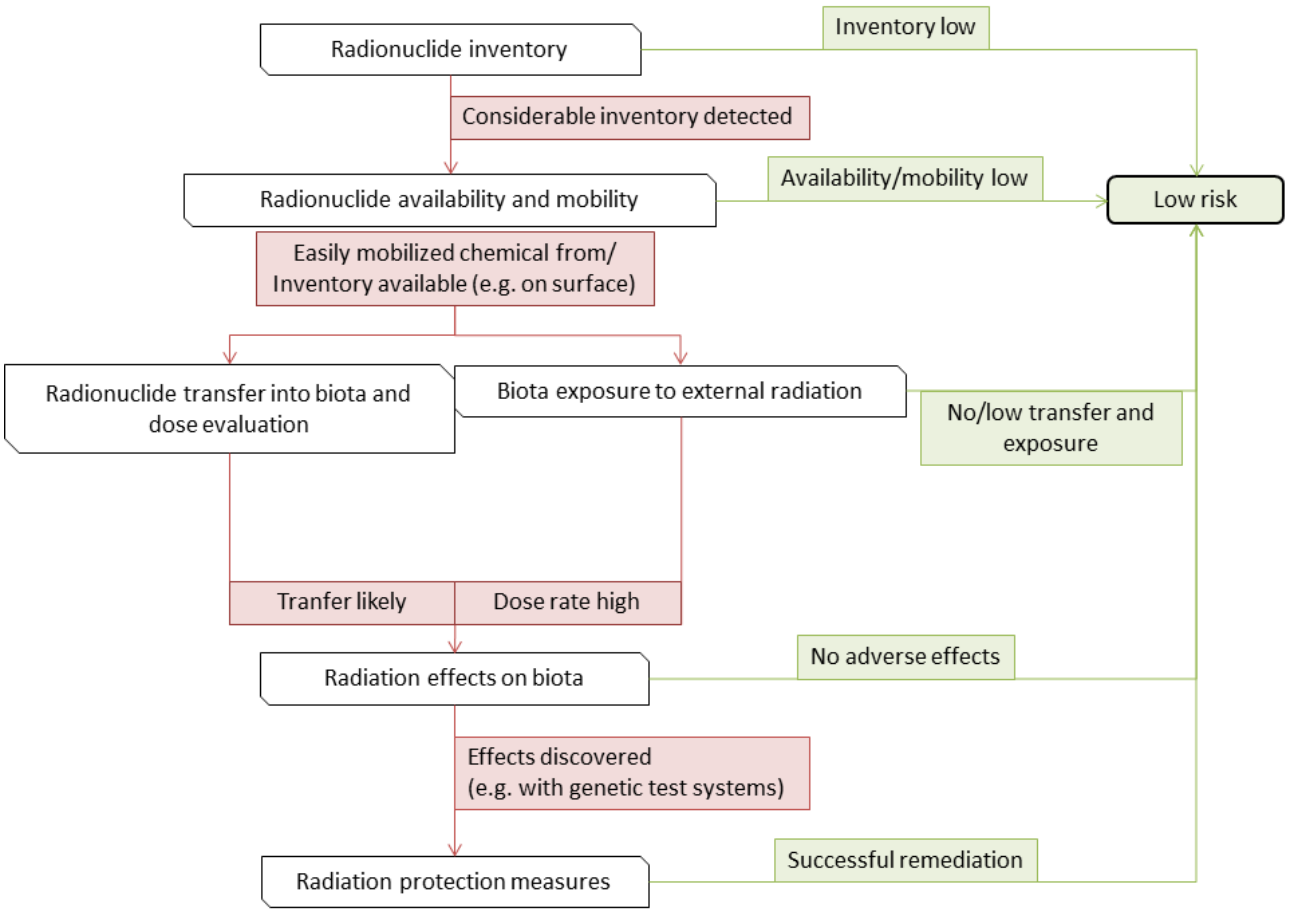

Figure 1 A simplified flowchart depicting a possible method for risk assessment in a site containing NORM (Michalik, 2008)

The exposure potential of NORM can be increased in two different ways. The concentration of NORM can be increased in a product, by-product, or residue; or the potential of the NORM to be released into the environment from a product, by-product or residue can be increased. The latter can happen either through physiochemical changes induced by a process or by the handling of the material, for example residues may be left exposed to the elements (IAEA, 2004).

Several processes can be identified which can alter the activity concentration of radionuclides in a process, a few of these are discussed shortly in this chapter. Extraction of groundwater, either in the oil and gas industry or for drinking water purposes, can affect the pH, redox potential and partial gas pressure of the water, which in turn can disturb the chemical equilibrium of radionuclides. Additionally, any process that involves burning material may lead to certain radionuclides being volatilized and non-volatile ones being left, at times in concentrated amounts, in residues. Physical milling and grinding processes in turn alter the surface area of the material, which increases the potential for dispersal and dissolution. If radionuclides are in solution, sedimentation may increase concentrations of nuclides that accumulate in the sediment. Finally, adsorption to surfaces may also

increase concentrations of some nuclides, as some nuclides may be preferentially bound to surfaces. It is important to assess the process and to identify instances where these types of interactions may lead to increased concentrations of NORM (IAEA, 2004).

Even if the process used does not concentrate radionuclides in any material by a significant degree, it may be that the NORM has been brought to a state form which radionuclides are released more readily into the environment. An example of this would be tailings at a mine. While the tailings might contain activity concentrations comparable to regular soil, the radionuclides are more available to be released into the environment, for example by leaching into surface waters (IAEA, 2004). The large quantities of waste can also create problems for safe disposal, for example remediation solutions like deep underground disposal might not be economically viable.

5.2 Mining and mineral processing

While some processes that can increase the activity or exposure potential of NORM were presented in section 5.1, the mining and mineral processing industry specifically has a few interesting types of processes that can affect the concentration of radionuclides and exposure potential of NORM. Indeed, many mining and mineral processing industries were listed in section 5 as industries that may need additional regulation due to NORM. In these mining and mineral processing industries four main types of processes that may affect the concentration of NORM have been identified. They are: mining, crushing, and milling of ore; physical mineral separation processes; wet chemical separation processes; and thermal processes for extraction, processing and combustion of minerals (IAEA, 2013). These four processes are discussed in more detail below.

5.2.1 Mining and comminution of ores

In mining operations overburden and insufficiently mineralized rocks are waste rocks. This waste is often stored in large piles at the mining sites. While it may not be economically viable to use the waste rock as a raw material, the activity concentration found in the large piles may at times be large enough for them to be considered NORM. Another feature that should be considered is the presence of pyritic material which may enable acid mine drainage (IAEA, 2013). This phenomenon will be discussed in more detail in section 7. It should be also noted that the activity concentrations in NORM remain largely undisturbed in the mining and comminution of ores, but the exposure potential is increased as the material is dug up, and in the case of waste rock, left in piles above ground. Dust is another potential exposure route that should be considered in crushing and milling processes (IAEA, 2013).

5.2.2 Physical separation of minerals

The physical separation of minerals can be done either by dry or wet processes. In dry processes, much like in milling and crushing, the concentrations of radionuclides remain almost the same. However, the concentration of radionuclides in a specific mineral is important. Because radionuclides associated with a specific mineral tend to stay with that mineral, an elevated or depleted concentration of radionuclides may be found the product, the separated mineral. The properties of the mineral and process in question define whether the activity concentration is increased or decreased in the product (IAEA, 2013).

Another risk associated with dry physical processes is the formation of dust. As mentioned before radionuclides tend to stay with their respective minerals in the separation process. This feature may lead to elevated concentrations of radionuclides if a mineral is soft and forms dust easily. An example of such a mineral would be monazite, which typically contains thorium, so the formation of monazite dust leads to increased concentrations of thorium in dust particles as opposed to the bulk material (IAEA, 2013). In addition to inhalation of dust, another risk in dry physical separation processes is the radon that can escape more easily from the small particles (UNSCEAR, 2008).

5.2.3 Wet chemical separation

Acid and alkaline leaching are common wet chemical extraction methods for ores and their concentrates. In situ leaching is a special form of wet chemical extraction where chemical leaching is performed directly to the ore which is still underground. In these processes, radionuclides mobilize readily and migrate into residues, which are formed in large amounts. Activity concentrations of these residues are not necessarily high, but the residues can still sometimes be classified as NORM (IAEA, 2013).

In wet chemical extraction mobilization of radionuclides is expected, however conditions may be favorable for the precipitation of some radionuclides (IAEA, 2013). Radionuclides can then concentrate in the precipitation process. If the chemical leaching is done with sulfuric acid, precipitates, in the form of scales containing radioisotopes of lead and radium (sulfates and coprecipitates), can be found. These scales can be significant from a radiation protection standpoint during maintenance and cleaning of equipment (IAEA, 2006).

5.2.4 Thermal processes

Thermal processes are used to refine both metals and minerals. During any thermal process, be it the combustion of coal or the calcining of minerals, fumes and dust are pathways of exposure for workers. Volatilized radionuclides can also be of concern as low boiling point elements are often present in raw materials in the mining industry. The most important volatilized isotopes are ^{210}Pb and ^{210}Po, with some radium isotopes being of concern in extreme temperatures found, for example, in plasma furnaces (IAEA, 2006). The enrichment of nonvolatile radionuclides in ash and other residues formed in thermal processes may be of concern as well, although the concentrations of radionuclides in these residues are moderate due to the typically large masses of these types of residues (IAEA, 2013).

6 Residues and wastes

There is a slight difference between a residue and waste. Residue is the material that remains from a process and waste is defined as material for which no further use is foreseen (IAEA, 2007). Residues may still be recycled into the processes that produced them or otherwise used. For example, waste rock produced in mining can be used to fill the underground tunnels of the mine, so despite its name waste rock may not in fact be waste if a use for it is found.

In concentrating processes found in the mining industry, the unwanted portion of the raw material is at times also concentrated, which can the lead to wastes and residues having high enough activity concentrations of radionuclides to be considered NORM. The physical state of the waste and NORM content depends on the raw materials and processes used (Michalik, 2008).

6.1 Waste rocks and tailings

Mining operations produce waste rock as overburden and poorly mineralized rock is removed from the mine. This rock may be classified as NORM depending on its activity concentration, which depends on the activity concentration of the mined rock itself. The total amount of waste rock generated is typically large, which again creates its own problems for remediation. Large piles of waste rocks are often stockpiled on the mining site that produced them (IAEA, 2013).

Leaching of radionuclides and other harmful elements can be an issue with waste rock piles, as can be seen in the case of Paukkajanvaara in Finland where no action was taken towards rehabilitating the site for nearly 30 years. Radionuclides were found to be leaching from tailings and waste rocks

stockpiled on site (Sillanpää et al., 1989). Later studies found that the leaching of radionuclides might still be ongoing, even after remediation (Tuovinen et al., 2016).

In contrast to waste rock, which is produced in the mining process, tailings are generated in the extraction of the valuable ore. Tailings is not a very descriptive term as it covers a broad range of residues created in, for example, aluminum, coal, oil sand, uranium, and precious and base metal processing (Kossoff et al., 2014). However, some common general properties can be identified for tailings. The grain size of tailings is usually small, less than 0.01 – 0.1 mm, ranging from sand to clay sized particles (Lottermoser, 2007a; Bjelkevik, 2005). The porosity of tailings is high, and their shear strength is moderate to high compared to geological materials, considering their porosity and grain size (Bjelkevik, 2005).

Tailings comprise of solids and some liquids and the chemical composition of tailings is defined by the mined ore body and the processing fluids and methods used. Efficiency of the extraction and weathering of the tailings after disposal also play a role in shaping the chemical composition of the tailings (Kossoff et al., 2014). While the ore body mainly determines the composition of the solid material, the composition of the liquid portion of tailings is determined by the extraction process. At least some process chemicals will find their way into the disposed tailings, while evaporation and rainfall lead to changes in the composition of the tailings water (e.g. left-over process water and porewater). In addition, process chemicals, for example thiosalts ($S_2O_3^{2-}$, $S_3O_6^{2-}$, $S_4O_6^{2-}$) can cause acidification after being oxidized into sulfate, further affecting the behavior of metals and other elements (Lottermoser, 2007a).

While the composition of tailings solids is dependent on the ore body, one should not assume that the tailings are the same as the ore. The grain size, mineralogy, and chemistry of the tailings is very different from the ore. After all, the whole point of the process is to change the physical and chemical properties of the ore (Lottermoser, 2007a). The minerals found in tailings can be divided into three categories. These are: the gangue fraction, the residual uneconomic sulfide-oxide fraction, and the secondary mineral fraction (Kossoff et al., 2014). The secondary mineral fraction consists of minerals formed during weathering (Lottermoser, 2007a).

Tailings are typically stored in tailings dams that are built on site and expanded as the operations go on. The tailings dams can be described as sedimentation lagoons for the tailings, from which water is removed and pumped back into the process (Lottermoser, 2007a). The tailings created by different mining operations vary in radionuclide content and indeed some tailings can be considered NORM.

These types of residues are formed for example in dry separation of heavy minerals, production of aluminum and production of uranium (IAEA, 2013).

Some environmental concerns associated with tailings dams are dam spillages, pipeline ruptures, dust generation, and release and seepage of elements into surrounding waters (Lottermoser, 2007a). These concerns are valid for both stable and radioactive contaminants.

6.1.1 Uranium mill tailings

As with tailings produced in any other mining process, the chemistry and mineralogy of the uranium mill tailings heavily depends on the mineralogy of the mined ore. Another important factor is the extraction method, as the leaching can be acidic or alkaline (Abdelouas, 2006). In uranium mining operations the ore is commonly milled and then leached with sulfuric acid. These types of tailings will always contain some uranium since no extraction process is 100% efficient.

Primary and secondary minerals are also found in uranium mill tailings. The primary minerals being minerals that remain form the leaching, surviving fairly unchanged. Silicate minerals such as quartz and feldspar are examples of such minerals and these are typically found in uranium mill tailings. As in other types of tailings, the secondary minerals encountered in uranium tailings are formed by precipitation from different components of the ore and reagents used in the extraction (Abdelouas, 2006).

The potential release of uranium from tailings is affected by contact time, solid-liquid ratio, particle size and pH, as shown in laboratory experiments done on uranium mill tailings (Liu et al., 2017). Two properties controlled by particle size can promote the leaching of uranium. These are higher porosities caused by larger particles and higher surface areas caused by smaller particles. pH plays a role by changing the surface charge of the tailings and facilitating the dissolution of some minerals, in both high and low pH (Liu et al., 2017).

7 Acid mine drainage

Sulfidic minerals are found in many sedimentary rocks and many ores are sulfidic or associated with sulfidic minerals. These minerals can be oxidized, and, in the process, some of them form acid. The formation of acid and the subsequent increase of solubility of metals and dissolution of minerals is referred to as acid mine drainage (AMD). It is a worldwide problem affecting many different types of mines (IAEA, 2004). Abundant sulfides can be found alongside metallic ores, phosphate ores, coal seams, oil shales and mineral sands (Lottermoser, 2007b).

As mineral resources are exploited, sulfidic minerals can be brought to the surface where they can be exposed to a more oxygenated environment, i.e. the atmosphere or oxygenated waters, tailings dams, waste rock piles and surfaces of open pit mines are some of the places where sulfidic minerals may be exposed and oxidized (Lottermoser, 2007b). Control of water flow at an AMD site is key in mitigating contamination, as water is the main transport mechanism of pollutants in these types of sites. Surface water, groundwater and hydrological seepage should be considered along with controlled placement of wastes to ensure successful mitigation of AMD (Akcil and Koldas, 2006).

7.1 Pyrite oxidation

The most common sulfidic mineral behind AMD is pyrite (FeS_2) due to its abundance and chemistry. Some factors affecting the rate of acid generation are the quantity of sulfide minerals, water and humidity, presence of oxidants and bacterial activity. The oxidation of pyrite can be expressed in a simplified way as two chemical reactions. The first describing the oxidation of pyrite by oxygen, shown in equation 2 and the second describing the oxidation of pyrite by ferric iron (Fe^{3+}), shown in equation 3 (Akcil and Koldas, 2006).

$$FeS_2(s) + {}^{7}/_{2}\ O_2(g) + H_2O(l) \rightarrow Fe^{2+}(aq) + 2\ SO_4^{2-}(aq) + 2\ H^+(aq) \qquad 2$$

$$FeS_2(s) + 14\ Fe^{3+}(aq) + 8\ H_2O(l) \rightarrow 15\ Fe^{2+}(aq) + 2\ SO_4^{2-}(aq) + 16\ H^+(aq) \qquad 3$$

As can be seen from the above equations, the oxidation of pyrite by either of the described reactions produces acid and sulfate. The oxidation of pyrite is a cyclic system, since the oxidation of pyrite produces ferrous iron (Fe^{2+}) which in turn can be oxidized into ferric iron that can oxidize more pyrite thus starting the cycle again. The oxidation of ferrous iron into ferric iron is shown in equation 4.

$$Fe^{2+}(aq) + {}^{1}/_{4}\ O_2(g)\ +\ H^{+}(aq) \rightarrow Fe^{3+}(aq) + {}^{1}/_{2}\ H_2O(l) \qquad 4$$

This way pyrite can be continuously indirectly oxidized through ferric iron if it stays in solution and is produced via oxidation. In other words, pyrite itself does not necessarily have to be directly exposed to oxygen for AMD to happen (Akcil and Koldas, 2006).

7.2 Secondary minerals

Changing conditions on a waste site may lead to dissolution of certain minerals, and from the released elements new minerals can precipitate. These minerals are called secondary minerals and in the case of mines they may be further divided into pre-mining secondary minerals and post-mining secondary minerals. The former of these are formed naturally by, for example, weathering of exposed rocks. The formation of post-mining secondary minerals, on the other hand, is strongly dependent on the conditions of the disposal site and characteristics of the waste. As an example, a pyrite containing waste rock pile could start to weather and form AMD, which can eventually lead to the release of ferric iron. Ferric iron in turn can precipitate as jarosite ($KFe_3(SO_4)_2(OH)_6$) at pH values between 2.3 and 3.5. Jarosite is one of many secondary minerals commonly associated with AMD (Akcil and Koldas, 2006; Lottermoser, 2007b).

Common post-mining secondary minerals that have been found in sulfide mines are iron oxides, oxyhydroxides and -oxyhydroxysulfates, such as schwertmannite ($Fe_8O_8(OH)_8(SO_4)\cdot nH_2O$), goethite (α-FeO(OH)), ferrihydrite ($Fe_2O_3\cdot 0.5H_2O$) and the previously discussed jarosite (Kumpulainen et al., 2007). Hydrous metal sulfates such as gypsum ($CaSO_4\cdot 2H_2O$), halotrichite ($FeAl_2(SO_4)_4\cdot 22H_2O$), and melanterite ($FeSO_4\cdot 7H_2O$) are also common. In addition, other low crystalline metal phases can be found in such sites (Carbone et al., 2013).

7.3 Signs of acid mine drainage

There are some easily recognizable indicators of AMD and sulfide oxidation in general that can be used in the field to quickly asses the state of a given site. The most important indicators are decreased pH, increased electrical conductivity, and increased concentrations of metals and major cations (Na, K, Ca, Mg). Among these, other signs of AMD are decreased oxygen concentration in porewaters and increased waste temperature, both of which are direct consequences of sulfide oxidation reactions. Visual clues of ongoing AMD are yellow or red staining of surfaces and flocculants in various bodies of water on site, lack of vegetation, and surface precipitates on exposed wastes.

Secondary iron minerals and colloids are usually responsible for the staining and flocculants. Sulfurous odors are produced on some AMD sites as well (Lottermoser, 2007b).

Mine waters impacted by acid mine drainage show very high sulfate concentrations, over 1000 mg/l. Concentrations of metals in these types of waters are high (usually Fe and Al) or at least elevated. Iron and aluminum might be found in concentrations of over 100 mg/l in some cases and other metals, such as copper, chromium, nickel, lead and zinc in concentrations of over 10 mg/l (Lottermoser, 2007c).

Field indicators of AMD in waters are low pH (<5.5), lack of aquatic life, precipitates on beds and banks of waterways, discoloration (commonly yellow-red-brown caused by suspended iron hydroxides), and abundant algae and bacterial slimes (Lottermoser, 2007c).

Part II: Experimental

8 Site descriptions

In all mining operations, even those that do not primarily involve uranium or other radioactive ores, a risk of contaminating the environment with naturally occurring radioactive material (NORM) exists. As mines are closed, it is important to evaluate the environmental impact of past operations and any wastes that might have been left behind. In the case of NORM contamination remediation may be needed in order to bring the dose rate of the closed site back to acceptable levels and to prevent the transport of radioactive elements. Such actions may include covering tailings, removing tailings, encouraging growth of vegetation and even limiting the use of the affected area. Contamination in the form of stable heavy metals may also warrant remediation. Two closed mine sites were studied in this thesis and their descriptions are found below.

8.1 Korsnäs

8.1.1 Geology

In Korsnäs the host rock comprises of mainly carbonatite, with wall rocks comprising of mica gneiss and granite. The mined ore is found in a fault zone stretching North-South. Its notable minerals include apatite and galena, with smaller quantities of ancylite, barytocalcite, bastnäsite, britholite and carbocernaite. It is worth mentioning that the main carriers of the rare earth elements mined in Korsnäs are apatite, monazite and allanite (GTK, 2018).

8.1.2 History

In 1951 the Geological survey of Finland (GTK) started to look for ore in the Korsnäs area located 50 km southwest from Vaasa. GTK eventually succeeded in finding a deposit in 1955. Full mining operations didn't start until 1961 and shortly afterwards, in 1962, due to a drop in the price of lead operations were temporarily ceased, continuing in 1964. The mine remained active until 1972, having produced some 860 000 metric tons of ore and leaving behind 760 000 tons of waste. The total amount of enriched lead produced was 45 000 tons. In addition to lead, the mine produced around 36 000 tons of enriched lanthanide ore that was never sold and still remains on the site (Timonen, 1991).

8.1.3 Waste

The 760 000 tons of waste have been piled on a 6 ha area located north of the mine. The unsold enriched lanthanide is in a separate pile west of the mine. In 1992, the Finnish radiation and nuclear safety authority (STUK) measured the activity concentrations of ^{226}Ra, ^{232}Th, ^{238}U, ^{235}U and ^{40}K from both piles. It was discovered that the activity concentrations of these radionuclides were higher than normal in both, with the lanthanide pile containing more ^{226}Ra, ^{232}Th, ^{238}U and ^{235}U than the tailings (Markkanen, 1992a).

8.1.4 Environmental impact

In 2016, the Finnish Centre for Economic Development, Transport and the Environment (ELY) analyzed sediment samples and water samples from the Korsnäs site. The results indicated that there have been recent releases of metals from the site. The highest found lead concentration in the sediment samples was 1960 mg/kg and in the water samples it was 5.6 µg/l. The highest found concentration of uranium was 120 mg/kg in the sediment samples and 39.2 µg/l in water samples. Thorium was found only in the sediment samples with the highest concentration being 26 mg/kg (Leminen, 2016).

Significant concentrations of other metals were found in all sediment samples and it was concluded by Leminen (2016), that the harmful elements travel in the surface waters from the mine into the nearby sea. Measurements with a dose rate detector yielded readings comparable to background levels of radiation around the site (Leminen, 2016).

8.1.5 Remediation

In his report Markkanen (1992a) states that without any remediation the yearly dose for a member of the critical group could be 0,3 mSv, which is high enough to warrant some form of remediation. Markkanen also states that the amount of solid material that has been transported form the waste pile into the sea might be as high as 200 tons. While the amount is significant it has been transported slowly and it has been distributed over a large area, thus making it much less harmful.

Markkanen stated that in order to prevent dust from spreading and to attenuate the gamma radiation emitted by the piles, the waste piles should be shaped into mounds and covered with a tight layer of soil with vegetation growing on top. The lanthanide pile should be covered with at least 50 cm of soil and the tailings with at least 30 cm (Markkanen, 1992a).

According to a later report from 1998, dose rate measurements showed that the waste piles had been adequately covered (Markkanen, 1998). The radiation dose rate had been lowered to acceptable levels, and this has been corroborated by measurements done by ELY (Leminen, 2016). While radiation safety on the site is adequate, ELY has stated that further research is needed on the area regarding the high metal concentrations measured in water and sediment samples (Leminen, 2016).

8.2 Vihanti

8.2.1 Geology

The major component of the host rock in Vihanti is porphyry with quartz-plagioclase gneiss and impure dolostone being present. Skarn is also found in the host rock as a minor component. The ore found in the Vihanti site is sulfide ore, which includes in major proportions chalcopyrite, galena, pyrite, pyrrhotite and sphalerite minerals (GTK, 2019).

8.2.2 History

The Vihanti mine is located in Lampinsaari, Raahe. Ore containing rocks found in the Vihanti area during the 1930s 1940s prompted GTK to launch a full search for a deposit and in 1947 the first deposit of zinc-bearing ore was found. Mining started in 1954 with 12 800 tons of zinc ore and gradually the amount increased to around 400 000 tons per year, totaling 22 800 000 tons of zinc-bearing ore when the mine closed. Alongside zinc the mine produced sulfur, copper, lead and silver. When the mine closed in 1992, the total amount of ore mined was almost 28 000 000 tons (Pelkonen, 1992).

In the 1970s significant amounts of radon in the air and water was discovered. The source of the radon was investigated, and it was found that the deposit also had uranium phosphate mineralization. Because of this discovery, the dose monitoring of employees and the ventilation of the mine was improved (Pelkonen, 1992).

The uranium deposits, while significant enough to produce a harmful amount of radon, are not large enough to be considered economically viable for mining. The total amount of uranium phosphate mineralization is estimated to be only a few million tons. These typically contain around 0.03% of uranium with peak values reaching 0.15% (Pelkonen, 1992).

8.2.3 Waste

The extensive mining operations in the Vihanti site produced 24.4 million tons of tailings, while 10.7 million tons of this waste was used to fill the some of the underground tunnels of the mine, some 13.7 million tons were left above ground in the 90 ha waste area. The average uranium concentration of the tailings is estimated to be 30 ppm, but it should be also noted that the average concentration of all metals is lower in the newer parts of the pile (Pelkonen, 1992).

8.2.4 Environmental impact

During the mine's operative years STUK measured samples from the area to find out the then state of the area. The samples included soil, water, deposition, and plants. All measured radionuclides were in the normal range for environmental samples. The highest amount of uranium reported (40 mg/kg of dry weight) was found in alpine pondweed (Potamogeton alpinus), and the highest amount of ^{210}Pb (258 Bq/kg of dry weight) was found in lichen (Cladonia alpestris). The ^{210}Pb-finding is explained by deposition and the fact that lichen has a longer life span than the studied plants (Lemmelä, 1982).

During 1992, STUK conducted an inspection to the mine. Samples of the tailings were analyzed due to concerns caused by the previously detected radon concentrations inside the mine. Since the radon concentrations were so high it was suspected that the mined rock itself might contain more uranium than expected. Measurements showed that the activity concentrations of ^{226}Ra, ^{232}Th, ^{238}U and ^{40}K were around 300 Bq/kg, 10 Bq/kg, 400 Bq/kg and 200 Bq/kg, respectively. The activity concentrations for radium and uranium were higher than normal, while the activity concentrations for thorium and potassium were lower than normal (Markkanen, 1992b).

More recently GTK has taken water samples from the Vihanti site and discovered that the waters coming from the underground tunnels of the mine contained uranium. This is most likely due to the

uranium phosphate mineralization found in the mine. An elevated concentration of uranium was also discovered in the waters of Alpuanoja, a ditch flowing away from the waste area. However, it was unclear at the time if the uranium originated from the tunnels or from the tailings (Tornivaara et al., 2018).

8.2.5 Remediation

As the mine closed in 1992 it was already decided that the tailings were to be covered with a layer of soil with vegetation growing on top (Pelkonen, 1992). These are the same actions that STUK recommended later in 1992. The soil layer is expected to be enough to attenuate the gamma radiation emitted by the pile making it practically impossible for a person to receive a yearly dose greater than 0.1 mSv by spending time in the area. The soil layer also prevents any dust form the tailings from spreading (Markkanen, 1992b). The tailings have been covered and there is vegetation growing on top of almost the whole area. The center of the pile is sometimes covered in water and is not as well covered by vegetation (Tornivaara et al., 2018).

9 Sampling

Sampling was conducted in June of 2019 on the two sites. Various sampling locations are shown in Figure 2 and Figure 3 for Vihanti and Korsnäs respectively. The water sampling locations for Vihanti are shown in Figure 4. Water samples were stored at 5 °C and all other samples were stored frozen. The solid samples were frozen and water samples were cooled on the same day as they were collected. A description of the sampling sites is found in section 8. All samples were named by sample matrix and with sequential numbering, except for reference samples which were abbreviated as ‘ref.’ samples (e.g. ref. water). Waste samples were named ‘NORM’ and sediment samples were abbreviated as ‘sedi’. Soil, water, porewater and core samples were simply named ‘soil’, ‘water’, ‘porewater’ and ‘core’ respectively. The two parallel water samples taken from a single location were labeled as A and B (e.g. water 1A). The same naming convention was applied to both sites.

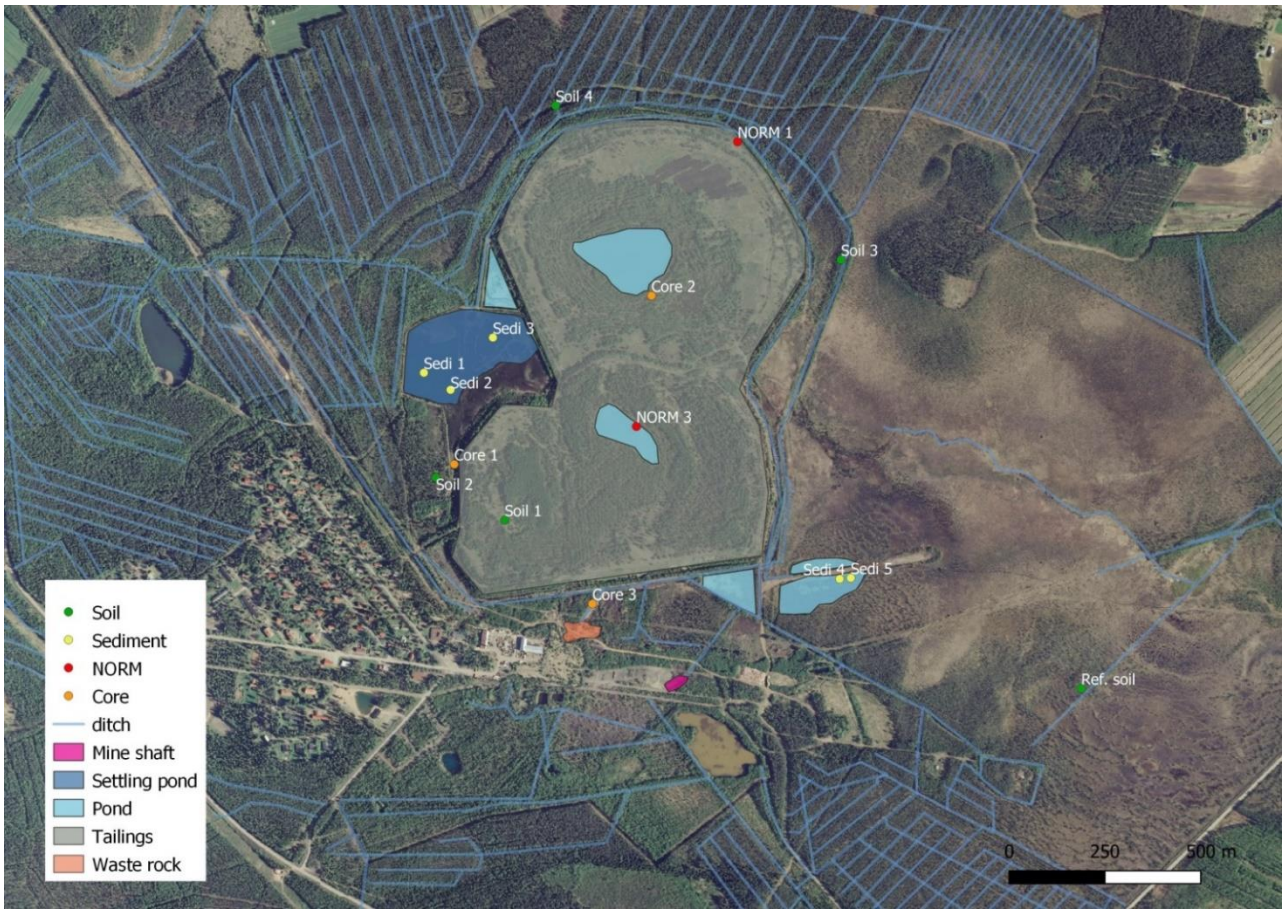

Figure 2 Map of the Vihanti site, showing various sampling locations. Porewater samples were collected from the same locations as core samples and from sampling location NORM 3.

9.1 Soil sampling

Five soil samples were collected from each of the two sites. Each of these sample sets included a reference sample collected nearby, from an area expected to be unaffected by the mining activities of the sites (see Figure 2 and Figure 3) . Soil sampling was performed using an Oxland golf hole cutter. The hole cutter cuts a core of soil which is around 20 cm in length resulting in a cylindrical core which can be sectioned based on soil type.

From each sampling location three parallel samples were collected to reduce the uncertainty of the sampling due to the highly heterogeneous nature of soil. Parallel samples were collected inside a 10 m radius of each other, while also avoiding taking the samples from places too close to one another. The samples were removed from the hole cutter in one piece and wrapped in cling film which was then secured with tape. The samples were then packed into plastic bags and frozen on the same day. For one soil sample, Korsnäs soil 4, four parallel samples were taken, because a higher dose rate was detected in the area.

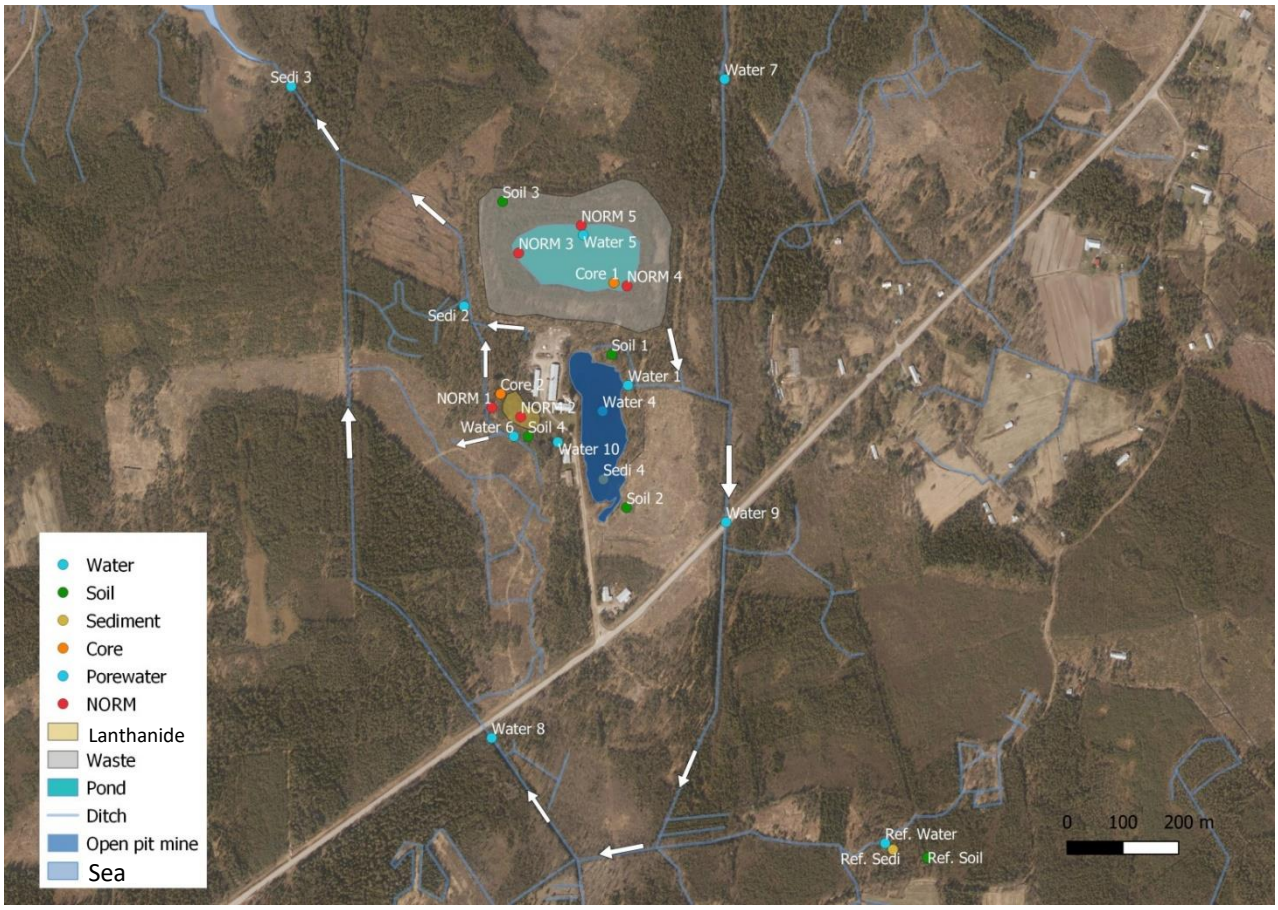

Figure 3 Map of the Korsnäs site, showing various sampling locations. Porewater samples were taken from the same locations as core samples. Water samples water 2 and 3 were taken from locations sedi 2 and 3, respectively. Sediment sample sedi 1 was taken from location water 1.

9.2 Water sampling

Water sampling locations of Korsnäs can be seen in Figure 3 and in Figure 4, the water sampling locations of Vihanti are shown. Both sites had a large number of ditches surrounding the waste piles. In Korsnäs, the old open pit mine (marked with blue in Figure 3) has filled with water and samples were collected from it. In Vihanti, water from the old settling pond was sampled along with two other ponds that have formed on the southeastern side of the waste pile. Both sites also had pools of water on top of the waste piles, water from these was also collected. In addition to surface water, porewater was sampled from both sites in the same locations where core samples were taken.

9.2.1 Surface water

Surface water was sampled from various ponds and ditches from both sites. From Vihanti, 17 water samples were taken (Figure 4) and from Korsnäs, 15 water samples were taken (Figure 3). Water samples were collected into 1L plastic bottles. In addition to these larger samples, two 12 mL syringes were used to collect water from each sampling location and filter it through a 0.45 µm syringe filter (VWR, PP membrane). The water was filtered into a 15 mL test-tube (VWR, metal-free PP), which contained 50 µL of concentrated nitric acid (Romil, Suprapur HNO_3, 67-69%). The volume of the filtered samples was around 10 mL. In areas where the water was hard to reach, the smaller samples were collected with syringes from the 1L plastic bottle instead. Water samples were also collected from various depths from the former settling pond in Vihanti and the old open pit mine in Korsnäs using a Limnos water sampler capable of sampling water from different depths. The sampling depth of such samples was added to the name of the sample (e.g. water 4 – 1m).

Figure 4 Map of the Vihanti site, showing water sampling locations and the flow of the surface water. Sampling location water 17 is not show on the map. This location was a ditch close to water 12 flowing away from the settling pond.

9.2.2 Porewater

Porewater was sampled from both sites at the same locations where the core samples were taken (see section 9.5). These sampling locations are shown in Figure 2 and Figure 3 for Vihanti and Korsnäs, respectively. Sampling was performed using Rhizon CSS 5 cm porewater samplers, which have a pore size of 0.15 µm and the length of the membrane is 5 cm. Porewater sampling with Rhizon samplers can be seen in Figure 5. The porewater was sampled after a hole was dug for the core sample. Rhizon samplers were inserted to the wall of the hole and a syringe was attached to the Rhizon sampler. The piston of the syringe was then pulled back and porewater flowed through the Rhizon sampler's membrane into the syringe. From each hole, porewater was sampled in around 10 cm intervals. Each porewater sample was divided into two 15 mL test-tubes, one was filtered through a 0.45 µm syringe filter and acidified with 50 µL of conc. HNO_3, the other was not. An argon float was added to the non-acidified test-tubes to replace any air in the headspace. These test-tubes were then stored in air-tight argon filled glass jars. These samples were collected from six different locations.

Figure 5 Porewater sampling in Vihanti, sample porewater 1 taken together with core 1B

9.2.3 Groundwater

Groundwater samples were sampled by Pöyry Oy during 3.-4.9.2019. A liter of groundwater was pumped from groundwater pipes into 1 l plastic bottles, however only 0.5 l of sample P114 could be pumped. Three parallel samples were taken from the plastic bottles and filtered and acidified similarly to the surface water samples. The pH of the samples was measured in the laboratory using pH paper prior to acidification (see Appendix 1).

9.2.4 Field measurements

Water quality was measured in the field at the same locations form where the water samples were collected. A YSI Professional meter was used to measure the pH, oxidation reduction potential, temperature, specific conductivity and dissolved oxygen of the water. Calibration of the meter was done on each sampling day prior to sampling. The obtained results are discussed in section 13.2. Dose rate measurements were also conducted while sampling using a portable NaI gamma spectrometer. The results from these measurements are discussed in section 14.

9.3 Sediment sampling

In Vihanti, sediments form the settling pond and one of the smaller ponds were sampled, see Figure 2. In Korsnäs, sediments were sampled from the ditches surrounding the waste piles and from the old open pit mine, see Figure 3. The samples taken from the open pit mine were taken using a Limnos sediment sampler and all other samples, including the ones taken from Vihanti, were taken using a Wildco® Ogeechee corer, seen in Figure 6. Five sediment samples were collected from Vihanti and seven from Korsnäs. Sediments were not sectioned due small sample amounts and concerns that the corer might be compressing the samples.

Figure 6 Ogeechee corer being prepared for sampling in Korsnäs (Sediment 2)

9.4 Mine waste sampling

In both sites most of the mine wastes were piled above ground and later covered as a part of site remediation, except for the main waste pile in Korsnäs. Samples of the wastes were collected by digging through the covering layer of soil and then collecting a sample of the waste into a plastic container with a trowel. These sampling sites are labeled as 'NORM' samples in Figure 2 and Figure 3. In Korsnäs, samples were taken from both the tailings pile and the pile of enriched lanthanide. Slightly higher external dose rates in the range of 0.5 µSv/h were observed near the lanthanide pile, in Korsnäs, and samples were collected from this area.

9.5 Core samples

Six core samples were taken from Vihanti and four form Korsnäs. The cores were taken from wet spots near the waste piles and two parallel samples were taken from each sampling location. The parallel samples were, however, handled differently, one was preserved and the other was sectioned on the field. Figure 7 shows a core (core 3B, Vihanti) that was sectioned on the field. In Vihanti the samples were cored using 50 cm plastic tubes with a diameter of around 10 cm, while in Korsnäs the coring tubes were 40 cm in length and around 7,5 cm in diameter.

The samples were cored by hammering a plastic tube into the soft, wet soil. After the coring tube was almost completely in, a stopper was inserted into the upper end of the tube. Once the stopper was in place, a hole was dug next to the tube, exposing one side of the tube. After the bottom end of the tube could be seen a stopper was slid into it and the whole tube was lifted from the hole. The coring was performed in the same way for both preserved and sectioned cores. The upper portions of the sectioned samples were cut into 1 cm slices and the lower portions were cut in 2 cm intervals. Each slice was packed into either a plastic bag or container and carefully labelled.

Preservation of the other cores was achieved with an argon float that was added to the coring tubes, after which both ends of the tubes were sealed. Finally, the sealed tubes were packed in black plastic bags and frozen. The preserved cores were handled and stored upright.

Figure 7 Core sample Core 3B from Vihanti ready to be sectioned. The length of this core was around 35 cm.

10 Pretreatment of samples

10.1 Pretreatment of soils

Soil samples thawed overnight in room temperature. The samples were sectioned in the laboratory based on soil type and if no change in soil type could be seen, the sectioning was done based on depth, in around five-centimeter increments. Corresponding sections from each of the parallel samples were combined and placed on an aluminum pan with a plastic film in between the pan and the sample. The soil samples were dried overnight at 105 °C, one complete soil sample at a time. After drying, the samples were sieved through a 2 mm sieve. Any roots or rocks larger than 2 mm were collected and weighed. A portion of the sieved <2 mm fraction was taken into a tared plastic container and weighed. The containers were sealed with tape and then vacuum sealed in vacuum bags.

10.2 Pretreatment of waters

Water samples were collected into test-tubes containing 50 µL of concentrated nitric acid as described in section 9.2.1. The purpose of the acidification was to preserve the sample by ensuring all analytes remain in solution. All samples were measured undiluted with an ICP-MS system to find out the ideal dilution factor for each sample. Multiple dilutions were made of some samples in order to measure each analyte at a concentration covered by the calibration curve (see section 12.1**Virhe. Viitteen lähdettä ei löytynyt.**). Dilutions varied from 1.5-fold to up to 4000-fold. Up to 300-fold dilutions were done in 15 mL test-tubes by pipetting a desired amount of sample on top of 50 µL of conc. HNO_3, which was then diluted to either 10 or 15 mL depending on the desired dilution. Dilutions greater than 300-fold were done in volumetric flasks or 50 mL test-tubes. Samples diluted in volumetric flasks were acidified with 50 µL of conc. HNO_3 after an aliquot of 15 mL was taken into a test-tube. Samples diluted in 50 mL test-tubes were acidified with 0.15 mL of conc. HNO_3.

10.3 Pretreatment of sediments

Sediments were frozen in plastic Ogeechee coring tubes or in plastic containers depending on the sampling method. The frozen samples were thawed overnight in room temperature and moved from the coring tubes and plastic containers onto stainless steel pans lined with a plastic film or into small plastic containers depending on sample amount. Excess water was evaporated from the samples using heat lamps, time under the heat lamps varied based on the amount of water. After this the samples were frozen again and then put into a freeze dryer. The drying time was around 40 h for each sample. Once dry, the samples were homogenized using a mortar and pestle. Some samples contained notable amounts of plant matter and these samples were sieved before homogenization. Finally, the samples were packed into plastic containers, sealed with tape and then vacuum sealed.

10.4 Pretreatment of mine wastes

The mine wastes were moved onto stainless steel pans lined with a plastic film and put into a freeze dryer. The samples were dried for around 40 h. The dried samples were first sieved through a 2 mm sieve and then homogenized with a mortar and pestle. The samples were packed into plastic containers and vacuum sealed the same way as soil and sediment samples were.

10.5 Pretreatment of core samples

The core samples that were sectioned in the field were freeze dried in plastic bags that were opened for the duration of the drying. The drying time of the core samples was around 40 h. The samples were sieved prior to homogenization if large amounts of stones or roots could be seen. Homogenization was done with a mortar and pestle until a talc like consistency was achieved. Due to low sample volume of some sections, a few samples had to be combined in order to completely fill the plastic containers used during measurement. The core samples were vacuum sealed the same way as the other solid samples.

10.6 Pretreatment of SR-XRPD and XRF samples

A total of ten samples were selected for analysis with SR-XRPD and XRF these samples included seven mine waste samples and three sections from a core sample (see section 13.1). A subsample from each of the selected samples was taken. At this point the samples had already been pretreated as described in sections 10.4 and 10.5. The subsamples were ground even finer by hand with a mortar and pestle and then sieved through a 25 µm sieve. To avoid introducing additional bias the subsamples were ground and sieved completely.

11 pH measurements of solid samples

The pH of select core sample sections and mine wastes were also measured. The method used was performed according to the international standard ISO 10390:2005(E) (ISO, 2005). A 0.01 mol/l calcium chloride ($CaCl_2$) solution was prepared by dissolving 1.47 g of calcium dihydrate ($CaCl_2 \cdot 2H_2O$) in water (purified with reverse osmosis) and then diluting the solution into 1000 mL of solution. A sampling spoon was used to sample 5 mL of solid sample into a 50 mL test-tube to which 25 mL of the $CaCl_2$ solution was added. Two parallel samples were made from each individual sample measured. The samples were shaken for around 60 minutes and left to stand for 60 to 180 minutes. The pH was measured using an Orion pH meter model 420A. The results of these measurements are presented in section 13.3. The pH of all waste samples was measured; however, the organic top layers (0-10 cm) were excluded. The sections of core samples which were measured were selected based on observed color changes between the sections.

12 Methods

In this thesis various sample matrices were analyzed using four different methods. Water samples were analyzed using inductively coupled plasma mass spectrometry (ICP-MS). Select mine waste samples were analyzed using both X-ray fluorescence (XRF) and synchrotron radiation X-ray powder diffraction (SR-XRPD). All solid samples were analyzed using gamma spectrometry. The results of the analyses are presented in section 13.

12.1 Inductively coupled plasma mass spectrometry

In ICP-MS analyses, samples are atomized and ionized and then sent to a detector based on their mass to charge (m/z) ratios. The ICP-MS system used in the determinations of this thesis was an Agilent 7800 ICP-MS quadrupole mass spectrometer. The system was operated with helium as a collision gas for m/z ratios of less than 12 and more than 80. No collision gas was used for other elements. Sample introduction was handled by an automatic sample injector and pump. An internal standard was used to correct for loss of signal during analysis. The elements in the internal standard were: ^{72}Ge, ^{103}Rh, and ^{175}Lu. A diluted sample of certified reference material (CRM) was analyzed along the samples to assess the validity of the results.

The CRM was a SPS-SW2 batch 137 reference material for measurement of elements in surface waters (Spectrapure standards AS, Oslo, Norway) diluted 10-fold. The CRM was measured at the start of the run and at the end. If the measured concentrations in the CRM sample were to differ by more than 10 % from the stated concentrations, the results of the run would be rejected. Table 1 shows the concentrations of analytes in the undiluted CRM and standard used in the measurements.

Table 1 The concentrations of analytes in the undiluted CRM and standard sample used in the ICP-MS measurements. The isotope and the unit are shown in the in the first column along with the element.

Element [unit]	CRM	Standard
27 **Al** [ppb]	250	1000
28 **Si** [ppm]	5	400
31 **P** [ppb]	500	1000
51 **V** [ppb]	50	100
52 **Cr** [ppb]	10	50
55 **Mn** [ppb]	50	2000
56 **Fe** [ppb]	100	4000
59 **Co** [ppb]	10	20
60 **Ni** [ppb]	50	100
63 **Cu** [ppb]	100	200
66 **Zn** [ppb]	100	1000
75 **As** [ppb]	50	20
78 **Se** [ppb]	10	30
95 **Mo** [ppb]	50	100
111 **Cd** [ppb]	2,5	20
208 **Pb** [ppb]	25	100
238 **U** [ppb]	2,5	1000

Six standard samples were prepared for calibration. One blank and five dilutions of a solution containing known concentrations of the analyzed elements, Al, Si, P, V, Cr, Mn, Fe, Co, Ni, Cu, Zn, As, Se, Mo, Cd, Pb and U, were prepared. The five dilutions made were 10-, 20-, 50-, 100- and 200-fold dilutions. All samples were acidified with ultra-pure concentrated HNO3 prior to analysis. The concentrations of the analytes in the undiluted standard are given in Table 1.

12.2 X-ray fluorescence

In X-ray fluorescence (XRF) an X-ray source is used to knock electrons out of their orbitals. The vacant orbital is filled by an electron from an orbital with a higher energy level. As the electron moves from a higher energy state to a lower one energy is released in the form of X-rays that are characteristic to the transition and the element.

To analyze the samples in this work, XRF was performed on glass beads made in 1:10 ratio of sample to flux, which comprised of 49.75% $Li_2B_4O_7$, 49.75% $LiBO_2$ and 0.5 % LiBr. The mixture was fluxed in a platinum crucible at 1000 °C. One sample had to be ignited, since the bead would not set in the crucible otherwise. The measurements were done with a wavelength dispersive XRF PANanalytical axios mAX system. Both a quantitative run and a semi-quantitative run were done. The system was calibrated with standard samples with known concentration of elements analyzed in the quantitative run before the analysis.

12.3 Synchrotron radiation X-ray powder diffraction

Two techniques are combined in synchrotron radiation X-ray powder diffraction (SR-XRPD). These are the production of X-rays with high speed electrons moving in a circle (synchrotron radiation, SR) and the determination of the structure of matter using X-ray powder diffraction (XRPD).

As a charged particle, in the case of SR an electron, accelerates it produces electro-magnetic radiation. Now, if the particle is moving close to the speed of light the characteristics of the emitted radiation are different than at lower speeds. The features that make SR a good choice for powder diffraction are tunable photon energy, spectral brightness, polarization, pulsed time structure and coherence (Gozzo, 2012).

In X-ray diffraction, X-rays are diffracted from the electrons of atoms. Measuring the intensity of the scattered radiation yields a diffraction pattern, form this pattern it is possible to deduce the position of the atoms relative to each other. Much like in a diffraction grate it is possible to find out the distance between the individual grates, but in XRD the electrons act as the grate (Billinge and Dinnebier, 2008).

The SR-XRPD analyses in this work were done in the material science beamline at the swiss light source in the Paul Scherrer Institute. The storage-ring energy of the swiss light source is 2.4 GeV, which allows accelerated electrons to circle the storage-ring for hours at a time. The material science beamline has a photon energy range of 5-40 keV. An undulator produces the X-rays used in the

analysis, which continue through two beam position monitors and then two diaphragms which intercept soft X-rays. After this the beam continues through a diamond filter and window, meant to protect the X-ray optics, continuing on through beam defining slits, three diamond beam position monitors, a double crystal monochromator, a double mirror chamber, a bremsstrahlung blocker and, finally, the beam ends up at the powder diffractometer (Willmott et al., 2013).

Data collection of the SR-XRPD analyses was done with a Dectris Pilatus 6 M single photon counting hybrid detector. The samples were pretreated as described in section 10.6. A vibrating sample holder was also used. The benefit of a vibrating sample holder is the better particle statistics that can be obtained with it. This feature stems from the fact that a higher number of orientations of a single crystal are exposed to the beam (Sarrazin et al., 2005).

Dioptas software was used to create the two-dimensional diffraction patterns, for which a Rietveld refinement was done. The identification of mineral phases in the samples was done with PanAnalytical High Score+ software, by matching the obtained diffractograms with ones in a database (ICDD PDF4 Minerals database).

12.4 Gamma spectrometry

Gamma spectrometry is used to detect and quantify certain radioactive elements. As a radioactive element decays it may decay into an extremely short-lived excited state of the daughter nucleus, which then relaxes into the ground state of the nucleus by emitting gamma radiation. These gamma rays are often characteristic to a certain decay event and can thus be used to identify the decaying nucleus and to quantify its activity.

In this work, broad energy germanium detectors (BEGe) with thin carbon epoxy windows were used. The relative efficiencies of the detectors were around 50% (at 1.33 MeV). This type of detector was selected so that ^{210}Pb could be measured at the same time as other radionuclides of interest. Eight radionuclides of interest were studied using gamma spectrometry. These were: ^{232}Th, ^{228}Th, ^{228}Ra; ^{238}U, ^{226}Ra, ^{210}Pb; ^{235}U and ^{40}K. The energies used to quantify the radionuclides of interest are given in Table 2. Gamma radiation was also measured on the field using a portable NaI spectrometer. The portable detector measured the dose rate while sampling was conducted.

All samples were packed in cylindrical plastic containers of two sizes. The bigger containers had a radius of 37 mm, from the center to the inside wall, and the smaller containers had a radius of 21 mm. The height of both containers, on the inside, was 26 mm. The thickness of the bottom of both containers was 1.2 mm and the thickness of the walls were 1.9 mm for the smaller containers and 2.1

mm for the larger ones. To obtain reliable results for radon's progeny, the samples analyzed with gamma spectrometry were packed in completely filled containers, to minimize uneven distribution of radon's progeny inside the container, and sealed in vacuum bags, to prevent radon from escaping. Counting times ranged from 24 to 72 hours, depending on the activity of the sample.

12.4.1 Calculation of results

The calculation of results was done with UniSampo Shaman spectral analysis software. For ^{40}K and ^{210}Pb the calculation of activity concentration is straightforward since both radionuclides emit gamma radiation as they decay. The activity concentration of these radionuclides can then be calculated from their corresponding peaks. The low energy of the emission from ^{210}Pb causes some difficulties due to absorption, which are discussed further in section 12.4.2.

The rest of the radionuclides of interest are harder to quantify as they do not have suitable gamma emissions of their own or the energies overlap with other peaks. Table 2 shows the radionuclides of interest, the progeny used to quantify some of them, and the energies of the peaks used in the calculations (Säteilyturvakeskus, 2019a).

Table 2 The radionuclides measured to quantify the activity concentrations of the radionuclides of interest and their energies.

Radionuclide of interest	Radionuclide(s) measured	Energy/Energies used (keV)
Th-232	Ac-228; Tl-208	338.3, 911.2; 583.2, 2614.5
Th-228	Pb-212; Tl-208	238.6, 300.1; 583.2, 2614.5
Ra-228	Ac-228	338.3, 911.2
U-238	Pa-238m	1001.0
Ra-226	Pb-214; Bi-214	295.2, 351.9; 609.3, 1120.3, 1764.5
Pb-210	Pb-210	46.5
U-235	U-235	185.7
K-40	K-40	1460.8

For some of the radionuclides multiple peaks were used to quantify their activity concentration, in these cases an average weighted with the inverse of the variance of the peaks was used to get the activity of a given radionuclide. Equation 5 shows how the weighted average was calculated,

$$\hat{V} = \sum_{1}^{N} \alpha_i V_i \qquad 5$$

where

$$\alpha_i = \frac{w_i}{\sum_1^N w_i}$$

and

$$w_i = (var_i)^{-1}$$

So $\hat{V}$ is the weighted average of intensities, α_i is the weighting factor for the intensity of a given peak V_i, and w_i is the inverse of the variance.

The error of the measurements was calculated as 1 sigma from the number of counts in a peak and the counting time.

The activity concentration of ^{232}Th has been calculated from its progeny ^{228}Ac and ^{208}Tl using a weighted average that was calculated according to Equation 5. Similarly, the activity concentration of ^{228}Th was calculated from ^{212}Pb and ^{208}Tl, and the activity concentration of ^{228}Ra was calculated from ^{228}Ac. The energies of the progeny used in the calculations are listed in Table 2. Equilibrium between ^{232}Th and its progeny (^{228}Th, ^{228}Ra) was assumed based on the observed equilibrium between ^{228}Th and ^{228}Ra in the samples and because Th is known to be a very immobile element. Thus, the activity of ^{232}Th has also been reported.

Unlike with the Th series the activity concentration of ^{238}U was calculated from a single peak of a single progeny, ^{234m}Pa at 1001 keV.

The activity concentration of ^{226}Ra was also calculated as a weighted average of intensities of its progeny, ^{214}Pb and ^{214}Bi. This was done so that the activity concentration of ^{235}U could be calculated from its own peak at 186 keV by correcting the counts from ^{226}Ra in this peak. Once the activity of ^{226}Ra is known the activity of ^{235}U can be calculated as shown below in Equation 6.

$$A(^{235}\mathrm{U}) = A(^{235}\mathrm{U}; 186\ \mathrm{keV}) * \left(1 - \frac{A(^{226}\mathrm{Ra})}{A(^{226}\mathrm{Ra}; 186\ \mathrm{keV})}\right) \qquad 6$$

Where $A(^{235}\mathrm{U})$ is the corrected activity of ^{235}U, $A(^{235}\mathrm{U}; 186\ \mathrm{keV})$ is the activity of uranium calculated as if the whole peak at 186 keV belongs to ^{235}U, $A(^{226}\mathrm{Ra})$ is the activity of ^{226}Ra calculated form its progeny and $A(^{226}\mathrm{Ra}; 186\ \mathrm{keV})$ is the activity of ^{226}Ra calculated as if the whole peak at 186 keV belongs to ^{226}Ra.

12.4.2 Self-attenuation of ^{210}Pb

The low energy radiation emitted by ^{210}Pb is absorbed more efficiently by matter, including the sample itself. In this work all containers had to be vacuum sealed and filled completely which is not ideal since a thicker sample has more matter to absorb the radiation. All results are corrected mathematically for both height and density (Säteilyturvakeskus, 2019b), but very thin samples are preferred for determinations of ^{210}Pb (Säteilyturvakeskus, 2019a).

Industrial waste samples, like the ones studied in this thesis, typically contain relatively high concentrations of elements with high atomic numbers, which attenuate radiation more efficiently. Failing to adequately correct for self-attenuation leads to underestimation of ^{210}Pb activity concentrations (Bonczyk, 2018). While the results in this work have been corrected by mathematically addressing the effect of sample height and density, self-attenuation may still cause underestimation of ^{210}Pb activity concentrations. A better way to determine the activity of ^{210}Pb would be to measure an extremely thin sample for a longer time, but this was not done due to time constraints.

13 Results and discussion

13.1 Characterization of wastes

13.1.1 Tailings from Vihanti

Three tailings samples were taken from Vihanti, the two samples designated NORM 1 and NORM 3 and the core sample core 3B. The tailings samples and three slices from core 3B were analyzed with XRF and SR-XRPD. The core slices selected were 4-5 cm, 16-18 cm and 24-26 cm, the slices were selected based on color changes in the core. Concentrations of some elements obtained by XRF and activity concentrations of ^{238}U, ^{226}Ra and ^{232}Th for the samples are presented in Table 3 below. The full XRF results can be seen in Appendix 2.

Table 3 The concentrations and activity concentrations of select analytes in waste samples of Vihanti. If no number is given, the result was under the limit of detection of the method. All results are for dry weight of sample

Sample	**U-238** (Bq/kg)	**Ra-226** (Bq/kg)	**Th-232** (Bq/kg)	**Fe** (%)	Mn (%)	Cu (ppm)	Ni (ppm)	**Zn** (ppm)	**U** (ppm) [XRF]
NORM 1 25 cm	60	290	6.9	12	0.047	730	22	410	-
NORM 3 60 cm	200	320	11	4.2	0.070	380	65	1960	26
Core 3B 4-5 cm	-	67	11	10	0.023	200	31	180	6
Core 3B 16-18 cm	-	250	3.0	19	0.023	840	39	540	-
Core 3B 24-26 cm	-	270	3.5	4.7	0.031	4770	26	270	-

As can be seen from the above table, the wastes are quite heterogenous, with radium showing the least difference in its activity concentration between samples. Assuming uranium and radium were in equilibrium in the ore, it seems the enrichment process or weathering of wastes has mobilized uranium relative to radium. This will be discussed in section 13.5.5 for core 3B, for NORM 1 and 3 it would seem conditions of NORM 1 have been more favorable for uranium mobilization. Probable causes for this are depth and acidity of the waste. The pH results for the solid samples from Vihanti highlight the potential of the waste to produce acid. NORM 1 was acidic while NORM 3 was near neutral (see section 13.3). Rainwater is more likely to reach the depth in NORM 1 than NORM 3 which, together with acidity, explains the difference in the activity concentrations of uranium. The thorium series showed no signs of disequilibrium.

The iron concentration in core 3B at 24-26 cm drops significantly compared to 16-18 cm. Porewater samples show that iron concentrations in the porewater behave in the opposite way, going from 4 610 mg/l at 15 cm to 32 990 mg/l at 25 cm iron seems to be mobilized from the core at the deeper depth owing, at least partially, to the more reducing condition down the core favoring Fe^{2+} ions rather than less soluble Fe^{3+} ions. All measured elements follow the same pattern except for silicon and zinc. Silicon concentrations are almost the same between the two porewater samples and zinc concentrations are higher in the 15 cm sample than the 25 cm one. The observation in the zinc concentrations could be explained by heterogeneity as core 3B slice 16-18 cm shows higher zinc concentrations than core 3B slice 24-26 cm.

The most abundant mineral phases detected in samples NORM 1 and NORM 3 were diopside ($MgCaSi_2O_6$), quartz (SiO_2), albite ($NaAlSi_3O_8$) and tremolite, ($Ca_2Mg_{4.95}Fe_{0.05}Si_8O_{22}(OH)_2$), while calcite ($CaCO_3$) was quite abundant in NORM 3 it was detected in very small amounts in NORM 1. However, NORM 3 showed a much lower concentration of gypsum than NORM 1. It could be that

pyrite oxidation in NORM 1 has produced sulfuric acid that has dissolved calcite and formed gypsum instead.

The three most abundant mineral phases throughout core 3B were quartz, albite and pyrite for the 4-5 cm slice, quartz, albite and jarosite for the 16-18 cm slice and for the bottom slice, 24-26 cm, quartz, gypsum and diopside. Common secondary minerals found in AMD sites, gypsum, jarosite and goethite were detected in all samples (Carbone et al., 2013; Kumpulainen et al., 2007), except for goethite in slice 24-26 cm, this suggests ongoing AMD localized in the area with uncovered wastes on the south side of the waste pile. Chalcopyrite ($CuFeS_2$) detected in slices 16-18 cm and 24-26 cm explains the higher concentrations of copper found in these samples.

13.1.2 Tailings from Korsnäs

Three samples of tailings were collected form Korsnäs. Samples designated NORM 3-5 were collected from atop the waste pile from different locations. Concentrations of some elements obtained by XRF and activity concentrations of ^{238}U, ^{226}Ra and ^{232}Th in the samples are presented in Table 4 below. The activity concentrations of uranium and radium are close to each other in samples NORM 3 and NORM 4, in sample NORM 5 the activity concentrations are further apart suggesting uranium is leaching downward form upper layers of the waste. The concentrations of other elements measured with XRF seem to coincide well between the samples, with the lanthanides showing some differences between sample NORM 4 and samples NORM 3 and 5. The differences could be explained by heterogenicity of the ore that was processed. The thorium series showed no signs of disequilibrium. The full XRF results can be seen in Appendix 2.

Table 4 The concentrations and activity concentrations of select analytes in waste samples of Korsnäs. All results are for dry weight of sample

Sample	**U-238** (Bq/kg)	**Ra-226** (Bq/kg)	**Th-232** (Bq/kg)	**Fe** (%)	**Mn** (%)	**Y** (ppm)	**Ce** (ppm)	**La** (ppm)	**U** (ppm) [XRF]
NORM 1 20-30 cm	4100	7780	2190	4.5	0.12	670	12700	5540	420
NORM 3 30-40 cm	730	780	270	2.8	0.093	120	1480	780	84
NORM 4 25-30 cm	550	550	250	2.2	0.10	150	2370	1220	38
NORM 5 20-30 cm	600	480	360	2.6	0.077	100	1380	720	42

The four most abundant mineral phases identified in waste samples NORM 3-5 were calcite, albite, quartz, and microcline ($KAlS_3O_8$). In all samples hydroxylapatite ($Ca_5(PO_4)_3(OH)_2$) was also detected, which hosts a large fraction of the lanthanides, thorium, and uranium (Papunen and Lindsjö, 1972).

13.1.3 Enriched lanthanide from Korsnäs

Two samples from the enriched lanthanide pile were collected from Korsnäs. Sample NORM 2 turned out to be just the covering layer and showed no abnormal results which are not discussed further. NORM 1 was clearly enriched lanthanide. The enriched lanthanide is also enriched in radionuclides from the uranium and thorium series, as is evident from the high activity concentrations in this sample. Once again, the thorium series showed no signs of disequilibrium. The uranium series, however, shows large differences between activity concentrations of ^{238}U and ^{226}Ra. The same factors discussed in section 13.5.6 for core 2A are likely to cause the disequilibrium observed here as well, since the samples were taken so close to each other and the matrix containing the radionuclides is the same.

The most abundant mineral phases identified in NORM 1 were microcline, monazite ($(Ce,La,Th)PO_4$), calcite and hydroxylapatite. As discussed before monazite and apatite are the main carriers of the rare earth elements and radionuclides in Korsnäs (Papunen and Lindsjö, 1972). The abundance of these minerals (around 8.2% apatite, 9.6% monazite) explains the high concentrations of U, Ra, Th, Y, Ce and La seen in the sample. Thorium is often the radionuclide of concern in monazites (IAEA, 2013), but in this case the monazite has been described as “almost thorium free” with a thorium concentration of 0.15% (Papunen and Lindsjö, 1972).

13.2 Water quality

pH results of surface waters from both sites are presented in Figure 8 and Figure 9, for Vihanti and Korsnäs respectively. Additionally, all the results of field measurements for water samples from Vihanti and Korsnäs are shown in Appendix 3.

At Vihanti the lowest measured pH values were 2.10 (water 16) and 2.68 (water 15), both of which were measured in the same area and are marked with red in Figure 8. The area had a strong sulfurous odor and the water in the ditches was brownish red. The specific conductivity of the location was the highest measured across all water sampling locations, 20 041 µS/cm. The ICP-MS results of the water sample taken from this location also revealed very high concentrations of dissolved metals (see section 13.4.1). In contrast, the neighboring ditches had higher pH values and lower specific conductivities. The water in these ditches was cloudy with fine yellow particles and the cloudiest water was seen in sampling location ‘water 8’. In an earlier study, the pH from very close to this sampling location was measured and reported as 6.03 (Tornivaara et al., 2018).

The low pH, high specific conductivity, high concentrations of dissolved metals and the discoloration in one of the ditches (water 16) are clear signs of acid mine drainage (see section 7.3). In addition, the yellow particles, the relatively low pH of 4.91, and the high level of zinc (>10 mg/l) of the neighboring ditch (water 8) are clear signs of acid mine drainage as well. However, the effect seems to be localized.

A pH of 4.92 was measured from a ditch (water 6) coming from an old mine shaft, which is now completely under water. The bed and banks of this ditch were covered with a rust colored precipitate, but the water was clear. The precipitate could have formed as the pH of the ditch changed, after evaporation or due to oxidation of iron (II+) to (III+) followed by precipitation of iron hydroxide.

The pH of the two small ponds southeast of the waste pile was circumneutral (water 2A, 2B). In a previous study, the pH from the same location was found to be lower, around 4.3, and weathering of waste rocks on the banks of the pools was thought of as the cause (Tornivaara et al., 2018).

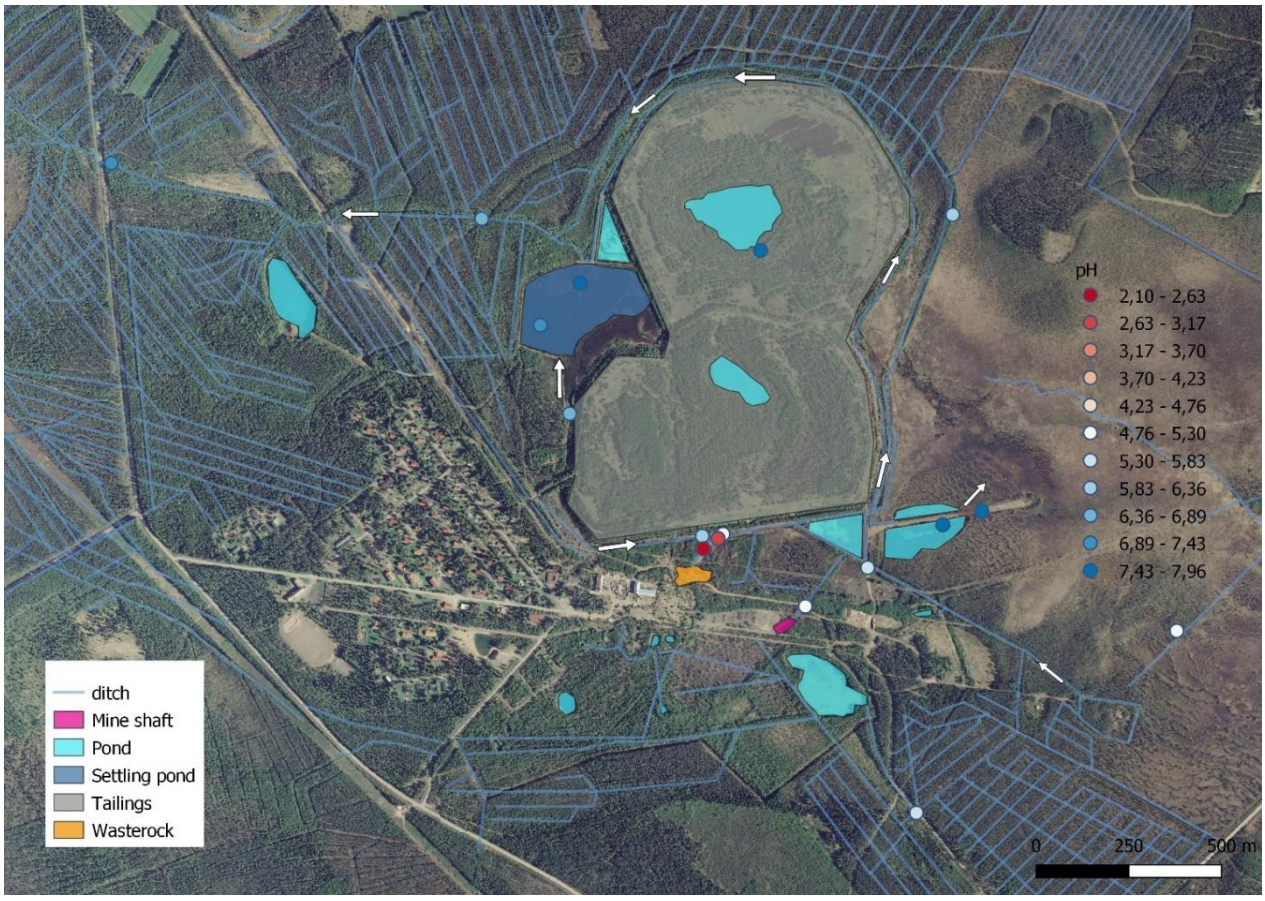

Figure 8 Water sampling locations where pH was measured in Vihanti. The colors of the dots represent the pH values with red representing lower pH and blue higher pH, as can be seen in the

Comparing the pH values from this work to earlier measurements presented by Tornivaara et al. (2018), it can be seen that the values change, going from acidic to neutral in the ponds southeast of the waste pile (water 2A, 2B) and from neutral to acidic in the ditch on the south side of the waste pile (water 8, 15, 16). The specific conductivities in the ponds also changed, going from around 20 000 µS/cm reported by Tornivaara et al. (2018) to around 1500 µS/cm measured in this work. The weathering of the waste rocks near the southeastern ponds may have stopped or slowed significantly allowing for the pH to rise back up again. As for the ditch south of the pile, the pH has most likely dropped due to weathering of the waste lining the ditch.

In Korsnäs the measured pH values were all circumneutral (Figure 9). As for specific conductivities, only measurements from the old open pit mine showed values significantly higher than the rest, rising from 2422 µS/cm measured at a depth of 1 m, to 6132 µS/cm measured at 5 m. For comparison, the specific conductivity measured from the sampling location of the reference water was 237 µS/cm.

In the field measurements of water quality, no abnormal results for any of the properties measured were found, aside from the elevated conductivities measured from the old open pit. pH values and specific conductivities measured in this work agree with those measured in an earlier study by Leminen (2016).

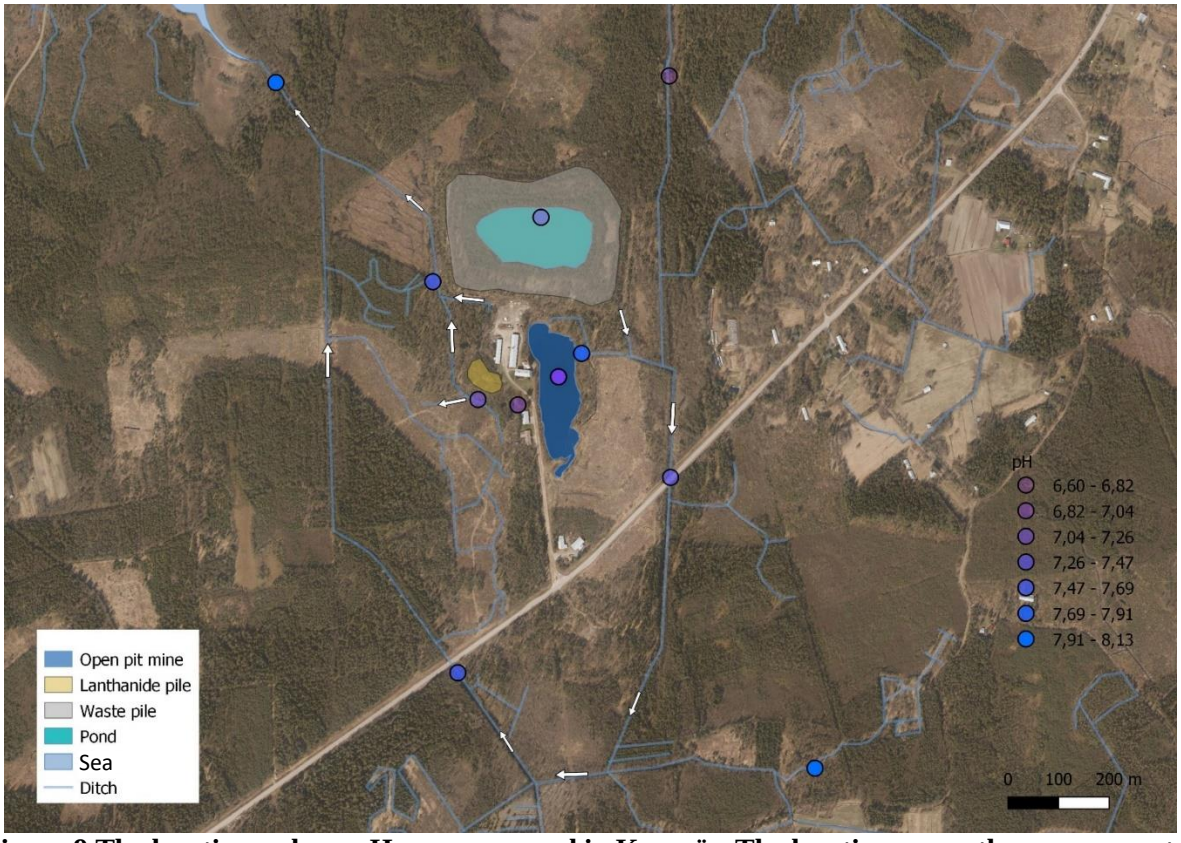

Figure 9 The locations where pH was measured in Korsnäs. The locations were the same as water sampling locations. The colors of the dots represent pH, as can be seen on the right side of the figure.

13.3 pH of solid samples

The pH values of selected solid samples can be seen in Figure 10 and Figure 11. Four samples from Vihanti showed clearly lower pH values than the rest, the values were: around 2.5 for three samples from Core 3B and around 3.2 for NORM 1. The rest of the Vihanti samples had a circumneutral pH.

One sample from Korsnäs showed slightly lower pH than the rest of the samples from the site, around 5.5, while the rest were neutral. As can be seen from Appendix 4 no two parallel measurements differ from each other more than 0.15 pH units which satisfies the repeatability requirement set in the followed ISO standard (ISO, 2005).

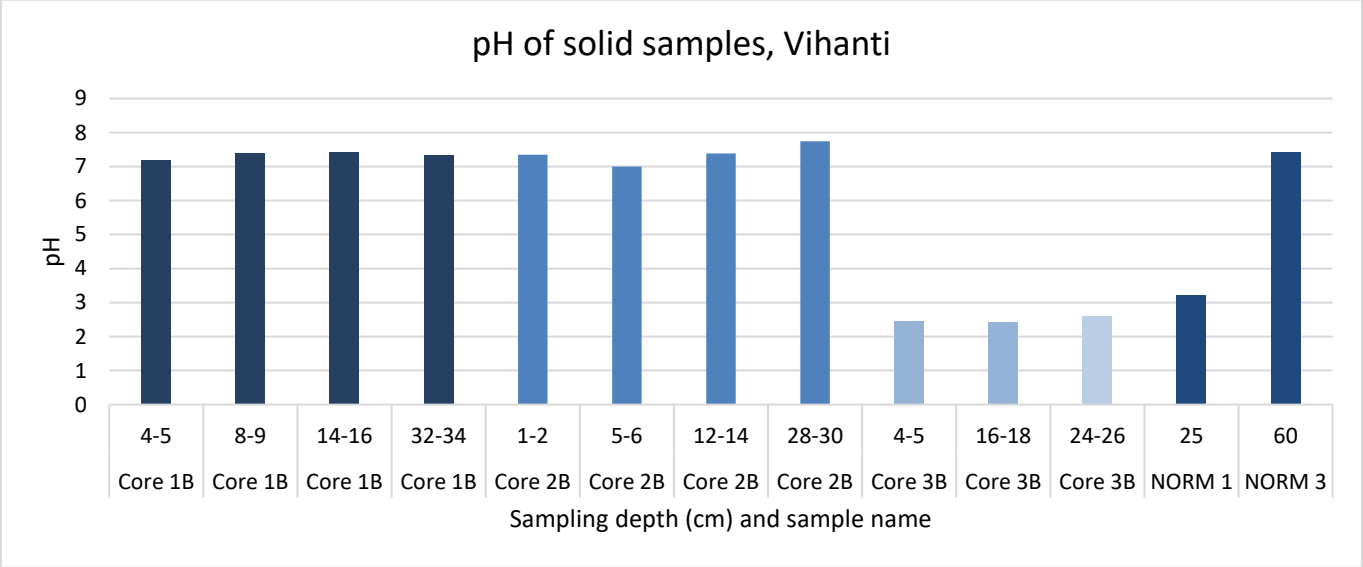

Figure 10 pH values of different solid samples from Vihanti. Sampling depth is given in centimeters above the sample name. The colors are meant to make it easier to distinguish between different samples and serve no other purpose.

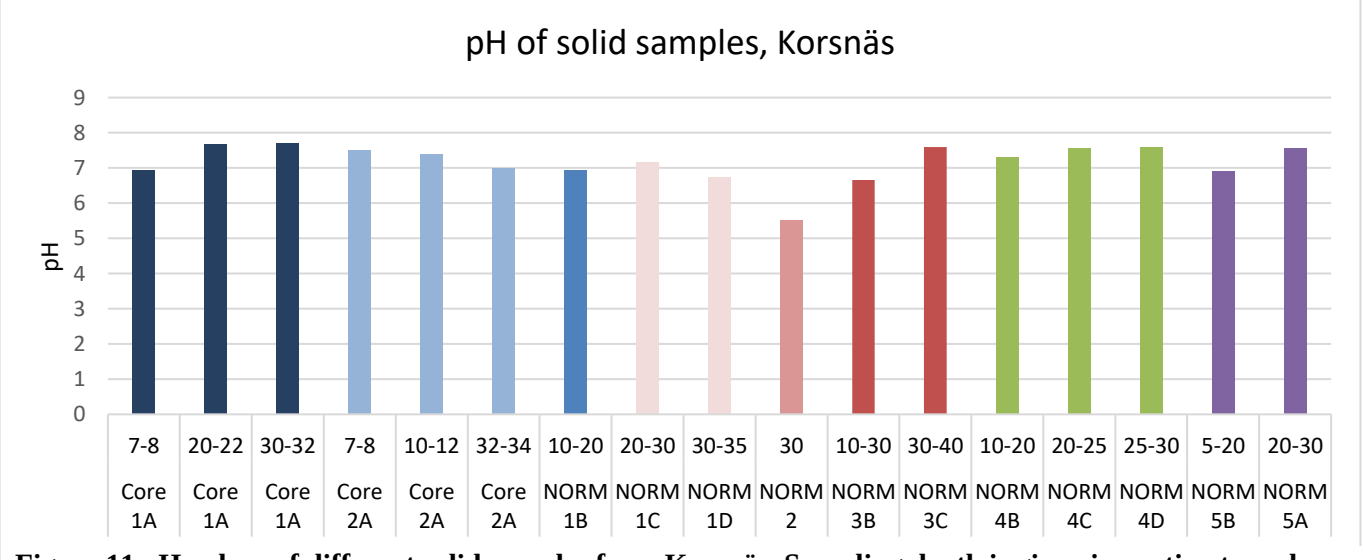

Figure 11 pH values of different solid samples from Korsnäs. Sampling depth is given in centimeters above the sample name. The colors are meant to make it easier to distinguish between different samples and serve no other purpose.

13.4 ICP-MS results

13.4.1 Surface water

Vihanti

The full ICP-MS results of surface waters from Vihanti are presented in Appendix 5 and the concentrations of uranium and zinc are presented alongside a map of the sampling locations in Figure 12 as bar plots.

The highest concentrations of all measured elements, except for molybdenum, were found in one sample, water 16. Compared to the reference water taken from the nearby Isoneva bog, the concentrations are from one to three orders of magnitude higher in water 16 than in the reference sample. Weathering of sulfide minerals and subsequent dissolution of other minerals as a result of lowered pH are the two most likely reasons for these high concentrations. Sphalerite (ZnS), pyrite (FeS_2), chalcopyrite ($CuFeS_2$), and galena (PbS) are the main minerals of Zn, Fe, Cu and Pb, respectively, that were found in the ores of Vihanti (Pelkonen, 1992). The exposed material (presumably tailings) around water 16 could still contain these minerals and their weathering would explain the abnormal metal concentrations observed in water 16.

Much like water 16, water 8, which was taken from a neighboring ditch, shows high concentrations of Al, Fe, Cu and especially Zn. The concentration of zinc in these samples is shown in Figure 12, along with all the other samples from Vihanti. The greater volume of water and abundance of small solid particles present in the ditch of water 8 most likely lower the concentrations of most of the measured elements compared to water 16. The observed lower concentration of iron relative to, for example, zinc might be due to formation of iron hydroxides, which are often seen as colloids in AMD sites (Lottermoser, 2007b). Iron hydroxide is known to coprecipitate many elements, which would lead to a drop in their concentrations as well.

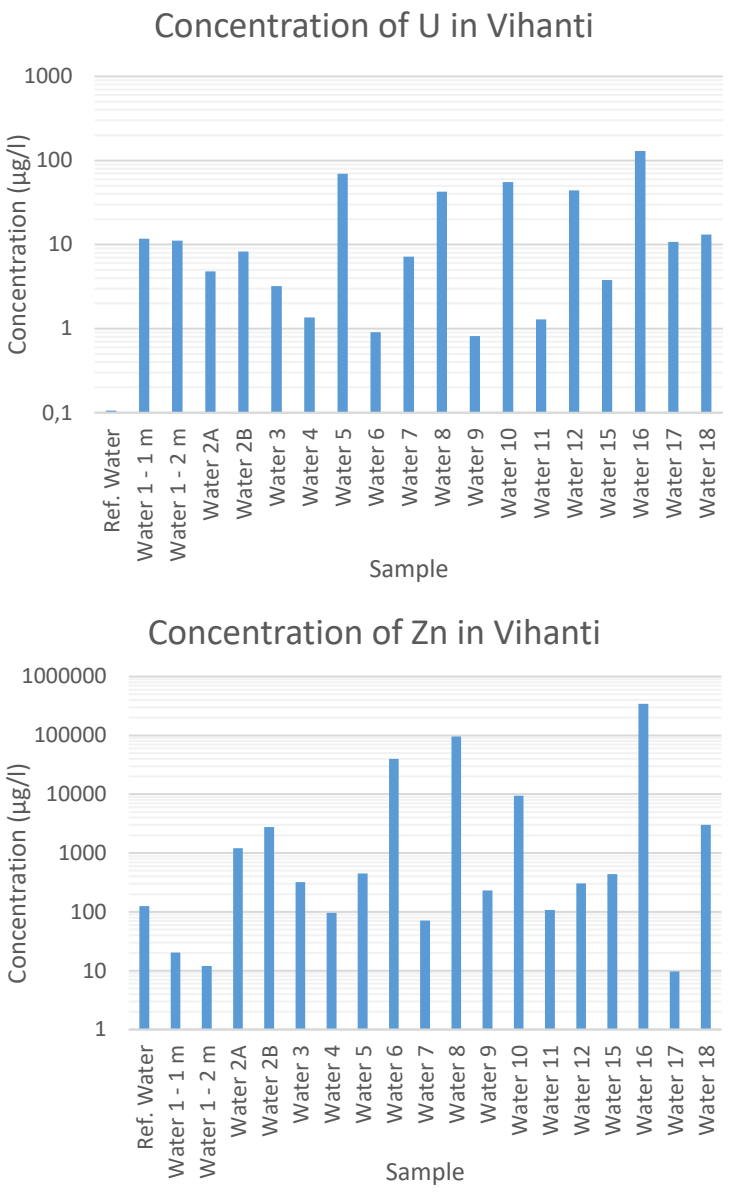

Figure 12 Concentrations of uranium and zinc in surface waters throughout the Vihanti site and water sampling locations. Note the logarithmic y-axes. Water samples water 3 and reference water are not shown in this picture to save space.

Sample water 6 also shows high concentrations of zinc and cadmium as well as elevated concentrations of cobalt, nickel, and copper. The high concentration of zinc compared to other samples from the site is seen clearly in Figure 12. Water 6 was collected from a ditch that receives its water from an old mine shaft, which is now completely flooded. The sample shows a low concentration of iron but as described in section 13.2 the beds and banks of the ditch where water 6 was taken were covered in a rust colored precipitate. The color of the precipitate suggests that it could very well be iron (III) hydroxide, the formation of which would explain the low iron concentration observed in the sample. As water flows from the mine shaft to the surface, a change in pH would promote oxidation and hydrolysis resulting in a loss of aqueous Fe (II+). The precipitation of iron coprecipitates many elements lowering their concentrations in the water phase. This phenomenon has been reported by Lottermoser and Ashley (2005) in the closed Mary Kathleen uranium mine.

The concentrations of the analytes in surface water sample water 6 and groundwater sample P115 are strikingly similar and both water 6 and the pipe where P115 was sampled are near the mine shaft. Water from the old mine shaft flows into the ditch of water 6 and it could be that the water in the old mine shaft also mixes with the groundwater sampled in P115. Comparing the results of water 6 and P115 suggests that the source of contamination of these samples could be the same or very similar in composition, but for water 6 at least the only logical option is the water flowing from the mine shaft. The results of P115 are discussed further in section 13.4.2.

Pöyry Oy has performed monitoring of the Vihanti site, and the two surface waters sampled coincide with water 6 and 12. The results from 2017 (Pöyry Finland Oy, 2018) compared to the results of this work indicate that the concentrations of Fe, Zn, Cd and Pb have not changed significantly in sampling location water 12. However, in water 6 the results show that the concentrations of zinc and cadmium have increased significantly, the zinc concentration measured in this work was around 40 000 µg/l (Figure 12), while the results from 2017 show a concentration of 8 400 µg/l. For cadmium, the concentration in this work was around 200 µg/l (Figure 13) and around 23 µg/l in 2017. The same increasing trend can be seen in groundwater P115 as with water 6 (see in section 13.4.2).

Samples were also taken from atop the tailings pile from the two ponds on the south and north sides of the pile. Water 5 which was taken from the northern pond shows higher concentrations of all analytes except for copper and lead. The greatest differences were observed in manganese, cobalt, and uranium concentrations. The differences between the two ponds may be explained by the heterogenous nature of the waste, the northern side is newer and should, on average, contain less of some heavy minerals, especially those of zinc (Pelkonen, 1992). Gamma results of samples NORM

3 and core 2B show that the activity concentration of ^{238}U is almost the same in these samples, which were taken from the shores of the ponds. Interestingly, the porewater results at around 30 cm show that the concentration of uranium is much higher in the porewater of NORM 3 than core 2B. The opposite can be said for the concentration of uranium in the corresponding ponds. To summarize, the northern and southern sides of the waste show similar activity concentrations of uranium in the waste, but the south side shows lower concentration of uranium in the pond, while also showing a higher concentration of uranium in the porewater.

The highest concentrations observed in this work seem to be localized on one area, much like the effects of the AMD. Additionally, water coming from the old mine shaft contains high concentrations of zinc and cadmium.

The concentration of uranium in all water samples was higher than in the reference sample form Isoneva bog, seen clearly in Figure 12. However, only five samples had concentrations above 30 µg/l, these were water 5, 8, 10, 12 and 16. Water samples 5, 8 and 16 are discussed above. Water 10 was taken from a ditch on the northwest side of the waste pile. Core sample core 1B was taken from the bank of the same ditch and its gamma results showed similar activity concentrations of ^{238}U as in the waste on top of the pile. The porewater results from the core at 9 cm, 19 cm, and 29 cm showed similar concentrations of uranium as water 5 and 10 and the porewater sampled near water 5. The concentration of uranium in water 10 is also close to the concentration in water 5. So, it seems that the banks of the ditch are lined with waste material from which some uranium can leach into the ditch.

Water sample water 12 was taken from the ditch receiving the outflow from the former settling pond (water 1) which shows lower concentrations of Mn, Fe, Zn and U than water 12. Water 17, which was sampled from a surface water pipe collecting outflow from the settling pond agrees with the results from the settling pond (water 1), unlike water 12. One of the smaller ditches that flow around the waste pile could be the source for the aforementioned elements in water 12. Unfortunately, water from this ditch was not sampled.

High concentrations of cadmium were measured in three samples: water 6, 8 and 16, and the concentration of cadmium in all samples from Vihanti is shown in Figure 13. The three water samples that had higher concentrations of cadmium also showed high concentrations of zinc and copper. Cadmium could be released alongside these elements into the water from the waste, which seems plausible as cadmium can be incorporated in minerals of zinc and copper as cation substitutions or small inclusions in the host mineral (Lottermoser, 2007b). The strongest positive correlation between cadmium and any element in surface waters is seen between cadmium and zinc (R=0.958). In

addition, a strong positive correlation between cadmium and copper in surface waters is also seen (R=0.934). The correlations between cadmium and zinc as well as cadmium and copper are also strong and positive (R>0.930) in groundwaters and porewaters.

Cadmium concentrations throughout the site can be compared to the European environmental quality standards (EQS) set in EU Directive 2008/105/EC (2008). The EQS cover inland surface waters which include rivers and lakes and related artificial or heavily modified water bodies. The concentration of cadmium in the surface waters from Vihanti are shown in Figure 13 along with the EQS and drinking water limits.

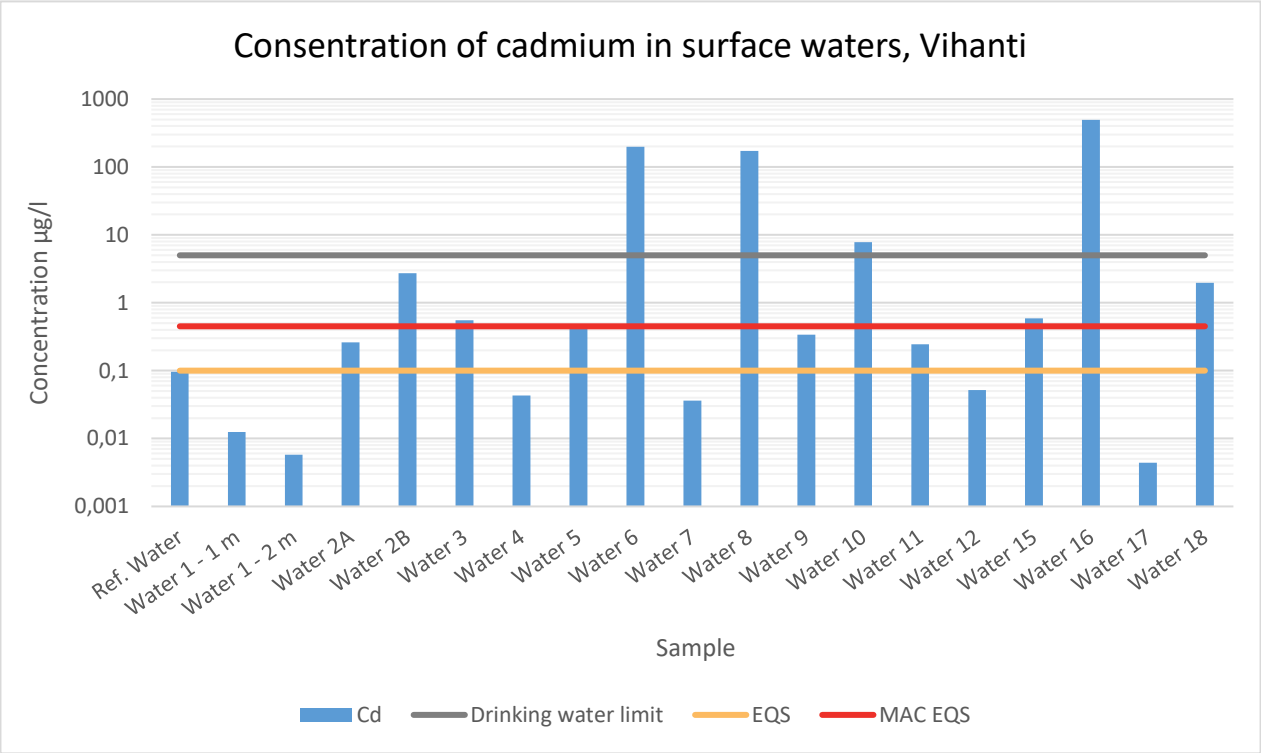

Figure 13 Concentration of cadmium in surface waters of Vihanti. Note the logarithmic y-axis. The EQS and maximum allowable concentration (MAC) EQS value along with the Finnish drinking water limit are also shown in the graph.

As can be seen from Figure 13 eight water samples are above the maximum allowable concentration environmental quality standard (MAC-EQS; 0.45 µg/l) and twelve water samples are above the environmental quality standard (EQS; 0.1 µg/l). The samples which are over the MAC-EQS are located around the low pH ditch and the old mine shaft, one sample, water 10, is located on the southwest side of the waste pile. Four samples across the Vihanti site show nickel concentrations above the value of the relevant EQS, these are water 6, 8, 16 and 18, and for lead two samples, water 8 and 16, show concentrations above the relevant EQS.

Korsnäs

Three surface water samples that showed clearly higher concentrations of uranium than other samples were found. These samples were water 1, water 4 – 1 m and water 6. Uranium concentrations of all surface water samples from Korsnäs are plotted in Figure 14. The uranium in samples water 1 and 4 most likely originates from mineralization on the surfaces of the open pit mine and this is discussed further in section 13.4.1.2. The uranium in water 6 most likely originates from the lanthanide pile, since gamma spectrometry data shows that the highest activity concentrations of ^{238}U are found in samples taken from the pile, in addition the porewater samples taken alongside core 2A show high concentrations of uranium. This suggests that uranium can be transported from the solid phase of the waste into the porewater in the waste, further leaching of this porewater into the ditch surrounding the lanthanide pile is then the most likely cause for the higher uranium concentration observed in water 6.

Comparing the results of water 10 with water 6 reveals that even though both samples were taken close to the lanthanide pile the slightly farther located water 10 has a much lower concentration of uranium, as seen clearly in Figure 14. This indicates that distance from the lanthanide pile is an important factor for the transport of uranium. The pond where water 10 was taken also has a greater volume of water in it which will, of course, affect the concentration of any element.

Three of the water sampling locations coincide with sampling locations in previous work of Leminen (2016), these sampling locations are water 1, 2 and 3. Mostly minor changes can be seen in the results from 2016 compared to this work. Water 1 is the closest sampling point to the old open pit mine, water 2 is downstream of the lanthanide pile and water 3 is even further downstream from water 2. The samples in this work were taken during the summer and the samples in the work of Leminen (2016) were taken during the fall. In all three samples cadmium concentrations decreased from around 0.2 µg/l to less than 0.1 µg/l. The largest change in concentration is seen in iron concentrations of water 2, where the concentration increased from 550 µg/l to around 1270 µg/l. Increases in uranium concentrations could be seen in water 1 and 2, from 39.2 µg/l to 80.5 µg/l and from 5.13 µg/l to 14.1 µg/l, respectively. Nickel concentrations increased in water 2 and 3, from around 10 µg/l to around 20 µg/l.

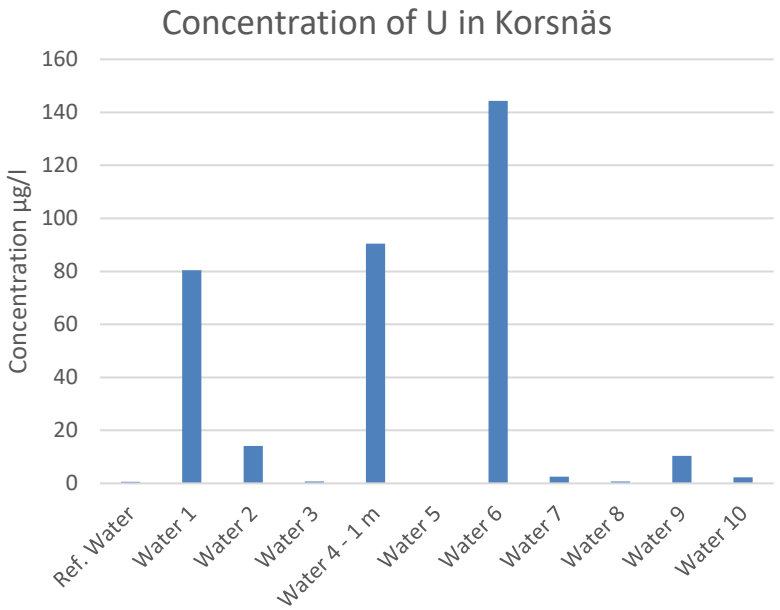

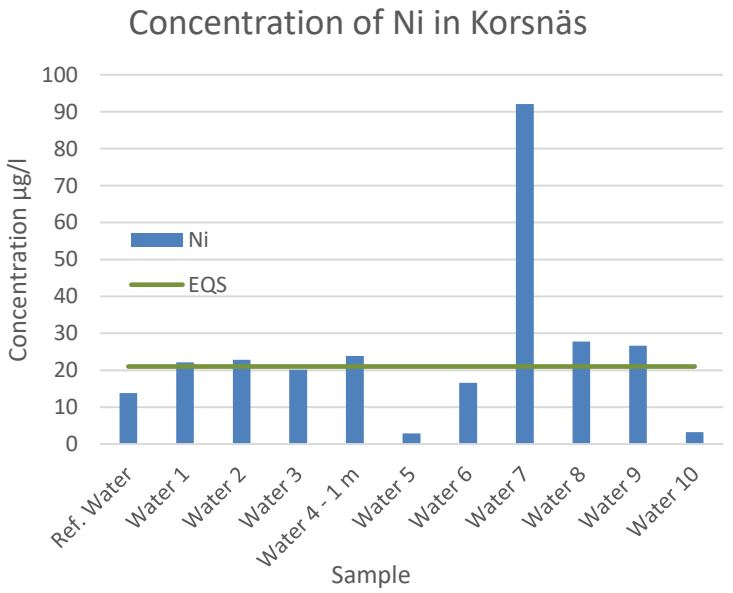

Figure 14 Water sampling locations of Korsnäs along with the concentrations of uranium and nickel in the samples. The values presented in this figure are averages of two parallel samples, the EQS of Ni is also shown. Water samples 2 and 3 were taken at locations sedi 2 and 3.

The two potential sources of contamination in the Korsnäs site are the waste pile and the lanthanide pile. The water samples that were taken closest to these two should, in theory, be the most contaminated. While water 6, the closest sample to the lanthanide pile, shows an elevated concentration of uranium (Figure 14) and manganese, water 5, the water sample taken from the pond atop the waste pile, shows very low concentration of all measured elements.

The highest concentrations of Al, Cr, Fe, Co and Ni in surface waters were detected in sample water 7, which was taken downstream of the old open pit mine to the south of the site. The concentrations of these elements are clearly higher than in other samples taken much closer to the waste piles and open pit mine. XRF results indicate that the concentrations of Al, Cr, Fe and Ni are low in both the waste pile and the lanthanide pile. No clear source for these elements in this sample could be identified and the source could be one of the other ditches that merge with the one sampled but based on the data at hand it most likely doesn't originate from the waste piles. The concentration of nickel throughout the site can be seen in Figure 14.

The cadmium and lead concentrations in all sampled surface waters were below their respective EQS values; 0.1 µg/l for cadmium and 7.5 µg/l for lead (EC, 2008; Verta et al., 2010). The concentrations of nickel in water samples water 1, 2, 4, 8 and 9 were slightly above the EQS value for nickel (21 µg/l), while the nickel concentration in water 7, 92 µg/l, is significantly higher than the EQS.

13.4.1.1 Flow paths

Vihanti

A single flow path can be constructed from the water samples collected from Vihanti. A ditch from the west side of the waste pile (water 10) flows north into the former settling pond (water 1). The water flows out of the pond into one ditch (water 12), which continues west away from the site (water 7 and 3). In these samples the highest concentration of uranium is observed in near the waste pile in sample water 10, the concentration then drops in the settling pond (water 1) and rises in the receiving ditch (water 12). In the following water samples the uranium concentration drops even further.

Korsnäs

In Korsnäs are two clear sources of uranium in the water, the first being the old open pit mine and the second the lanthanide pile. From the open pit mine (water 4) water flows out through one ditch (water 1), which eventually splits into two, one flowing north (water 7) and one flowing south (water 9). The ditch flowing south then loops around and turns to flow north (water 8) continuing until it merges

with another ditch flowing away from the site ending in the sea (near water/sedi 3). Yet another flow path is from a ditch near the lanthanide pile (water 6), which flows and merges with another ditch form the waste pile (near water/sedi 2). This ditch merges with the one flowing north from sampling location water 8 ending in the sea (near water/sedi 3). In all three of these described paths the uranium concentration is the highest in the first point decreasing with each sample, from around 100 µg/l in water 4 and water 6 to around 0.7 µg/l in water 3 and to around 2.5 µg/l in water 7. The gamma results also show increased activity concentrations of uranium and thorium series radionuclides in sediment sample 2 taken along the path from the lanthanide pile to the sea. A decrease in activity concentrations between sediment 2 and sediment 3 can be seen much like in their water sample counterparts.

13.4.1.2 Limnos water samples

Water samples taken from various depths of the old open pit mine of Korsnäs show that the concentrations of different elements vary with depth, as can be seen in Figure 15 and Figure 16. The concentrations of iron and manganese show the greatest change with depth across all measured elements, both showing an increase of three orders of magnitude as depth increased from 1 m to 10 m. The same kind of increasing trend with depth can be seen with most of the elements measured, Ni, Cu, Zn and Cd being the most notable exceptions. These elements showed higher concentrations in the samples taken from 1 m and 5 m than in samples taken from deeper. These trends can be seen in Figure 15 for Mn, Fe and U, and in Figure 16 for Ni, Cu and Zn.

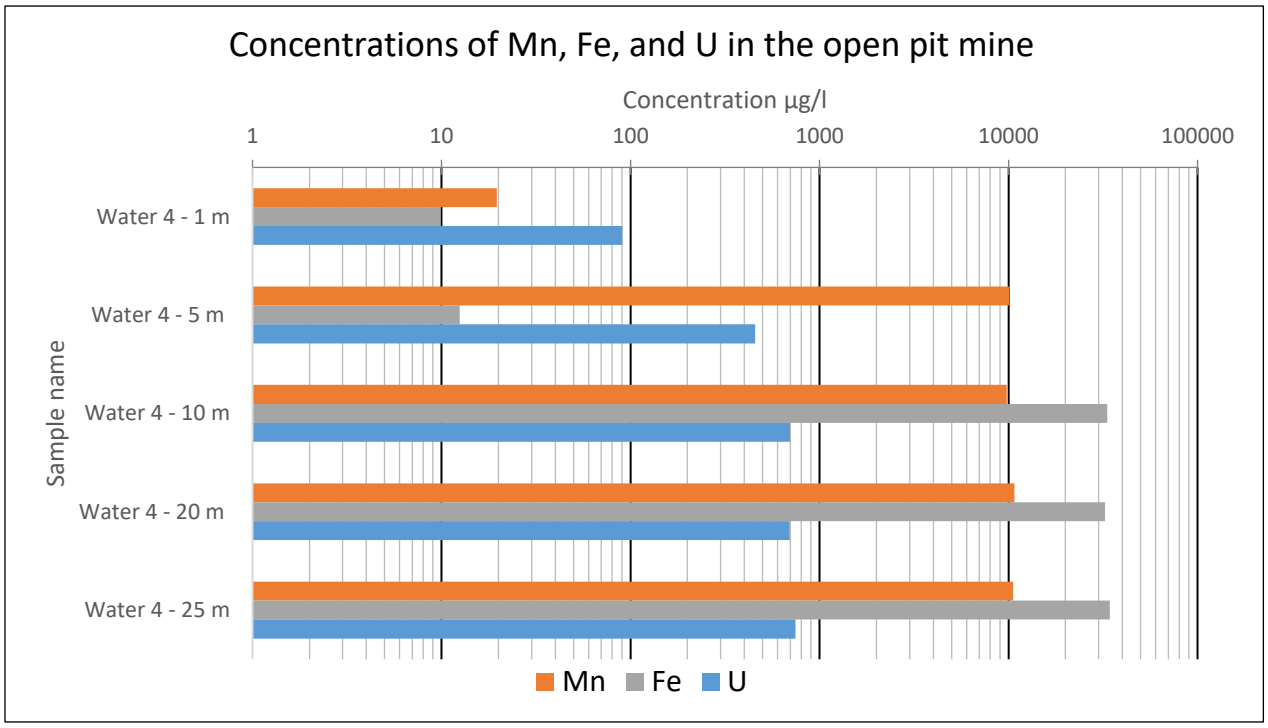

Figure 15 Concentrations of Mn, Fe and U in the old open pit mine in Korsnäs (Water 4). Note the logarithmic concentration axis. In this figure averages of both parallel samples are presented.

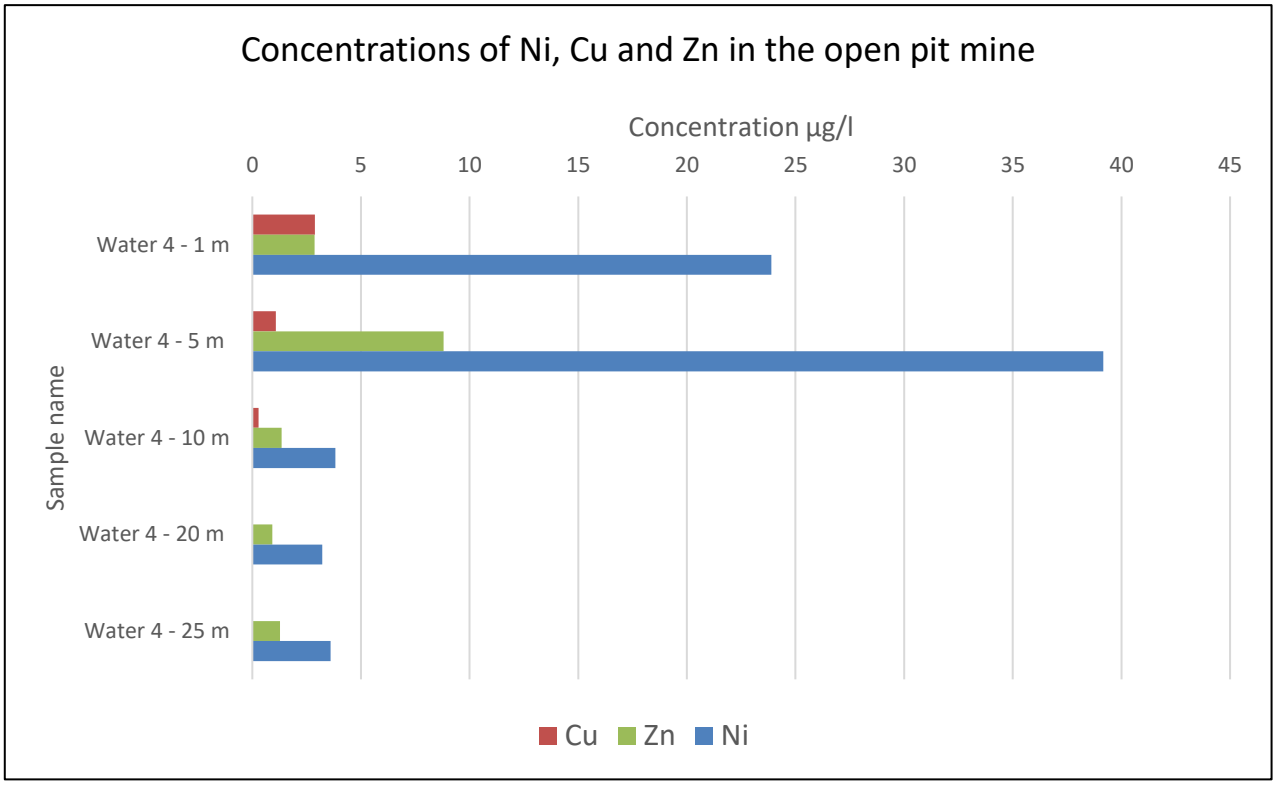

Figure 16 Concentrations of Ni, Cu and Zn in the old open pit mine in Korsnäs (Water 4). In this figure results from both parallel samples are presented.

Assuming none of the elements measured are mixing in the water of the old open pit mine, the different trend observed with Ni, Cu, Zn and Cd could be explained by a different source term that could be, for example, seepage waters from the surrounding area. Another option is that the conditions deeper in the pit are not favorable for soluble species of these elements and that they are present as colloids which do not pass the 0.45 µm filter used in this work. Nevertheless, compared to the typical background value of nickel in Finnish surface waters 1 µg/l (Verta et al., 2010) and to the reference sample collected near the site, the concentration of nickel is slightly elevated in the pit, and is in fact above the environmental quality standard set in EU Directive 2008/105/EC (2008).

The source of the other elements that were observed to have a positive trend with depth could be mineralization on the surfaces of the open pit. Since the pH of the pit was near neutral even at the deepest point sampled, the most likely cause of mobilization of elements are redox reactions and complexation. Measurements showed that the concentration of dissolved oxygen was low, and that the oxidation reduction potential was in the range of -100 mV. In reducing conditions, one would expect Mn and Fe to be in their lower oxidation states of II+. As for uranium, in anoxic alkaline or neutral conditions, the U-carbonate complex is usually the dominant species (Lehto and Hou, 2011).

13.4.2 Groundwater

The groundwater results from Vihanti are presented in full in Appendix 5 and some of the results are presented as bar plots in Figure 17 and Figure 18. The values presented in these figures are averages of results from two parallel samples, except for some rejected values of some dilutions (see section 13.4.3). No reference sample for groundwater was collected form an unaffected area, but the obtained results may be compared with corresponding concentration limits set for drinking water in Finnish legislation as groundwater is a common source of drinking water. No groundwater was collected from Korsnäs.

As can be seen from Figure 17 and Figure 18 the concentrations of chrome, arsenic and selenium are low in all of the groundwater samples. The concentrations of Al, Cu, Ni, Cd, Pb and U are low in most samples, but some samples show higher concentrations of these elements than the rest. Concentrations of manganese are constant across all samples; meanwhile large variation can be seen in iron concentrations and some variation in zinc concentrations can be seen across the samples.

Sample P115 shows the highest concentrations of Al, Co, Ni, Cu, Zn and Cd across all groundwater samples, while P114 shows the highest concentrations of V, Cr, Se, Mo and U. The highest concentrations of Mn and Fe can be found in the same sample, P110. Relative to the other samples, the concentrations of aluminum and copper in sample P115 are very high, over 1000-fold compared to the second highest concentrations. Also, the concentrations of cadmium and zinc are high in sample P115, around 100-fold and 200-fold, respectively, compared to the second highest concentrations. The concentrations of cobalt and nickel are slightly higher in P115 than in P114 which has the second highest concentrations of these elements.

For drinking water there are set concentration limits for eight of the measured elements, additionally there are limits for Al, Mn and F, which are not based on health effects (STM/1352, 2015). These values are presented in Table 5.

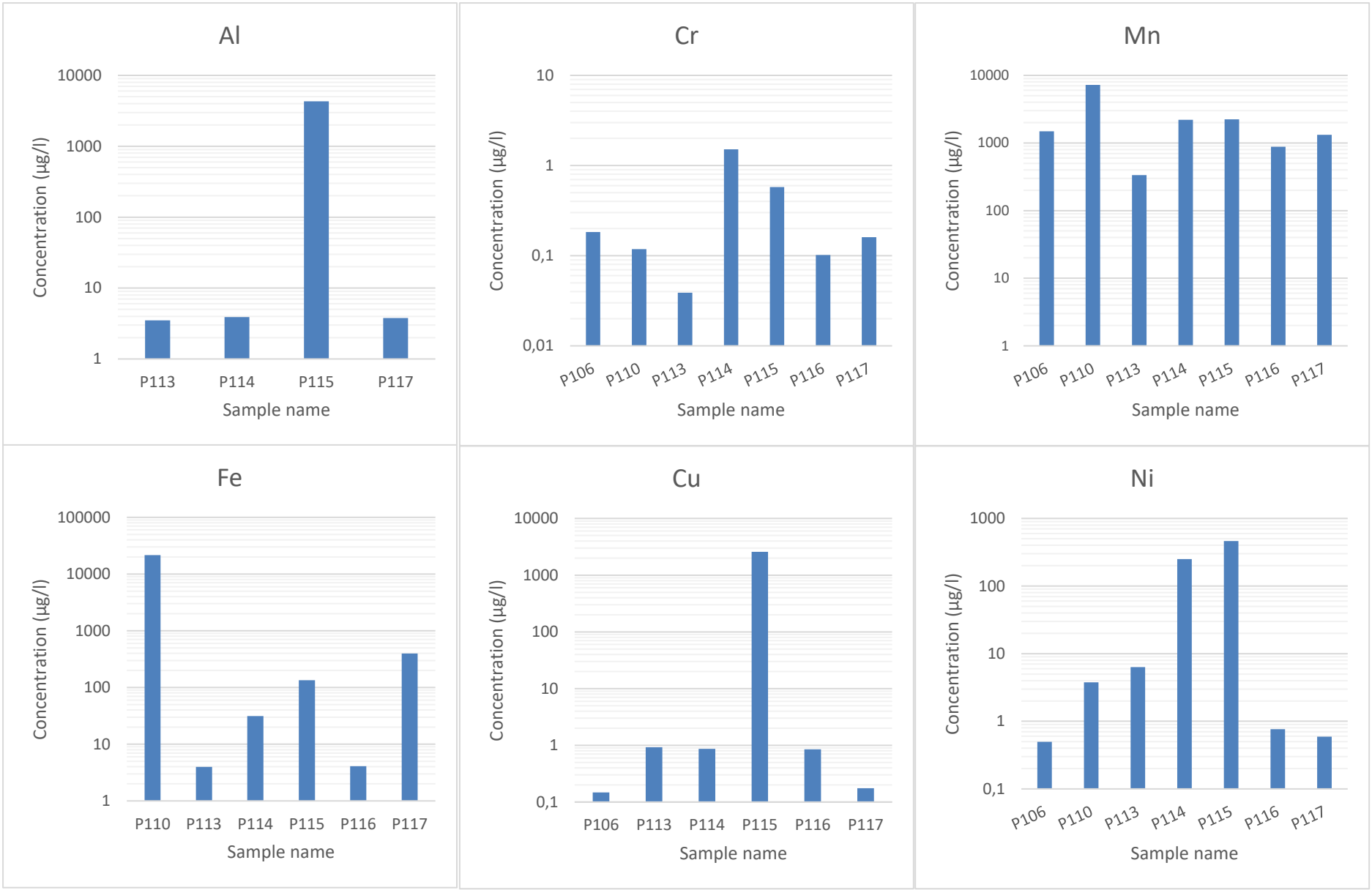

Figure 17 Bar plots of the concentrations of Al, Cr, Mn, Fe, Cu and Ni in ground water samples from Vihanti. Note the logarithmic scale of the y-axis. Concentrations below the limit of detection are not presented in this figure.

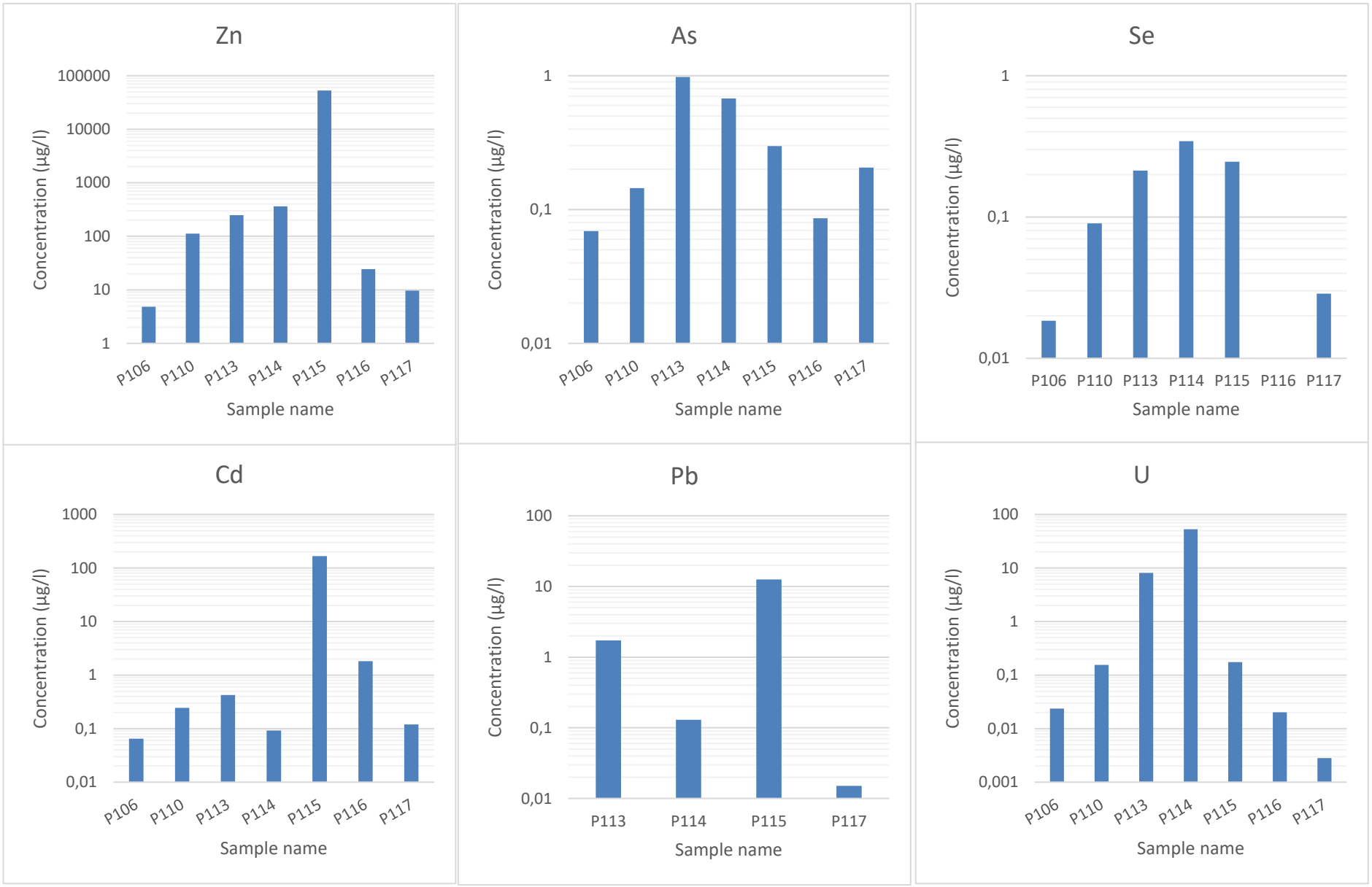

Figure 18 Bar plots of the concentrations of Zn, As, Se, Cd, Pb and U in ground water samples from Vihanti. Note the logarithmic scale of the y-axis. Concentrations below the limit of detection are not presented in this figure.

Table 5 Concentration limits of some elements in drinking water. Limits of Al, Mn and Fe are not based on health effects (STM/1352 2015).

Element	Concentration limit (STM/1352) µg/l
Cr	50
Ni	20
Cu	2000
As	10
Se	10
Cd	5
Pb	10
U	30
Al	200
Mn	50
Fe	200

Comparing the groundwater results with the limits in Table 5, it can be seen that none of the samples contain concentrations of Cr, As or Se that would be above the set limits. The concentration limit of 20 µg/l set for nickel is exceeded over 10-fold in two samples, P114 and P115. Sample P115 also shows concentrations of Cu, Cd and Pb that are over the limits set in STM/1352. The concentrations of Cu and Pb exceed the limit by around 500 µg/l and 2 µg/l, respectively. The cadmium concentration in sample P115 is, however, very high, exceeding the concentration limit of 5 µg/l by over 150 µg/l. Only in one sample, P114, is the limit set for uranium exceeded.

Pöyry Oy has performed monitoring of the Vihanti site, including analysis of the groundwaters. Since the sampling sites are the same it is possible to compare the results from this work to those of Pöyry Oy form 2017.

In all but two samples (P106, P116) the cadmium concentration increased compared to earlier results reported by Pöyry Oy (Pöyry Finland Oy, 2018). In sample P106 the concentration of cadmium went down and in sample P110 it remained almost the same, while in sample P115 the concentration was over triple compared to what it was in 2017. The smallest increase was seen in sample P114.

The concentration of iron decreased in all samples except for sample P114 where it remained almost the same. In two samples (P106, P115) a decrease in zinc concentration can be seen while the rest show an increase in the concentration of this element. The concentrations of lead cannot be compared for all samples as they are under the detection limit in either this work or in the results reported by Pöyry Oy (Pöyry Finland Oy 2018). For samples P114 and P115 the concentrations are above the

detection limit in both works and it can be said that the concentration of lead decreased in P114 and remained around the same in P115.

Based on the data at hand, it is difficult to find a reason for the change in the measured concentrations compared to earlier results, aside normal yearly variation. Oxidizing conditions in groundwater P114 could explain the relatively high uranium and low iron concentrations. Uranium is mobile in its oxidation state of VI+ (Lehto and Hou, 2011), meanwhile iron oxidized to the oxidation state of III+ would most likely precipitate in near neutral pH. The source of the uranium could very well be the uranium-phosphorous mineralization found in some parts of the site (Pelkonen, 1992). The highest concentration of molybdenum (around 100 µg/l) was also found in sample P114, which also supports the notion of oxidizing neutral conditions as molybdenum is often found in higher concentrations in oxic conditions (Smedley and Kinniburgh, 2017).

The relatively low pH of 4 of sample P115 is together with redox conditions the most likely reason for the high concentration of elements found in this sample. Oxidizing acidic conditions would likely increase the concentration of the elements that were found in relatively high concentrations in this work.

The sources of cadmium in P115 are most likely sphalerite and galena, in which cadmium is commonly found in high concentrations (Lahermo et al., 2002). The weathering of these minerals would also release zinc and lead into the solution as well as lower the pH. The high concentration of copper, on the other hand, could be explained by the weathering of chalcopyrite. Sphalerite, galena and chalcopyrite along with some iron sulfides were the main minerals found in the ores of Vihanti (Pelkonen, 1992).

13.4.3 Evaluation of Data

In most of the ICP-MS results variation can be seen between the two parallel samples. These differences are likely a result of multiple factors, mainly dilution, heterogenicity and artifacts of the method. A large difference in the concentrations of the analytes can be seen in water 8 from Vihanti. This sampling location likely had abundant colloids in the water, and it is possible that during filtering some of these colloids ended up in one sample due to small differences in the used filters or the size distribution of the colloids.

Comparing the results of different dilutions of P115 revealed that the 5-fold dilution of parallel sample P115A failed, thus the results for Si, P, V, Cr, Fe, As, Se, Pb and U for sample P115 are obtained from a single dilution.

For sample P114 the concentration of aluminum is too high in the 1.5-fold dilution of parallel sample P114A compared to other dilutions of the same sample and its parallel sample. Other elements in between all dilutions and between the parallels are congruent, leading to the conclusion that the 1.5-fold dilution of P114A might be contaminated with aluminum.

Water sample water 9A (Korsnäs) shows a copper concentration that is too high compared to other samples from the site and to the parallel sample 9B. The copper is most likely from copper sulfate that was handled in the same fume hood.

The problematic results discussed in this chapter have been left out of the plots presented in this work, but can be seen in Appendix 5 nonetheless.

13.5 Gamma spectrometry results

In addition to radionuclides from the uranium and thorium series, ^{40}K and ^{235}U were also measured. The results of these radionuclides are not discussed below, since ^{40}K is not a part of a natural decay series and the activity concentration of ^{235}U was low across all samples. The results of these radionuclides can be found in Appendix 6 for each of the samples. The results of all radionuclides are reported as becquerels per kilogram of dry weight, unless said otherwise.

13.5.1 Soil samples of Vihanti

A reference soil sample was collected from the nearby Isoneva bog, however after measurement it was found that most of the activities measured were below their corresponding minimum detectable activities, because of this the results of the reference soil are not discussed further.

Soil samples form Vihanti show higher activity concentrations of uranium series radionuclides than thorium series radionuclides. The activity concentrations of uranium series radionuclides in two soil samples are shown in Figure 19. In most soil samples the uranium series is in disequilibrium, however the activity concentrations of ^{238}U and ^{226}Ra are fairly close to each other in many samples. One major exception to this is soil 3 where in sections 3-9 cm and 9-15 cm the difference is large. Particularly, in the 9-15 cm section, around 50 Bq/kg of ^{226}Ra compared to around 210 Bq/kg of ^{238}U are seen. These numbers indicate that either radium is being mobilized more efficiently than uranium or that uranium is enriched in this layer. Sequential extractions on Finnish boreal soils have indicated that uranium is more leachable in topsoil horizons, while radium showed better leachability in subsoil horizons (Virtanen et al., 2013). Based on this information one would expect the activity concentration of uranium to be lower than that of radium.

During sampling and pretreatment, soil 3 seemed organic and homogenous with no apparent changes in layers and the soil was saturated with water. Mobility of uranium has been found to increase in soil layers that are oxidizing and less saturated with water (Dowdall and O'Dea, 2002). The conditions in soil 3 could be unfavorable for the mobilization uranium compared to radium. Previous studies on a similarly organic rich wetland soil have indicated that uranium can be retained efficiently by organic complexation (Fuller et al., 2020). Carboxyl groups of organic acids in soil 3 could complex U(VI) and these complexes are then stable enough to immobilize at least some of the uranium. This could explain the apparent excess of uranium in the sample. The higher activity concentration of ^{210}Pb compared to ^{226}Ra supports the idea that radium is moving through the soil horizon.

The activity concentrations of ^{238}U and ^{226}Ra seem to be the lowest in the bottom sections of the soil samples, except for soil 1. The activity concentration throughout soil 1 is shown in Figure 19. This discrepancy is explained by the fact that soil 1 was sampled from atop the waste pile, but the covering soil layer was shallow enough that the bottom 5 cm of the core already contained some tailings. The ^{238}U activity concentrations ranged between 28 Bq/kg and 218 Bq/kg across all samples, with most of the sections having concentrations below the MDA. The activity concentration of ^{226}Ra on the other hand ranged from 6.4 Bq/kg to 206 Bq/kg, the lower minimum value of radium compared to uranium is explained by the lower MDA of radium. The typical ranges of ^{238}U and ^{226}Ra activity concentrations are 13-110 Bq/kg with mean values of 41 Bq/kg for both (UNSCEAR, 2008). Based on these numbers, the activity concentration of ^{238}U is elevated in soil 1 section 15-20 cm and soil 3 sections 3-9 cm and 9-15cm, while ^{226}Ra is elevated only in soil 1 section 15-20 cm. Considering that soil 1 section 15-20 cm is tailings, the only elevated activity concentrations found in soils were in soil 3 sections 3-9 cm and 9-15 cm. The activity concentrations of the measured uranium series radionuclides in samples soil 1 and 3 can be seen along with a map of the sampling sites in Figure 19. The effect of atmospheric deposition of ^{210}Pb and diffusion of radon followed by its decay into ^{210}Pb can be seen in the sections closest to the surface in all soil samples.

The activity concentration of measured thorium series radionuclides was found to be very low in all soil samples from Vihanti. Across all depths, the thorium series showed no signs of disequilibrium. However, lower activity concentrations were measured in the sections closest to the surface than in the deeper sections. The lowest measured activity concentration of ^{232}Th was 1.3 Bq/kg, which was measured in soil 3 in the 0-3 cm section. On the other hand, the highest measured activity concentration of ^{232}Th was 13 Bq/kg, which was measured in soil 2 at 17-22 cm. The average activity concentration of ^{232}Th in the soils of Vihanti was around 7.3 Bq/kg, which is lower than the mean value of 46 Bq/kg typically found in Finnish soils (UNSCEAR, 2008).

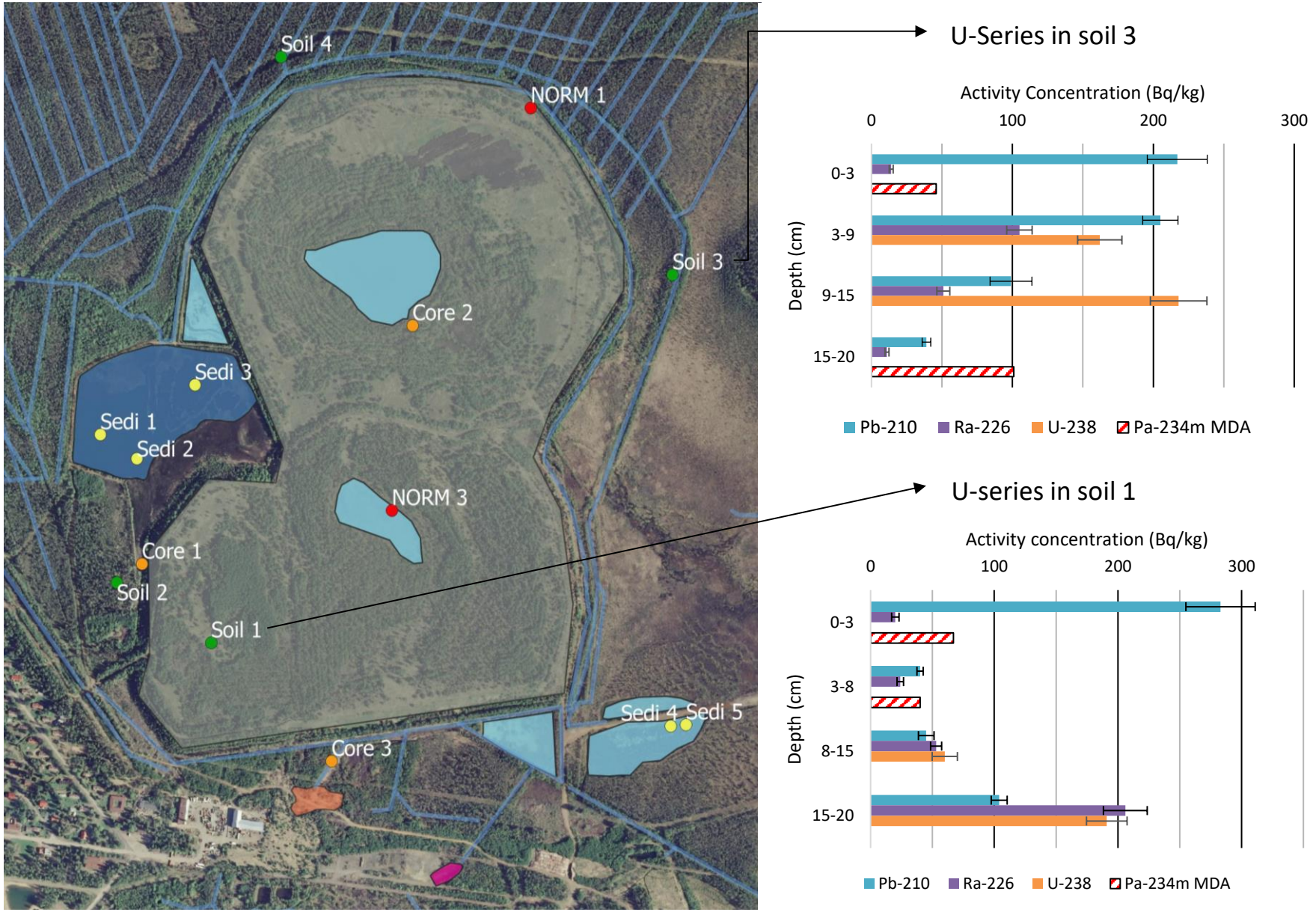

Figure 19 Activity concentrations of Uranium series radionuclides in soil 1 and soil 3 along with sampling locations in Vihanti. The red striped bars represent the minimum detectable activity values of Pa-234m from which the activity of U-238 is calculated. The error bars show 1 σ of uncertainty.

13.5.2 Soil Samples of Korsnäs

A reference soil sample was collected southeast of the site, far enough to reasonably assume it was not contaminated by the site's mining activities. The results for this sample are presented in Figure 20. The activity concentrations of all measured radionuclides were low and in the range of typical background values in this sample (UNSCEAR, 2008). As can be seen from Figure 20, the activity concentrations in both series increase with depth, reaching their maximum values in the depth of 15-20 cm. Based on this data there is no reason to suspect that Ref. Soil is unfit to be used as a reference for uncontaminated soil for the Korsnäs site.

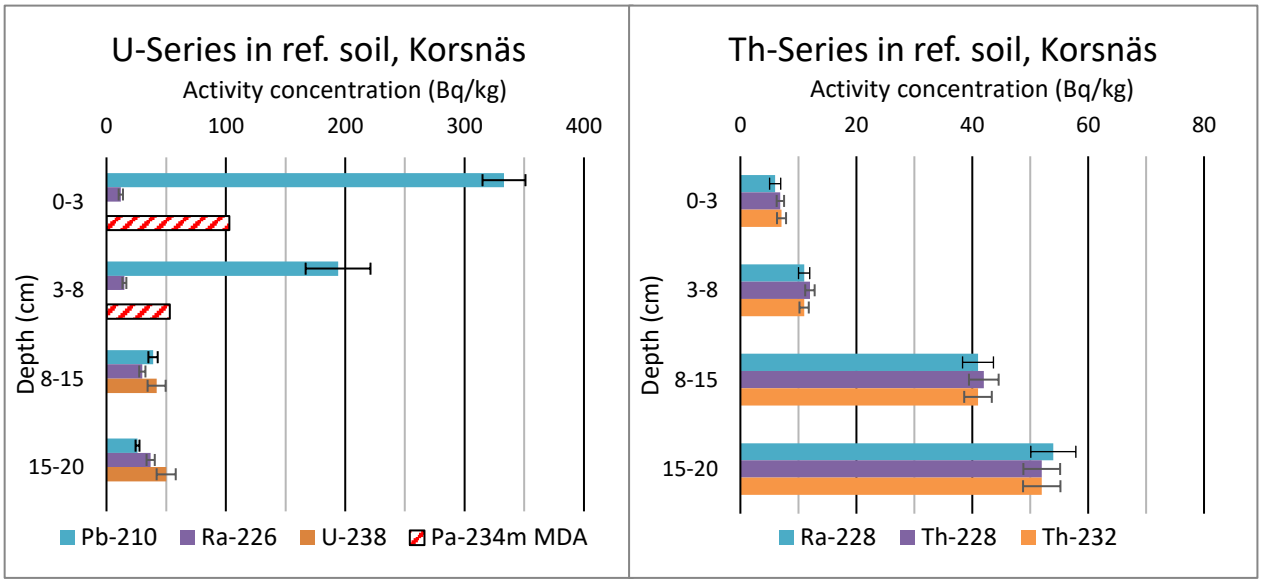

Figure 20 Activity concentrations of uranium (left) and thorium (right) series radionuclides throughout sample Reference Soil (Korsnäs). The red striped bars represent the minimum detectable activity values of Pa-234m from which the activity of U-238 is calculated. The error bars show 1 σ of uncertainty.

Compared to both the reference soil and the mean activity concentration in soils from literature, all soil samples exhibit elevated activity concentrations for the uranium and thorium series, however soil sample soil 2 was not analyzed due to time constraints. Soil samples 3 and 4 were taken from the main waste pile and the lanthanide pile, respectively, and present elevated activity concentrations throughout the samples. The results of soil 4 are presented in Figure 21. Because of the lack of a covering layer on top of the waste pile, soil 3 comprises solely of waste and is very homogenous. Soil 4, in turn, presented a thick (6 cm) layer of soil followed by a uniform sandy layer continuing down the rest of the sample. Since the sample was taken right next to the lanthanide pile it is plausible that this sample consists of the cover laid on top of the waste (~6 cm) during remediation and a coarser fraction of the waste itself.

Soil 1 was taken from a forested area in between the waste pile and the old open pit mine, and its depth profile is presented in Figure 21. The activity found in this soil sample seems to be concentrated between 2 cm and 13 cm, which is clearly seen in the figure. These layers were soil, where the 2-7 cm section seemed to contain abundant organic matter while the 7-13 cm section was more sandy. The activity concentrations in sections 0-2 cm and 13-20 cm of this sample were in the range of typical background values, however the activity concentrations in the top layer were higher than in the top layer of the reference sample. In the bottom layer the concentrations were the same magnitude as in the reference. The radioactivity in the depth of 2-13 cm could trace back to the mine's operational years. Dust may have contaminated the soil or waste may have been laid temporarily on top of it explaining the shallow contamination of the soil observed today, however it is difficult to say with certainty from the data at hand.

Soil 3 shows constant activity concentrations of all measured radionuclides throughout the sample, except a small increase in ^{210}Pb activity in the first two centimeters, which is caused by deposition of ^{210}Pb. The radionuclides from the thorium series are in equilibrium and the activity concentration of ^{232}Th averages around 225 Bq/kg throughout the sample, while the average activity concentrations of ^{238}U and ^{226}Ra throughout the sample are around 463 Bq/kg for uranium and 554 Bq/kg for radium. The lower activity concentration of uranium is most likely influenced by its higher tendency to mobilize because of its redox sensitivity as compared to ^{226}Ra.

Soil 4 shows activity concentrations of ^{238}U, ^{226}Ra; ^{232}Th, ^{228}Th and ^{228}Ra exceeding 1000 Bq/kg (1 Bq/g), which can be seen in Figure 21. These relatively high activity concentrations, which are localized in the 6-20 cm sections, and the sandy composition of the sample suggest that a portion of the enriched lanthanide waste was sampled in soil 4. However, even the 0-6 cm layer shows clearly elevated activity concentrations of ^{238}U, ^{226}Ra and thorium series radionuclides. Interestingly, the ^{226}Ra/^{238}U ratio in the whole sample is less than one indicating that uranium is enriched in the sample. This could be caused by preferential leaching of uranium from the lanthanide pile followed by accumulation in the nearby soil. The opposite can be seen in soil 3. In addition, the ratio of ^{210}Pb:^{226}Ra in soil 4 is low, which indicates that the process used to produce the enriched lanthanide has caused partitioning of these radionuclides. The same effect is also caused, to an extent, by the exhalation of radon as can be seen in soil 1 (Figure 21).

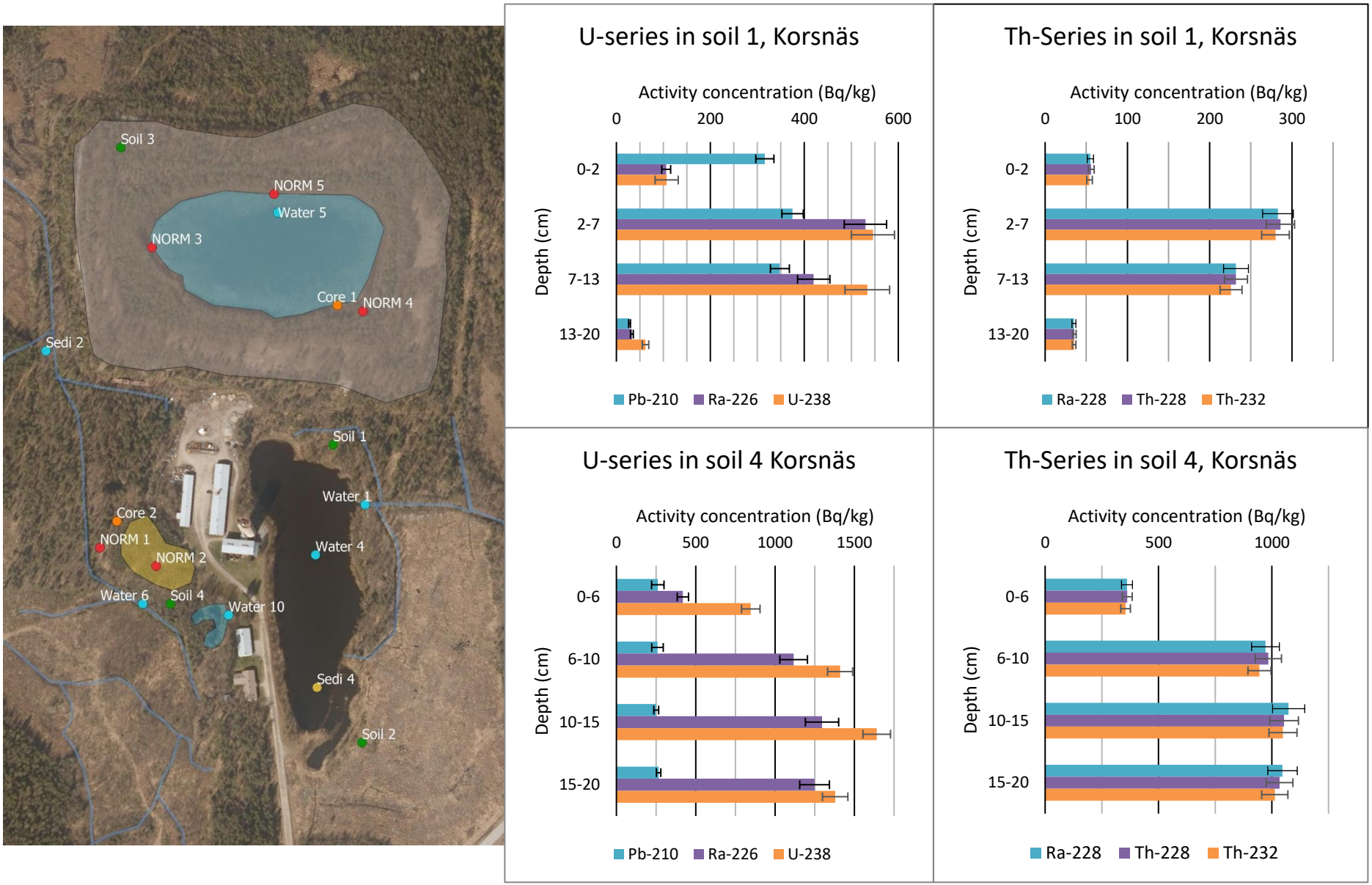

Figure 21 A map showing some sampling locations in Korsnäs and bar plots of the activity concentrations of some uranium and thorium series radionuclides in samples soil 1 and soil 4. The error bars show 1 σ of uncertainty.

13.5.3 Sediment samples of Vihanti

The activity concentrations of all sediment samples from Vihanti can be seen in Figure 22. Activity concentrations measured from sediment samples taken from different parts of the settling pond in Vihanti (Sedi 1-3) are consistent with each other. Activity concentrations of thorium series radionuclides are around 20 Bq/kg each and the activity concentrations of ^{238}U and ^{226}Th are around 34 Bq/kg and 23 Bq/kg, respectively, in these samples.

The activity concentration of thorium series radionuclides is low in samples taken from the ponds southeast of the waste pile, around 5 Bq/kg in sedi 4 and below the MDA in sedi 5. Compared to sediments from the settling pond the activity concentration of ^{238}U, 91 Bq/kg, in sedi 5 is elevated. The activity concentration of ^{238}U is much higher than ^{226}Ra, which could be explained by transport of uranium into the pond. In earlier studies of the site the water of these ponds was measured to be slightly acidic and uranium was suspected to be seeping from the old mine shaft into the surface waters (Tornivaara et al., 2018). These two factors may explain the large difference between the activity concentrations of ^{238}U and ^{226}Ra in sedi 5.

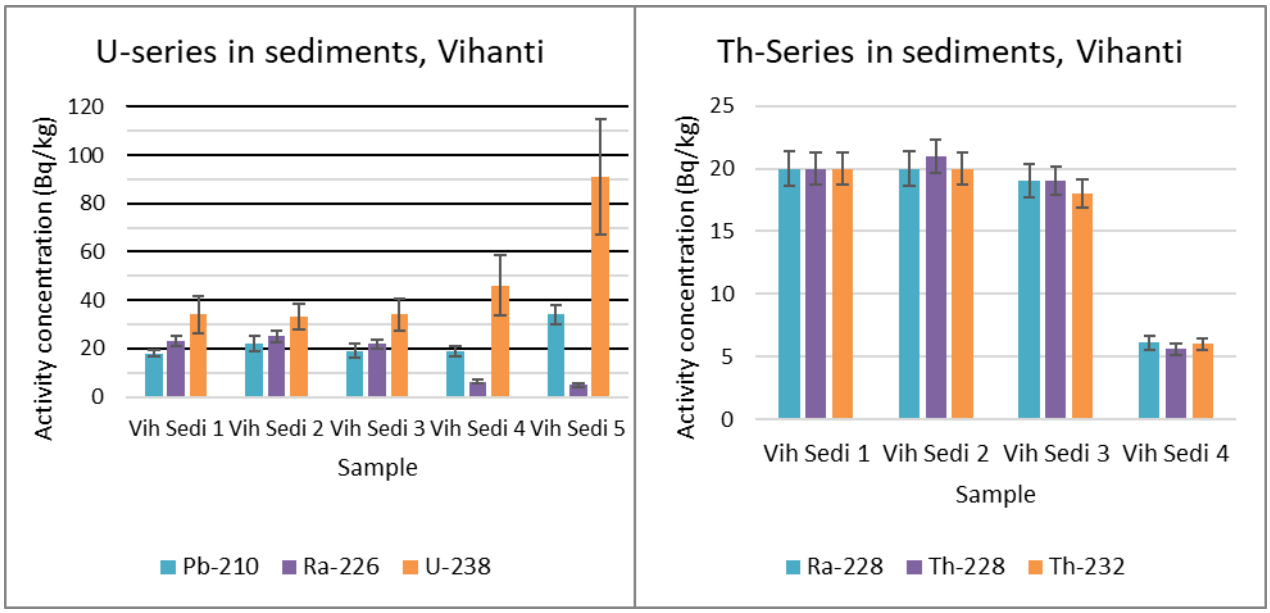

Figure 22 The activity concentrations of sediment samples from Vihanti. The results of the thorium series were below the minimum detectable activity for sedi 5. The error bars show 1 σ of

13.5.4 Sediment samples of Korsnäs

The activity concentrations of some uranium series radionuclides in sediments samples from Korsnäs are shown in Figure 23. As can be seen from the figure, compared to the reference sediment sample collected from Korsnäs, the activity concentrations in sedi 1 and sedi 3 are at background levels. Sedi 1 was a ditch coming out of the old open pit mine and sedi 3 was a ditch that flows into the sea. Sedi 2 showed higher activity concentrations than the reference, the radioactivity in this sample most likely traces back to the lanthanide pile. Before the site was remediated, the lanthanide pile was exposed, and dust could have been transported from the pile into the ditches where it was either transported into the sea or settled on the bottom of the ditch. Of all the sediment sampling locations sedi 2 is the closest to the lanthanide pile.

Sediment sample sedi 4 was taken from the open pit mine. The sampling was done with a Limnos sediment sampler, but the sediment was so loose that it was impossible to slice by depth and was collected as three separate subsamples instead. Of these subsamples, sedi 4 B1 is the top fraction of the sediment sample, 4A is the middle fraction and B2 in the deepest fraction. As can be seen from Figure 23, in sedi 4 there is variation in the activity concentration of ^{238}U and ^{210}Pb, while the activity concentration of ^{226}Ra is constant. This suggest that the rate of sedimentation is greater for uranium compared to radium.

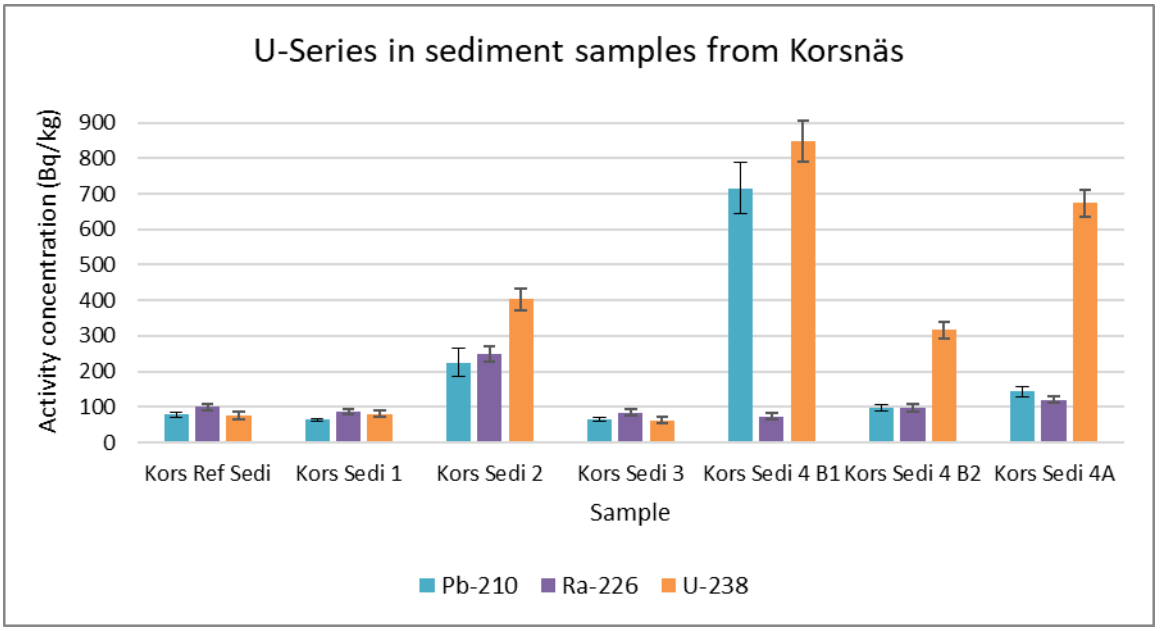

Figure 23 Activity concentrations of select uranium series radionuclides in sediment samples from Korsnäs. The error bars show 1 σ of uncertainty.

13.5.5 Core samples from Vihanti

The results for core 1B from Vihanti are shown in Figure 24. As the figure shows, the uranium series is not in equilibrium, however throughout most of the core the activity concentrations follow the same pattern but differ in magnitude. In the first 12 cm the activity concentration of ^{226}Ra is higher than ^{238}U, and after 15 cm the activity concentrations differ only slightly. The region with the higher concentration of radium compared to uranium corresponds with a color change seen in the core. The first 12 cm are light brown after which the color changes to gray. Changes in color often indicate a change in the redox state of, for example, iron. The conditions in the first 12 cm appear to be favorable for partial mobilization of uranium. The color change and the observed mobilization of uranium hint at oxidizing conditions in the upper parts and more reducing conditions in the bottom parts. Porewater samples taken from core 1B at depths of 9, 19 and 29 cm show uranium concentrations from 34 µg/l to 44 µg/l which are consistent with results of water samples from the closest ditch.

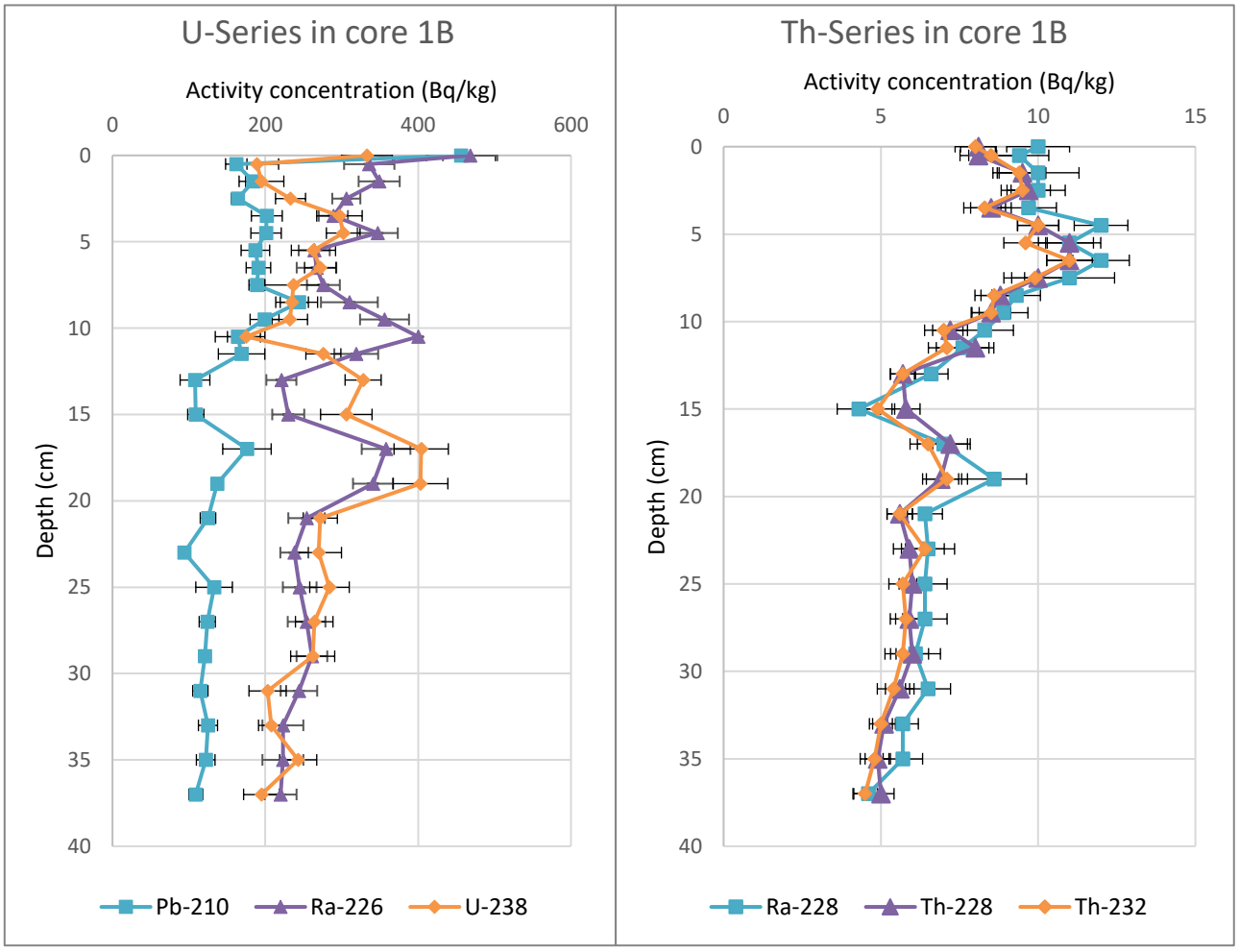

Figure 24 Plots of depth and activity concentration of uranium series radionuclides (left) and thorium series radionuclides (right) in core sample core 1B (Vihanti). The error bars show 1 σ of uncertainty.

The thorium series radionuclides in core 1B show no evidence of disequilibrium and their activity concentrations are very low. A slight downward trend can be seen for these three radionuclides.

Activity concentrations of uranium and thorium series radionuclides throughout core 2B are plotted in Figure 25, which shows that the uranium series is not in equilibrium. Two clear peaks in ^{238}U activity concentration can be seen in the figure at depths of 3 cm and 10 cm. The depths of these peaks coincide with depths at which the color of the core changed. At 3 cm the color was observed to change slightly from yellowish brown to a more grayish brown. At 10 cm the color had changed to almost completely gray. The observed peaks could be formed by uranium leaching downward from the layers above. The uranium is then retained in one layer due to a change in redox conditions or strong adsorbing material. Porewater samples taken at 16 and 26 cm along the core show uranium concentrations of 62 µg/l and 53 µg/l, which are again consistent with the closest water sample.

The results for the thorium series in core 2B show no evidence of disequilibrium. The activity concentrations are low, like in sample core 1B.

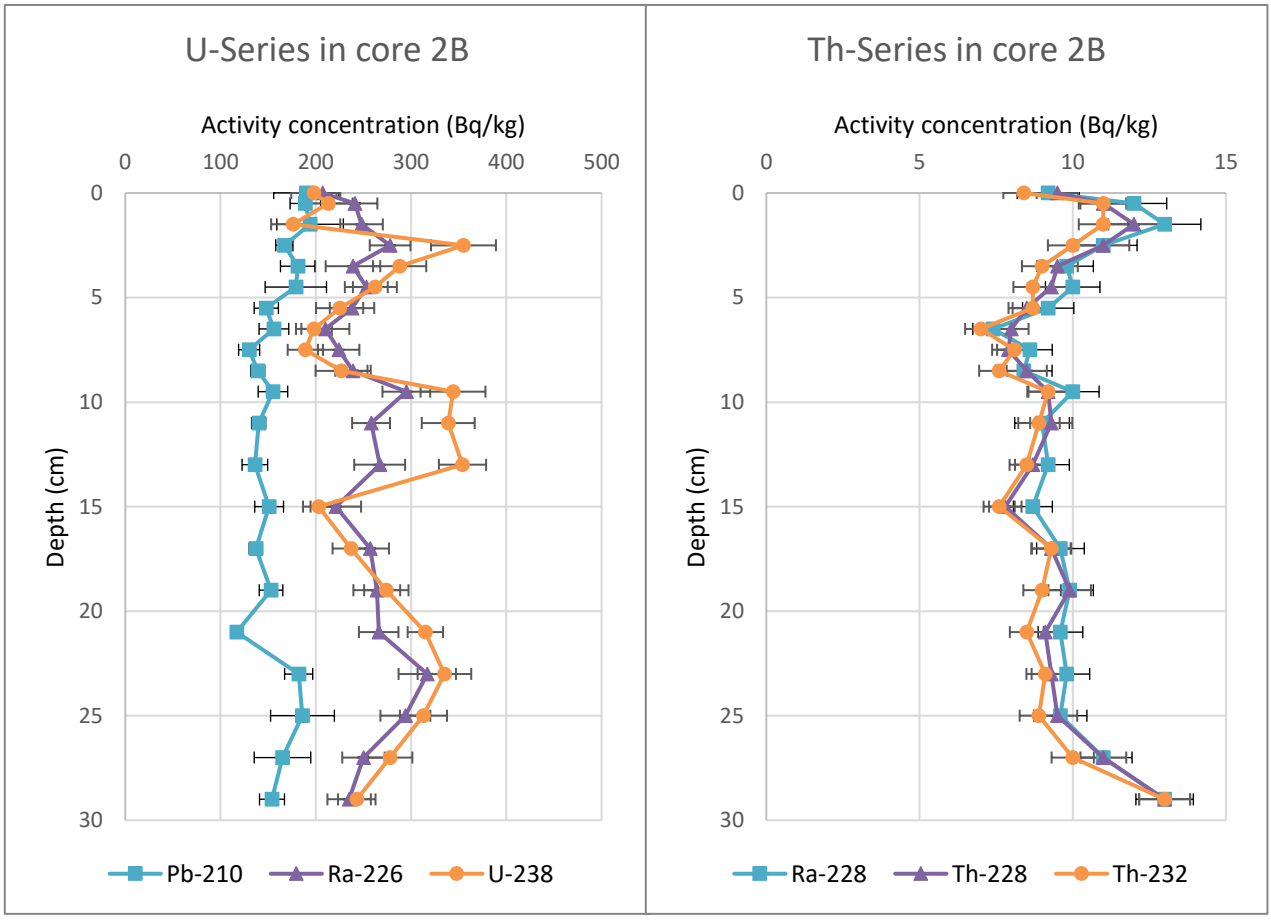

Figure 25 Plots of depth and activity concentration of uranium series radionuclides (left) and thorium series radionuclides (right) in core sample Core 2B (Vihanti). The error bars show 1 σ of uncertainty.

Figure 26 shows the activity concentration of uranium and thorium series radionuclides in sample Core 3B. In this sample the activity concentration of ^{238}U was below the minimum detectable activity throughout the core. Both an increase in uranium series radionuclides and a decrease in thorium series radionuclides can be seen at 10 cm. This suggests that the matrix changes, since it is unlikely that thorium would be mobilized more efficiently than radium as thorium is known to be very immobile (Lehto and Hou, 2011) The change in both series' activity concentrations coincides well with the depth at which a color change is seen from brown to a rust-like reddish brown. Despite the low pH of the core the thorium series seems to be in equilibrium.

The absence of ^{238}U coupled with the low pH that was measured from both the ditch near the sample and the core sample itself suggest that uranium has been mobilized from the sample. The porewater samples taken from depths of 15 and 25 cm show uranium concentrations of around 109 µg/l and 489 µg/l, which are much higher than in the other cores, these numbers support the idea of uranium

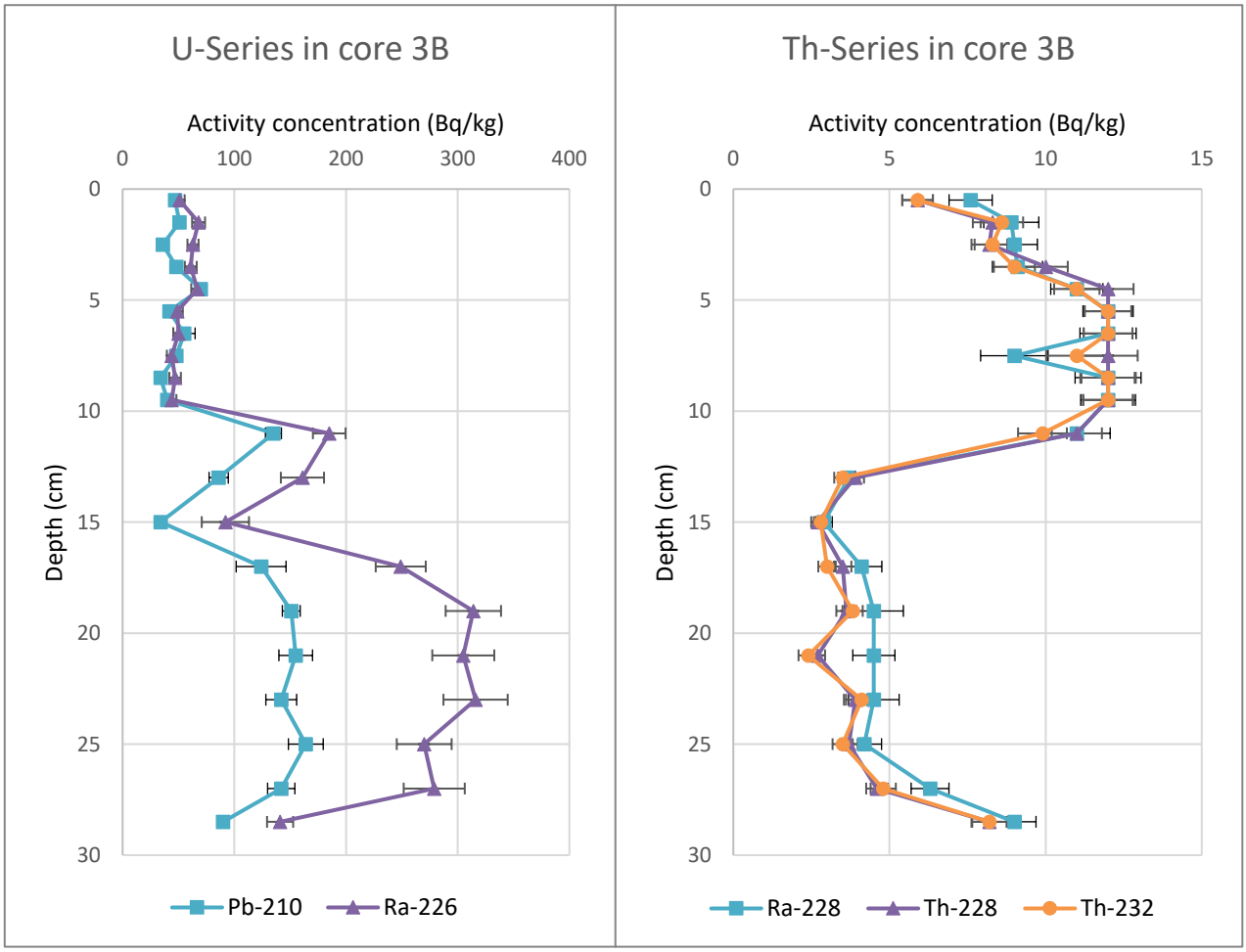

Figure 26 Plots of depth and activity concentration of uranium series radionuclides (left) and thorium series radionuclides (right) in core sample Core 3B (Vihanti). The activity concentration of U-238 was lower than the minimum detectable activity and therefore only Pb and Ra are plotted in the figure on the left. The error bars show 1 σ of uncertainty.

mobilization. Very high concentrations of other elements are seen in these porewater samples as well; high concentrations of dissolved metals are commonly associated with AMD (Lottermoser, 2007b). XRF analysis of the core yielded a uranium concentration of 6 ppm for slice 4-5 cm, while the other slices from the same core (16-18 cm and 24-26 cm) had uranium concentrations below the limit of detection (3.64 ppm). Sulfide oxidation (mainly pyrite) in this waste has created an acidic environment where elements from the waste are mobilized. Mineral dissolution has been shown to release uranium into solution in low pH (Liu et al., 2017), and similar mobilization of uranium (and other elements) from mine wastes under AMD conditions has been reported in the past (Lottermoser and Ashley, 2005).

13.5.6 Core samples from Korsnäs

The activity concentrations of uranium and thorium series radionuclides in sample core 1A from Korsnäs are plotted in Figure 27. After the first 5 cm the activity concentrations of ^{238}U and ^{226}Ra are the same magnitude and follow the same patterns. Activity concentrations of thorium series

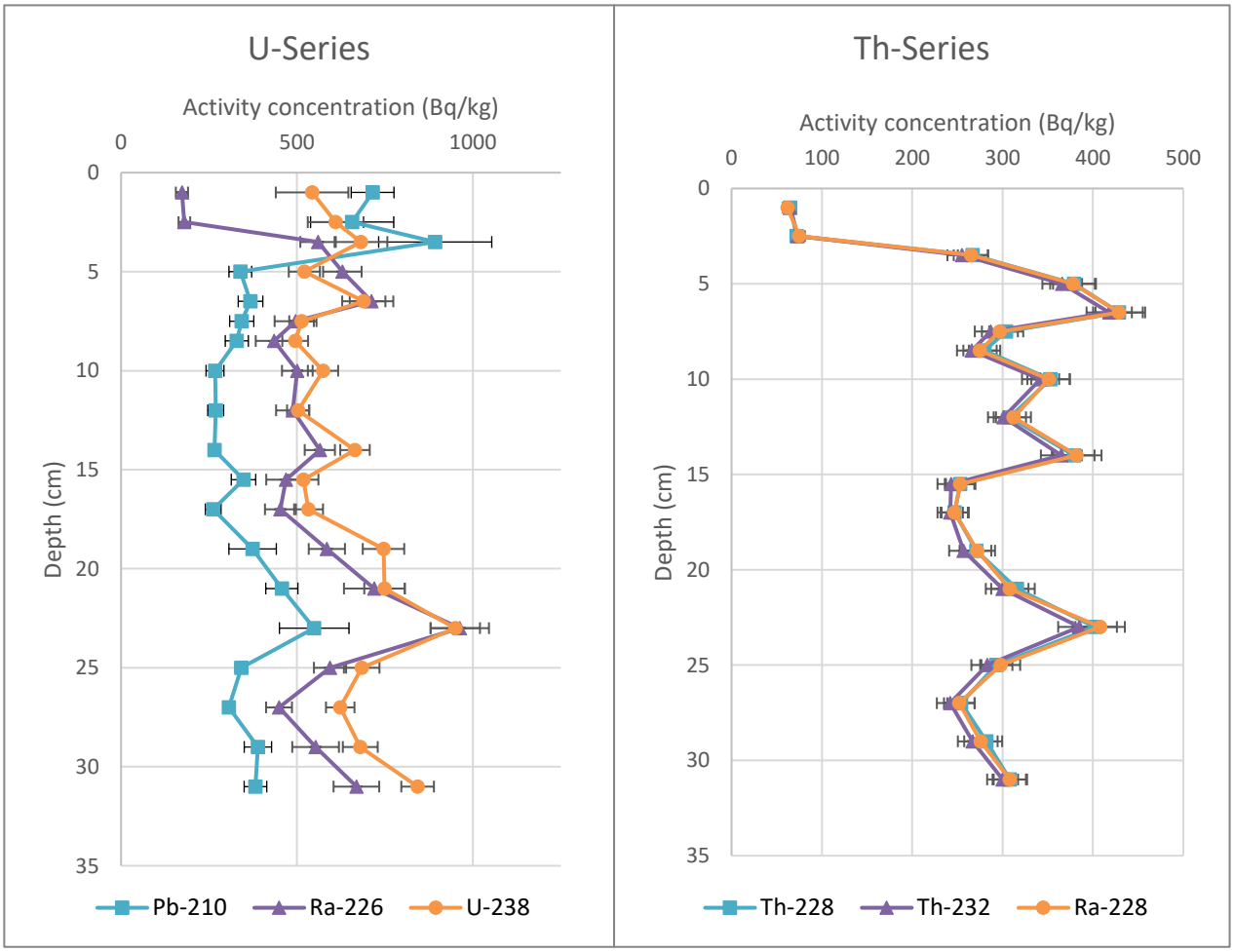

Figure 27 Plots of depth and activity concentration of uranium series radionuclides (left) and thorium series radionuclides (right) in core sample Core 1A (Korsnäs). The error bars show 1 σ of uncertainty.

radionuclides rise rapidly in the first 5 cm, as can be seen from Figure 27., after which the activity concentrations fluctuate but remain relatively high. The rise in activity coincides with the end of the organic layer. The activity concentrations of both series are high compared to typical values found in soils (UNSCEAR, 2008). Core 1A consists of tailings from the waste pile and as can be seen from the figure below the waste shows no signs of major disturbances.

Figure 28 shows the variation of activity concentration of the uranium and thorium series with depth in sample core 2A from Korsnäs and Figure 29 show the core prior to sectioning. The maximum activity concentrations found in this sample are among the highest found in this work. Two distinct peaks, one for uranium and one for radium, can be seen in the uranium series located around 5 cm apart. The peak of ^{226}Ra is at the depth where in Figure 29 the yellowish clay-like material can be seen. The peak of ^{238}U can be seen at the depth of 14 cm, which corresponds with the change in layers, form a clay-like layer to an organic layer. Based on these results, it seems uranium is leaching from the waste into the organic layer below where it is more efficiently retained.

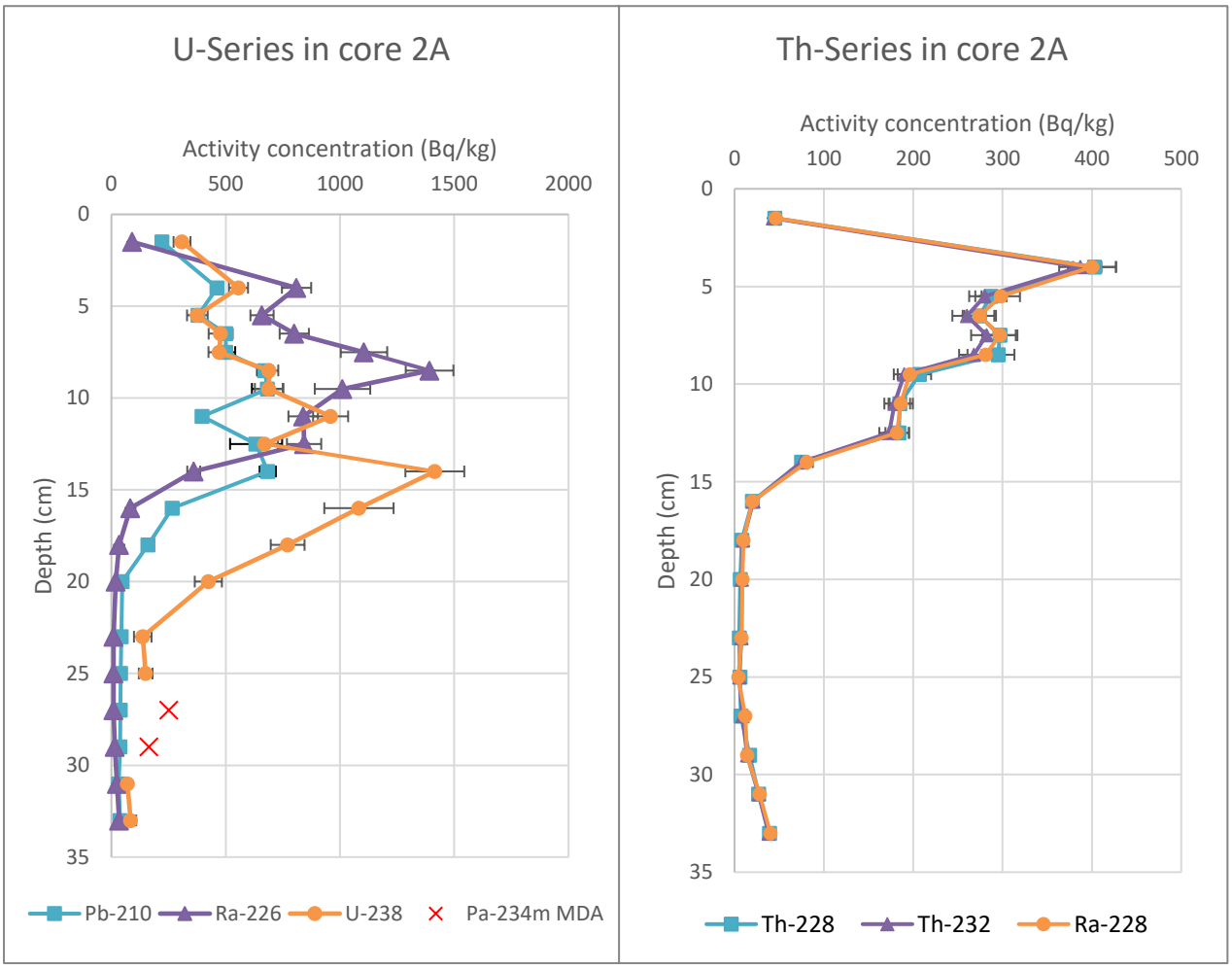

Figure 28 Plots of depth and activity concentration of uranium series radionuclides (left) and thorium series radionuclides (right) in core sample core 2A (Korsnäs). The red crosses in the uranium series plot are the minimum detectable activity values of Pa-234m from which the activity of U-238 is calculated. The error bars show 1 σ of uncertainty.

For all measured elements the actvity concentration drops quicly after the first peak and in the lower parts of the core the activity concetrations of all elements are at background levels. The thorium series seems to be in equilibrium and the depth of the peak matches the clay layer seen in Figure 29. Based on these results, it looks like the first layer is the cover layer placed during remediation followed by a layer of the enriched lanthanide, which is then followed by the original soil of the site. The assumed original soil shows two layers an organic layer and a sandy layer, which is seen at the very bottom of the core in Figure 29.

Figure 29 Picture of Core 2A before sectioning. The white arrow points from the top to the bottom. The length of the core is approximately 34 cm.

The main lanthanide carrying minerals reported in Korsnäs are monazite, apatite ($Ca_5(PO_4)_3(OH,F,Cl)_2$), and allanite ($((Ce,Ca,Y,La)_2(Al,Fe^{3+})_3(SiO_4)_3(OH)$), out of these three minerals apatite has been reported to contain the highest concentrations of uranium and thorium, while allanite and monazite contained around the same concentrations of uranium and thorium (Papunen and Lindsjö, 1972). Qualitative SR-XRPD analyses done on a sample from the lanthanide pile (NORM 1) show that the waste consists of approximately 9.6% monazite-(Ce) ($CePO_4$) and 8.2% hydroxylapatite, while allanite was not identified in the sample. It is reasonable to assume that the layer of the waste found in core 2A consists of a similar material.

The shapes of the curves of ^{226}Ra and ^{238}U are similar but uranium seems to have shifted downwards in the core, implying mobilization of uranium. Experiments have shown that leaching of uranium from monazite (Eyal and Olander, 1990; Oelkers and Poitrasson, 2002) and apatite (Köhler et al., 2005) is slow, but possible. Furthermore, the lanthanide pile has been exposed to the elements for

many years as the mine closed in 1972 and remediation was completed in 1998 (Markkanen, 1998), so it is safe to say that the pile has been exposed for at least 25 years, probably longer since it is unlikely that the pile was covered during production. Weathering of calcite in the pile could release carbonate into the pore solution, which can increase the mobility of uranium due to the formation of stable uranium carbonate complexes (Gunten, 1996). A sample from the lanthanide pile was measured qualitatively with SR-XRPD to contain approximately 9.4% calcite. Sulfuric acid (0.5% solution) was sprayed on the pile to promote the formation of a gypsum layer to prevent dust from spreading (Markkanen, 1992). The acid might have, at least on the top layers of the waste, increased the rate of weathering and mobilization of elements, thus weathering of the waste is not entirely natural.

In apatites uranium has been found in oxidation states of (IV) and (VI), in varying ratios. (Clarke and Altschuler, 1958), while in monazites the oxidation state of uranium has been reported as mainly (IV) (Ervanne, 2004). Based on this information, uranium has likely been released more readily from the apatite in the waste. However, this does not rule out weathering and subsequent oxidation and mobilization of U(IV) from, both, the apatite and the monazite.

The uranium appears to immobilize once it meets the organic layer at the depth of around 15 cm, which is most likely due to complexation with organic matter, such as humic acids, in the soil (Lehto and Hou, 2011; Zhang et al., 2020). Increasingly reducing conditions, however, may also immobilize the uranium by reducing it to U(IV). In soils uranium is known to be reduced by abiotic, biotic and coupled abiotic-biotic pathways from U(VI) to U(IV) forming crystalline and non-crystalline U(IV) depending on the pathway (Bernier-Latmani et al., 2010). The reduced species can be reoxidized and mobilized by changing conditions, for example intrusion of water containing dissolved oxygen or NO_3^- could oxidize U(IV) to U(VI) (Moon et al., 2007).

Full immobilization is not observed in core 2A. Porewater samples taken at 10 cm, 20 cm and 30 cm were found to have uranium concentrations of around 180 µg/l, 1140 µg/l and 721 µg/l, respectively. The higher two concentrations correspond to lower activity concentrations in the solid phase than the lowest porewater concentration, implying that uranium is leaching downwards and being only partially immobilized in the organic layer. Dissolved oxygen in rainwater could reach these depths leading to partial remobilization of uranium.

14 Dose assessment

Two factors are considered to briefly asses the dose caused to a member of the public spending time on the sites, inhalation of dust and external radiation. The dose rate from external radiation was measured on site with a portable detector. Assessing the activity concentration in dust in the areas can be done by assuming the activity concentration in the first centimeters of the soil samples corresponds to the activity concentration in the dust. Since the activity concentration of ^{234m}Pa was under the limit of detection in some samples ^{238}U could not be measured in these samples. However, the activity of ^{238}U can be estimated in two ways. First, is to assume equilibrium with ^{226}Ra, which was measured, and the second is to assume that the ratio of ^{238}U and ^{235}U is in its natural state. Since some mobilization of uranium was seen in the sites, estimating the activity concentration of ^{238}U from ^{235}U is likely more accurate. The activity ratio of ^{238}U to ^{235}U in samples where the isotopic ratio is undisturbed is around 21.4455, so multiplying the measured activity concentration of ^{235}U with this number yields an estimate for ^{238}U activity concentration (Lehto and Hou, 2011).

14.1 Vihanti

The average background external dose rate was measured to be 0.02300 µSv/h in the old mining town, while on top of the waste pile the average dose was measured to be 0.05402 µSv/h. Soil 1, the only soil sample taken from atop the tailings pile, is assumed to represent the situation across the pile (albeit this is a large extrapolation). The 0-3 cm section of the soil represents the layer that is being raised as dust by wind so the activity concentration in this section is the activity concentration in the dust inhaled by a member of the public. The activity concentrations of measured radionuclides in 0-3 cm of soil 1 are presented in Table 6 below.

The doses from the inhalation of dust containing measured radionuclides can be calculated by equation 7 (BfS, 2011).

$$E = V_j * \sum_r C_{air,r} * g_{inh,r} * t_{Exp} \quad (7)$$

Where V_j is the average volume of air inhaled by an adult in an hour, 0.93 m^3/h, $C_{air,r}$ is the concentration of a given radionuclide r in air in Bq/m^3, $g_{inh,r,j}$ is the inhalation dose coefficient of radionuclide r for the reference person in Sv/Bq and t_{Exp} is the exposure time in h. The doses from the measured radionuclides have been calculated in Table 6. The Activity concentration of the

radionuclides in air as dust was calculated using a reference value for airborne particles $5*10^{-7}$ kg/m^3, by multiplying the activity concentrations in 0-3 cm of soil with this number (BfS, 2011).

Two scenarios are considered in the table below, one where a person takes a walk once a day around the path on top of the pile, and the other, where a person takes a walk on the path three times a day. These scenarios are plausible for someone living in the old mining town. The length of the path atop the tailings pile is 3.9 km, with an average walking pace of 5 km/h this means that the exposure time is then 0.78 h, or almost 47 minutes, for a single walk around the path. In a year this translates to 284.7 h for a single walk a day and for three walks a day this translates to 854.1 h.

Table 6 The activity concentrations of measured radionuclides in 0-3 cm of soil 1 and the values relevant for dose calculations. ^{238}U activity concentration is calculated from ^{235}U marked with *.

Radionuclide	U-235	U-238*	Ra-226	Pb-210	Th-232	Th-228	Ra-228
Activity concentration in soil [Bq/kg]	0.79	16.9	20.0	283.0	6.3	6.9	6.1
Activity concentration in air as dust [Bq/m^3]	3.95E-07	8.47E-06	1.00E-05	1.42E-04	3.15E-06	3.45E-06	3.05E-06
Inhalation dose coefficient [Sv/Bq]	3.10E-06	2.90E-06	3.50E-06	1.10E-06	2.50E-06	2.60E-06	4.00E-05
Dose, one walk per day [mSv]	3.24E-07	6.50E-06	9.27E-06	4.12E-05	2.09E-06	2.37E-06	3.23E-05
Dose, three walks per day [mSv]	9.73E-07	1.95E-05	2.78E-05	1.24E-04	6.26E-06	7.12E-06	9.69E-05
Total dose per year (one walk per day) [mSv]	**9.41E-05**						
Total dose per year (three walks per day) [mSv]	**2.82E-04**						

The calculated effective dose for a person who takes a walk on the waste pile every day is around 15.47 µSv/a from both external radiation and inhalation of dust without subtracting the background, with inhalation of dust contributing around 0.094 µSv/a. For the other scenario, the dose from the two is around 46.42 µSv/a, without a background subtraction. These numbers are well below the 0.1 mSv/a limit set for a member of the public, even without background corrections. In these calculations only a few of the radionuclides from the natural decay chains were considered but given that the contribution of dust inhalation to the total dose was so small it is unlikely that the numbers would change dramatically if more nuclides were included, as their activity concentrations are likely low as well.

A simple subtraction of background dose rate from the observed dose rate yields a background corrected dose rate of 0.03102 µSv/h for external radiation. Considering both the dose rate from external radiation and inhalation of dust a person would need to spend around 3190 h on top of the waste pile per year, or around 8.7 h a day, to receive a dose of 0,1 mSv/a.

14.2 Korsnäs

In Korsnäs the effective dose rate measured while atop the pile was on average 0.2477 µSv/h, while the dose rate on the ground near the pile was 0.1079 µSv/h. The length of the path on top of the waste pile in Korsnäs is around 1.2 km, which leads to an exposure time of 0.24 h assuming a walking speed of 5 km/h. If a person takes this walk daily the exposure time becomes 87.6 h per year and if the person takes three walks a day on top of the waste the exposure time becomes 262.8 h.

Soil 3 and core 1A were both taken from atop the waste pile in Korsnäs and can be used to estimate the average concentration of radionuclides in the top part of the waste that is being raised up as dust. The average activity concentration of radionuclides in the top layer calculated from these two samples is presented in Table 7 along with the doses calculated with equation 7. Once again, the activity concentration of dust is estimated with a reference value for airborne particles (see above).

Table 7 The average activity concentration in 0-2 cm of samples soil 3 and core 1A and the values relevant for dose calculations and the results.

Radionuclide	U-235	U-238	Ra-226	Pb-210	Th-232	Th-228	Ra-228
Activity concentration in soil [Bq/kg]	18.0	472.0	352.5	515.5	128.0	130.5	129.5
Activity concentration in air as dust [Bq/m^3]	9.00E-06	2.36E-04	1.76E-04	2.58E-04	6.40E-05	6.53E-05	6.48E-05
Inhalation dose coefficient [Sv/Bq]	3.10E-06	2.90E-06	3.50E-06	1.10E-06	2.50E-06	2.60E-06	4.00E-05
Dose, one walk per day [mSv]	2.27E-06	5.58E-05	5.03E-05	2.31E-05	1.30E-05	1.38E-05	2.11E-04
Dose, three walks per day [mSv]	6.82E-06	1.67E-04	1.51E-04	6.93E-05	3.91E-05	4.15E-05	6.33E-04

Total dose, one walk per day [mSv]	3.69E-04
Total dose, three walks per day [mSv]	1.11E-03

The total calculated doses are 22,07 µSv/a and 66,20 µSv/a for the shorter and longer exposure times respectively, without background corrections. The contributions of inhaled dust are 0,37 µSv/a for the shorter exposure time and 1,11 µSv/a for the longer. As with the Vihanti site the contribution of inhaled dust is small, and the total doses are well below the 0.1 mSv/a limit, even without a background correction.

Assuming the dose rate measured on the ground near the pile accurately represents the background dose rate, the background corrected dose rate becomes 0.1398 µSv/h. Considering also the dose from inhalation of dust, a person would have to spend around 694 h on top of the pile in a year to receive a dose of 0.1 mSv/a. This translates to around 1.9 h every day per year.

Higher dose rates were detected near the lanthanide pile, which is not surprising considering the activity concentrations found in this waste. The highest readings were around 0.5 µSv/h measured on the west side of the pile. The cover seems to be thinner in this one location than on top of the pile, since the dose rate was near background levels on top of the pile. While this location exhibits an elevated dose rate the location is not easily accessible nor are there any paths on or around the lanthanide pile. A person would have to stand in this one spot for 200 hours a year, around 0.55 h every day, to receive a dose of 0.1 mSv/a. Standing in such a spot for extended periods of time is very unlikely.

15 Conclusions

15.1 Vihanti

In Vihanti the covering of wastes seems to have adequately lowered the dose rate from external radiation to near background levels. As can be seen from the example calculations in section 14.1 a person would have to spend over a third of a year on the pile to receive a dose of 0.1 mSv/a. The abundant vegetation growing on the waste helps to prevent largescale spread of dust from the site. It is unlikely that significant amounts of dust from the waste pile make it into the nearby town, furthermore even on top of the waste the contribution from inhaled dust to the total calculated dose was very small. No concerning activity concentrations in soil, sediment or waste samples were detected with gamma spectroscopy from the Vihanti site.

On the south side of the waste pile a small area was found which seemed to contain tailings that were not covered. Clear signs of acid mine drainage were found in this location. These were: discoloration of water, sulfurous odors, low pH, high electrical conductivity, high concentration of dissolved metals

and presence of secondary minerals. These effects were localized to this one area, but they highlight the potential of the waste to generate AMD, if left exposed to the elements.

The ICP-MS results of the surface water samples from the site show concerning concentrations in two areas, (i) the area on the south side of the waste pile showing signs of AMD, and (ii) the ditch flowing away from the old mine shaft. The concentrations of contaminants drop with distance from these locations, so the effects appear to be localized. Outflowing water from the site does not show indications of largescale spread of contaminants from the site.

Two groundwater samples, P115 and P114, showed worse water quality than others taken from the site. P115 had high concentrations of metals, especially of concern are the high concentrations of cadmium and zinc. P114 was the only groundwater sample that had uranium concentrations over the Finnish drinking water limit. The nearest groundwater used for drinking water is located around 1.2 km away from the site.

Comparison of the data form this work and old works indicated that the conditions on the site are changing. One location that used to be acidic had turned neutral and one that used to be neutral had turned acidic. The waters coming from the old mine shaft also showed an increase in cadmium and zinc concentrations, compared to earlier years.

The main hazards of the Vihanti site are the oxidation of possible exposed wastes and the following release of contaminants, as well as the water originating from the old mine shaft. Based on the results in this work the effects of both are localized near their respective sources. The waste on the north side of the pile had a lower pH than the south side, so some oxidation may have happened in this part, it is uncertain, however, if it has happened before or after the waste was covered. Nonetheless, no evidence of largescale AMD was found in this work, so the cover layer seems to function as intended.

15.2 Korsnäs

In Korsnäs the main waste pile has not been covered as evident from the clearly higher dose rate of external radiation measured on top of the pile. Despite the lack of a cover layer, plentiful vegetation is growing on the waste reducing the potential for the spreading of dust. In section 14.2 it was calculated that a member of the public would have to spend around 1.9 h on top of the waste every day to receive a dose of 0.1 mSv/a. While it is certainly possible to spend that amount of time on top of the waste, it is unlikely that anyone actually is, given that the length of the path atop it is short. The cover of the lanthanide pile seems to be adequate and only one spot with higher dose rates was

detected. The lack of paths and thick vegetation on the pile means that no one is likely to spend time standing in this particular spot. The high dose rate on top of the main waste pile highlights the importance of a cover layer in reducing the dose rate from external radiation.

Acid mine drainage in Korsnäs is unlikely to occur. The waste samples analyzed showed no decreases in pH, nor did they contain major concentrations of pyrite. In addition, the waste contains abundant calcite, which can act as a buffer. No abnormal pH values were measured in Korsnäs in this work.

Gamma spectroscopy revealed that the lanthanide pile contained higher activity concentrations of all measured radionuclides compared to the main waste pile, with some evidence of mobilization of uranium in the lanthanide waste. Porewater samples from the waste and surface water samples near the waste indicate that uranium is leaching from the waste into the water phase. The concentration of uranium in the closest ditch to the pile drops rapidly as distance from the pile increases. The sediment samples from the same ditch show the same trend.

Water samples taken from different depths of the old open pit mine revealed that the manganese and uranium concentrations are significantly higher in the deeper parts of the pit. Indicating that these elements might be released from the mineralization on the surfaces of the pit. Higher uranium concentrations were detected in the ditch flowing out of the pit. The concentration drops rapidly as distance from the pit increases.

The main hazards of Korsnäs are the relatively high dose rate of the exposed main waste pile, potential leaching of radionuclides from the lanthanide pile and the spreading of uranium containing waters of the old open pit mine. The waters from the site are all released into the sea, so it is unlikely anyone would be exposed to the uranium containing waters by, for example, drinking the water. The nearest groundwater used for drinking water is located 2.4 km away from the site.

16 References

ABDELOUAS, A., 2006. Uranium Mill Tailings: Geochemistry, Mineralogy, and Environmental Impact. *Elements*, vol. 2, no. 6 [viewed 6.5.2019], pp. 335-341 DOI 10.2113/gselements.2.6.335.

AKCIL, A. and KOLDAS, S., 2006. Acid Mine Drainage (AMD): causes, treatment and case studies. *Journal of Cleaner Production*, vol. 14, no. 12, pp. 1139-1145. Available from: http://dx.doi.org/10.1016/j.jclepro.2004.09.006 CrossRef. ISSN 0959-6526. DOI 10.1016/j.jclepro.2004.09.006.

BERNIER-LATMANI, R., VEERAMANI, H., VECCHIA, E.D., JUNIER, P., LEZAMA-PACHECO, J.S., SUVOROVA, E.I., SHARP, J.O., WIGGINTON, N.S. and BARGAR, J.R., 2010. Non-uraninite products of microbial U (VI) reduction. *Environmental Science & Technology*, vol. 44, no. 24, pp. 9456-9462.

BfS., 2011. *Calculation Guide Mining: Calculation Guide for the Determination of Radiation Exposure due to Environmental Radioactivity Resulting from Mining.* Salzgitter: BfS, Sep 5,.

BILLINGE, S.J.L. and DINNEBIER, R.E., 2008. Principles of Powder Diffraction. In: S.J.L. BILLINGE and R.E. DINNEBIER eds., *Powder Diffraction: Theory and Practice* Cambridge: Royal Society of Chemistry.

BJELKEVIK, A., 2005. *Water cover closure design for tailings dams.* Luleå: Luleå tekniska universitet Luleå.

BONCZYK, M., 2018. Determination of 210Pb concentration in NORM waste – An application of the transmission method for self-attenuation corrections for gamma-ray spectrometry. *Radiation Physics and Chemistry*, vol. 148, pp. 1-4. Available from: http://dx.doi.org/10.1016/j.radphyschem.2018.02.011 ISSN 0969-806X. DOI 10.1016/j.radphyschem.2018.02.011.

CARBONE, C., DINELLI, E., MARESCOTTI, P., GASPAROTTO, G.and LUCCHETTI, G., 2013. *The role of AMD secondary minerals in controlling environmental pollution: Indications from bulk leaching tests* ISBN 0375-6742. DOI 10.1016/j.gexplo.2013.07.001.

CLARKE, R.S. and ALTSCHULER, Z.S., 1958. *Determination of the oxidation state of uranium in apatite and phosphorite deposits.* ISBN 0016-7037.

DOWDALL, M. and O'DEA, J., 2002. *226Ra/238U disequilibrium in an upland organic soil exhibiting elevated natural radioactivity.* ISBN 0265-931X.

EC., 2013. *Council Directive 2013/59/Euratom of 5 December 2013 laying down basic safety standards for protection against the dangers arising from exposure to ionising radiation, and repealing Directives 89/618/Euratom, 90/641/Euratom, 96/29/Euratom, 97/43/Euratom and 2003/122/Euratom.,* Dec 5,.

EC., 2008. *Directive 2008/105/EC of the European Parliament and of the Council of 16 December 2008 on environmental quality standards in the field of water policy, amending and subsequently repealing Council Directives 82/176/EEC, 83/513/EEC, 84/156/EEC, 84/491/EEC, 86/280/EEC andamending Directive 2000/60/EC of the European Parliament and of the Council.,* Dec 24,.

ERVANNE, H., 2004. *Oxidation State Analyses of Uranium with Emphasis on Chemical Speciation in Geological Media.* Helsingin yliopisto

EYAL, Y. and OLANDER, D.R., 1990. *Leaching of uranium and thorium from monazite: I. Initial leaching.* ISBN 0016-7037.

FULLER, A.J., LEARY, P., GRAY, N.D., DAVIES, H.S., MOSSELMANS, J.F.W., COX, F., ROBINSON, C.H., PITTMAN, J.K., MCCANN, C.M., MUIR, M., GRAHAM, M.C., UTSUNOMIYA, S., BOWER, W.R., MORRIS, K., SHAW, S., BOTS, P., LIVENS, F.R.and LAW, G.T.W., 2020. *Organic complexation of U(VI) in reducing soils at a natural analogue site: Implications for uranium transport.* ISBN 0045-6535.

GOZZO, F., 2012. Synchrotron X-Ray Powder Diffraction. In: *Uniting Electron Crystallography and Powder Diffraction* Dordrecht: Springer Netherlands ISBN 9400755791.

GTK., 2019. *Mineral Deposit Report: Vihanti.* Geologian tutkimuskeskus, Feb 13, [viewed 3.4.2019]. Available from: http://tupa.gtk.fi/karttasovellus/mdae/raportti/525_Vihanti.pdf.

GTK., 2018. *Mineral Deposit Report: Korsnäs.* Geologian tutkimuskeskus, Nov 7, [viewed 3.4.2019]. Available from: http://tupa.gtk.fi/karttasovellus/mdae/raportti/171_Korsn%C3%A4s.pdf.

GUNTEN, H.R.V., 1996. Uranium series disequilibrium and high thorium and radium enrichments in Karst formations. *Environmental Science and Technology*, vol. 30, no. 4. DOI 10.1021/es950473j.

IAEA., 2013. Management of NORM Residues. Vienna: International Atomic Energy Agency ISBN 978-92-0-142710-6.

IAEA., 2007. IAEA Safety Glossary. Vienna: International Atomic Energy Agency ISBN 92–0–100707–8.

IAEA., 2006. *Assessing the Need for Radiation Protection Measures in Work Involving Minerals and Raw Materials.* Vienna: International Atomic Energy Agency ISBN 92-0-107406-9.

IAEA., 2004. *Extent of Environmental Contamination by Naturally Occurring Radioactive Material (NORM) and Technological Options for Mitigation.* Austria: International Atomic Energy Agency ISBN 9201125038.

ISO., 2005. *ISO 10390:2005, Soil quality - Determination of pH.* Second ed. Switzerland: International Organization for Standardization, Feb 15, Available from: https://www.iso.org/standard/40879.html.

KATHREN, R.L., 1998. NORM sources and their origins. *Applied Radiation and Isotopes; Naturally Occurring Radioactive Material in the Environment*, vol. 49, no. 3 [viewed 22.3.2019], pp. 149-168. Available from: http://www.sciencedirect.com/science/article/pii/S0969804397002376 ISSN 0969-8043. DOI //doi.org/10.1016/S0969-8043(97)00237-6.

KÖHLER, S.J., HAROUIYA, N., CHAÏRAT, C.and OELKERS, E.H., 2005. *Experimental studies of REE fractionation during water–mineral interactions: REE release rates during apatite dissolution from pH 2.8 to 9.2.* ISBN 0009-2541. DOI 10.1016/j.chemgeo.2005.07.011.

KOSSOFF, D., DUBBIN, W.E., ALFREDSSON, M., EDWARDS, S.J., MACKLIN, M.G.and HUDSON-EDWARDS, K.A., 2014. *Mine tailings dams: Characteristics, failure, environmental impacts, and remediation.* Available from: http://www.sciencedirect.com/science/article/pii/S0883292714002212 ISBN 0883-2927. DOI //doi.org/10.1016/j.apgeochem.2014.09.010.

KUMPULAINEN, S., CARLSON, L.and RÄISÄNEN, M., 2007. *Seasonal variations of ochreous precipitates in mine effluents in Finland.* ISBN 0883-2927.

LAHERMO, P., TARVAINEN, T., HATAKKA, T., BACKMAN, B., JUNTUNEN, R., KORTELAINEN, N., LAKOMAA, T., NIKKARINEN, M., VESTERBACKA, P., VÄISÄNEN, U. and SUOMELA, P., 2002. *Tuhat Kaivoa – Suomen Kaivovesien Fysikaalis-kemiallinen Laatu Vuonna 1999.* Espoo.

LANDA, E.R., 2007. Naturally occurring radionuclides from industrial sources: characteristics and fate in the environment. *Radioactivity in the Environment*, vol. 10, pp. 211-237.

LAURI, L.S., POHJOLAINEN, E. and ÄIKÄS, O., 2010. *Selvitys Suomen kallioperän U-pitoisuudesta.* Rovaniemi: Geologian Tutkimuskeskus.

LEHTO, J. and HOU, X., 2011. *Chemistry and analysis of radionuclides: laboratory techniques and methodology.* Weinheim: Wiley-VCH [viewed 26.3.2019]. ISBN 3527632786 e-book.

LEMINEN, M., 2016. *Korsnäsin Lyijykaivos: Tutkimusraportti: Alustavat Sedimentti-, Pintavesi- ja Säteilytutkimukset.* Etelä-Pohjanmaa: Etelä-Pohjanmaan elinkeino-, liikenne- ja ympäristökeskus, Nov 11.

LEMMELÄ, H., 1982. *Vihannin Kaivosalueen Radioaktiivisuuden Perustilatutkimus 24. - 28.08.1981.* Helsinki: Säteilyturvallisuuslaitos, Apr 20.

LIU, B., PENG, T., SUN, H.and YUE, H., 2017a. *Release behavior of uranium in uranium mill tailings under environmental conditions.* ISBN 0265-931X.

LIU, B., PENG, T., SUN, H. and YUE, H., 2017b. Release behavior of uranium in uranium mill tailings under environmental conditions. *Journal of Environmental Radioactivity*, vol. 171 [viewed 8.5.2019], pp. 160-168. ISSN 0265-931X. DOI 10.1016/j.jenvrad.2017.02.016.

LOTTERMOSER, B.G. and ASHLEY, P.M., 2005. *Tailings dam seepage at the rehabilitated Mary Kathleen uranium mine, Australia.* ISBN 0375-6742.

LOTTERMOSER, B.G., 2007a. Tailings. In: B.G. LOTTERMOSER ed., *Mine Wastes: Characterization, Treatment, Environmental Impacts* Berlin, Heidelberg: Springer Berlin Heidelberg, pp. 153-181 ISBN 978-3-540-48630-5. DOI 10.1007/978-3-540-48630-5_4.

LOTTERMOSER, B.G., 2007b. Sulfidic Mine Wastes. In: B.G. LOTTERMOSER ed., *Mine Wastes: Characterization, Treatment, Environmental Impacts* Berlin, Heidelberg: Springer Berlin Heidelberg, pp. 33-89 ISBN 978-3-540-48630-5. DOI 10.1007/978-3-540-48630-5_2.

LOTTERMOSER, B.G., 2007c. Mine Water. In: B.G. LOTTERMOSER ed., *Mine Wastes: Characterization, Treatment, Environmental Impacts* Berlin, Heidelberg: Springer Berlin Heidelberg, pp. 91-152 ISBN 978-3-540-48630-5. DOI 10.1007/978-3-540-48630-5_3.

MARKKANEN, M., 1998. *Korsnäsin Lantanidirikastekasan Tarkastus.* Helsinki: Säteilyturvakeskus, Dec 3.

MARKKANEN, M., 1992a. *Korsnäsin Kaivosalueen Säteilyturvallisuus.* Helsinki: Säteilyturvakeskus, Jun 25.

MARKKANEN, M., 1992b. *Vihannin Kaivoksen Lopettamista Koskeva Jätehuoltosuunnitelma.* Helsinki: Säteilyturvakeskus, Jul 15.

MICHALIK, B., 2008. NORM impacts on the environment: An approach to complete environmental risk assessment using the example of areas contaminated due to mining activity. *Applied Radiation and Isotopes*, vol. 66, no. 11, pp. 1661-1665. Available from: http://www.sciencedirect.com/science/article/pii/S0969804308002388 ISSN 0969-8043. DOI //doi.org/10.1016/j.apradiso.2008.01.025.

MOON, H.S., KOMLOS, J. and JAFFÉ, P.R., 2007. Uranium Reoxidation in Previously Bioreduced Sediment by Dissolved Oxygen and Nitrate. *Environmental Science & Technology*, vol. 41, no. 13, pp. 4587-4592. ISSN 0013-936X. DOI 10.1021/es063063b.

OELKERS, E.H. and POITRASSON, F., 2002. *An experimental study of the dissolution stoichiometry and rates of a natural monazite as a function of temperature from 50 to 230 °C and pH from 1.5 to 10.* ISBN 0009-2541.

PAPUNEN, H. and LINDSJÖ, O., 1972. Apatite, Monazite and Allanite; Three Rare Earth Minerals from Korsnäs, Finland. *Bulletin of the Geological Society of Finland*, no. 44, pp. 123-129.

PELKONEN, K., 1992. *Vihannin Kaivoksen Loppuraportti.* Outokumpu: Outokumpu Finnmines Oy, May 20.

Pöyry Finland Oy., 2018. *Outokumpu Mining Oy Vihannin Kaivoksen Jälkitarkkailu Tarkkailutulosten Yhteenveto v. 2017.*, Feb 23.

SARRAZIN, P., CHIPERA, S., BISH, D., BLAKE, D. and VANIMAN, D., 2005. Vibrating sample holder for XRD analysis with minimal sample preparation. *International Centre for Diffraction Data, Advances in X–ray Analysis*, vol. 48, pp. 156-164.

Säteilyturvakeskus., 2019a. *Luonnon radioaktiivisia aineita sisältävästä näytteestä mitatun gammaspektrin analysointi.* STUK, Aug 8,.

Säteilyturvakeskus., 2019b. *Kalibroinnit.* STUK, Aug 8,.

SILLANPÄÄ, T., IKÄHEIMONEN, T.K., SALONEN, L., TAIPALE, T. and MUSTONEN, R., 1989. *Paukkajanvaaran vanhan uraanikaivos- ja rikastamoalueen ja sen ympäristön radioaktiivisuustutkimukset.* Helsinki: Säteilyturvakeskus ISBN 951-47-1993-X nidottu.

SMEDLEY, P.L. and KINNIBURGH, D.G., 2017. *Molybdenum in natural waters: A review of occurrence, distributions and controls.* ISBN 0883-2927.

STM/1352., 2015. *Sosiaali- ja terveysministeriön asetus talousveden laatuvaatimuksista ja valvontatutkimuksista.*, Nov 17.

STRAWN, D., BOHN, H.L. and O'CONNOR, G.A., 2015. *Soil chemistry.* Fourth edition ed. Chichester, West Sussex, UK ; Hoboken, NJ, USA: John Wiley & Sons, Ltd ISBN 9781118629208.

STREBL, F., GERZABEK, M., KIRCHNER, G., EHLKEN, S. and BOSSEW, P., 2009. Vertical Migration of Radionuclides in Undisturbed Soils. In: *Quantification of radionuclide transfer in terrestrial and freshwater environments for radiological assessments* Vienna: IAEA, pp. 103-117.

TIMONEN, V., 1991. *Korsnäsin Kaivosalueen Kunnostus.* Vaasa: Vaasan vesi- ja ympäristöpiiri.

TORNIVAARA, A., RÄISÄNEN, M.L., KOVALAINEN, H. and KAUPPI, S., 2018. *Suljettujen ja hylättyjen kaivosten kaivannaisjätealueiden jatkokartoitus (KAJAK II).* Helsinki: Finnish Environment Institute, Jun 11 ISBN 9789-521149306/17961726.

TUOVINEN, H., POHJOLAINEN, E., VESTERBACKA, D., KAKSONEN, K., VIRKANEN, J., SOLATIE, D., LEHTO, J. and READ, D., 2016. Release of radionuclides from waste rock and mill tailings at a former pilot uranium mine in eastern Finland. *Boreal Environment Research*, Feb 4, vol. 21, no. 5-6 [viewed 6.5.2019], pp. 471-480.

UNSCEAR., 2008. *Sources and Effects of Ionizing Radiation: United Nations Scientific Committee on the Effects of Atomic Radiation: UNSCEAR 2008 Report to the General Assembly, with Scientific Annexes.* New York: United Nations.

VAARAMAA, K., ARO, L., SOLATIE, D. and LEHTO, J., 2010. Distribution of 210Pb and 210Po in boreal forest soil. *Science of the Total Environment*, vol. 408, no. 24 [viewed 12.4.2019], pp. 6165-6171. Available from: http://www.sciencedirect.com/science/article/pii/S0048969710009654 ISSN 0048-9697. DOI //doi.org/10.1016/j.scitotenv.2010.09.004.

VERTA, M., KAUPPILA, T., LONDESBOROUGH, S., MANNIO, J., PORVARI, P., RASK, M., VUORI, K.and VUORINEN, P.J., 2010. *Metallien taustapitoisuudet ja haitallisten aineiden seuranta Suomen pintavesissä – Ehdotus laatunormidirektiivin toimeenpanosta.* Suomen ympäristökeskus ISBN 9789-521137792/17961726.

VIRTANEN, S., VAARAMAA, K.and LEHTO, J., 2013. *Fractionation of U, Th, Ra and Pb from boreal forest soils by sequential extractions.* ISBN 0883-2927.

WILLMOTT, P.R., MEISTER, D., LEAKE, S.J., LANGE, M., BERGAMASCHI, A., BÖGE, M., CALVI, M., CANCELLIERI, C., CASATI, N., CERVELLINO, A., CHEN, Q., DAVID, C., FLECHSIG, U., GOZZO, F., HENRICH, B., JÄGGI-SPIELMANN, S., JAKOB, B., KALICHAVA, I., KARVINEN, P., KREMPASKY, J., LÜDEKE, A., LÜSCHER, R., MAAG, S., QUITMANN, C., REINLE-SCHMITT, M., SCHMIDT, T., SCHMITT, B., STREUN, A., VARTIAINEN, I., VITINS, M., WANG, X. and WULLSCHLEGER, R., 2013. The Materials Science beamline upgrade at the Swiss Light Source. *Journal of Synchrotron Radiation*. 2013/07/16 ed., vol. 20, pp. 667-682. Available from: https://www.ncbi.nlm.nih.gov/pmc/articles/PMC3747948/ ISSN 1600-5775. DOI 10.1107/S0909049513018475.

ZHANG, Y., LV, J., DONG, X., FANG, Q., TAN, W., WU, X.and DENG, Q., 2020. *Influence on Uranium(VI) migration in soil by iron and manganese salts of humic acid: Mechanism and behavior*. ISBN 0269-7491.

17 Appendix

Appendix 1 pH results of groundwater samples from Vihanti. Measured with pH paper in the laboratory

Sample ID	pH
P106	5.5
P110	5.5
P113	5.5
P114	7.5
P115	4.0
P116	5.0
P117	5.5

Appendix 2 Results of all elements measured with XRF in select waste samples. Empty cells signify concentrations below the relevant detection limit.

Sample	Si	Ti	Al	Fe	Mn	Mg	Ca	Na	K	P	Ba	Cu
	(%)	(%)	(%)	(%)	(%)	(%)	(%)	(%)	(%)	(%)	(ppm)	(ppm)
Vihanti NORM 1	17.10	0.17	3.56	12.21	0.05	4.92	7.22	0.45	0.37	0.11	4066	732
Vihanti NORM 3	21.33	0.20	4.97	4.17	0.07	6.57	8.74	0.58	0.71	0.13	11880	380
Vihanti Core 3B 5-6 cm	25.44	0.26	4.38	10.00	0.02	0.87	1.41	1.63	1.58	0.02	1570	200
Vihanti Core 3B 16-18 cm	16.43	0.11	1.70	19.28	0.02	2.56	3.50	0.50	0.61	0.03	7624	839
Vihanti Core 3B 24-26 cm	20.17	0.09	1.94	4.70	0.03	3.17	8.30	0.53	0.51	0.01	10630	4769
Korsnäs NORM 1	17.30	0.17	5.60	4.49	0.12	5.45	5.54	0.36	2.17	1.78	8373	31
Korsnäs NORM 2	33.45	0.31	6.57	2.16	0.05	0.73	1.48	2.21	2.54	0.08	786	23
Korsnäs NORM 3	20.94	0.17	5.40	2.83	0.09	2.30	9.77	1.31	2.97	0.64	12360	44
Korsnäs NORM 4	22.49	0.19	5.88	2.59	0.08	1.72	9.06	1.34	3.33	0.65	11850	166
Korsnäs NORM 5	22.26	0.16	5.12	2.22	0.10	1.47	9.73	1.14	3.28	1.19	18620	170

Sample	Cr	Ni	Sr	Zn	Zr	Rb	Nb	Y	Ce	La	V	U
	(ppm)	(ppm)	(ppm)	(ppm)	(ppm)	(ppm)	(ppm)	(ppm)	(ppm)	(ppm)	(ppm)	(ppm)
Vihanti NORM 1	43	22	126	406	58	11		19			137	
Vihanti NORM 3	88	65	208	1962	81	20	4	23		21	160	26
Vihanti Core 3B 5-6 cm	63	31	181	181	205	51		12	30		49	6
Vihanti Core 3B 16-18 cm	56	39	136	538	54		4	11		12	63	
Vihanti Core 3B 24-26 cm	42	26	178	268	54			11		20	73	
Korsnäs NORM 1	268	115	1190	132	130	33	6	668	12700	5536	92	423
Korsnäs NORM 2	124	62	278	44	294	105	8	30	85	54	48	36
Korsnäs NORM 3	109	74	3896	170	113	71	7	116	1480	776	99	84
Korsnäs NORM 4	108	62	3434	157	132	99	10	101	1381	716	92	42
Korsnäs NORM 5	170	110	4770	204	151	92	10	153	2365	1221	86	38

Appendix 3 Results of field measurements of water samples from Vihanti and Korsnäs. Values for temperature (T), dissolved oxygen (DO), specific conductance (SPC), pH, and oxidation reduction potential (ORP) are shown.

Vihanti						
Sample Name	**T [°C]**	**DO [%]**	**DO [mg/l]**	**SPC [µS/cm]**	**pH**	**ORP [mV]**
Ref Water	17.8	30.6	2.85	40.6	4.83	93.4
Water 2A	18.8	103.4	9.42	1458	7.50	-52.4
Water 2B	21.3	106.0	9.20	1970	7.96	-76.9
Water 3	14.6	99.8	10.11	866	7.37	-43.8
Water 4	12.5	40.9	4.37	929	6.30	10.0
Water 5	16.6	99.0	9.50	1724	7.50	
Water 6	14.5		4.38	15.0	4.92	86.3
Water 7	12.9	89.2	9.42	948	6.87	
Water 8	13.7	19.0	1.90	1960	4.91	89.9
Water 9	14.9	101.3	10.23	76.00	5.45	59.0
Water 10	12.3	77.0	8.20	920	6.80	
Water 12	14.1	63.2		2641	7.13	
Water 15	16.6	98.1	9.22	2212	2.68	2078
Water 16	18.8	20.4	1.28	20041	2.10	244.7
Water 17	17.8	81.7		1775	7.60	
Water 18	19.8	107.0	9.70	1489	7.92	-74.4
Water 1 - 1 m	17.6	104.1	9.90	1791	7.39	-48.0

Korsnäs						
Sample Name	**T [°C]**	**DO [%]**	**DO [mg/l]**	**SPC [µS/cm]**	**pH**	**ORP [mV]**
Ref. Water	15.4	84.4	8.35	237	8.13	-21.7
Water 1	18.6	93.2	8.50	2421	7.81	9.8
Water 2	14.1	44.5	4.28	782	7.51	-318.7
Water 3	13.5	98.8	10.10	265	8.08	0.8
Water 5	15.6	41.2	4.08	102	6.90	72.9
Water 6	12.9	53.5	5.47	1519	7.05	-88.0
Water 7	12.5	24.5	2.57	104.6	6.60	-150.5
Water 8	13.6	101.2	10.50	232	7.64	81.6
Water 9	13.8	55.5	5.70	633	7.37	80.9
Water 10	17.9	31	2.87	1102	6.91	120.4
Water 4 - 1 m	18.9	97.7	9.01	2422	7.59	39.1
Water 4 - 5 m	9.1	101.2	11.42	6132	6.83	56.1
Water 4 - 10 m	6.8	24.8	2.95	6783	6.76	-93.8
Water 4 - 20 m	6.7	13	1.55	6776	6.69	-160.6

Appendix 4 pH results of measured solid samples. Two parallel samples were measured for each sample. Shaking times and settling times are also given for each sample.

Vihanti								
Sample	**Depth (cm)**	**pH 1**	**pH 2**	**Difference**	**T 1 [°C]**	**T 2 [°C]**	**Shaking time**	**Settling time**
Core 1B	4-5	7.20	7.35	0.15	22.0	22.1	58 min	1 h 37 min
Core 1B	8-9	7.39	7.42	0.03	22.0	22.1	58 min	1 h 37 min
Core 1B	14-16	7.42	7.39	0.03	22.0	22.0	58 min	1 h 37 min
Core 1B	32-34	7.34	7.35	0.01	22.2	22.1	58 min	1 h 37 min
Core 2B	1-2	7.35	7.24	0.11	22.4	22.2	55 min	3 h
Core 2B	5-6	7.00	7.15	0.15	22.5	22.4	55 min	3 h
Core 2B	12-14	7.39	7.44	0.05	22.4	22.4	55 min	3 h
Core 2B	28-30	7.74	7.63	0.11	22.5	22.5	55 min	3 h
Core 3B	4-5	2.47	2.49	0.02	22.1	22.0	58 min	1 h 37 min
Core 3B	16-18	2.44	2.43	0.01	22.1	22.0	58 min	1 h 37 min
Core 3B	24-26	2.59	2.59	0.00	22.0	22.0	58 min	1 h 37 min
NORM 1	25	3.23	3.22	0.01	21.9	21.9	50 min	1 h
NORM 3	60	7.42	7.42	0.00	22.0	22.1	50 min	1 h 5 min
Korsnäs								
Sample	**Depth (cm)**	**pH 1**	**pH 2**	**Difference**	**T 1 [°C]**	**T 2 [°C]**	**Shaking time**	**Settling time**
Core 1A	7-8	6.95	6.96	0.01	22.4	22.5	58 min	2 h 13 min
Core 1A	20-22	7.68	7.72	0.04	22.5	22.6	58 min	2 h 13 min
Core 1A	30-32	7.71	7.67	0.04	22.6	22.7	58 min	2 h 13 min
Core 2A	7-8	7.51	7.48	0.03	22.4	22.5	58 min	1 h 45 min
Core 2A	10-12	7.39	7.54	0.15	22.3	22.4	58 min	1 h 45 min
Core 2A	32-34	7.00	6.86	0.14	22.4	22.5	58 min	1 h 45 min
NORM 1B	10-20	6.95	6.89	0.06	21.9	21.9	50 min	1 h 5 min
NORM 1C	20-30	7.15	7.12	0.03	21.9	21.9	50 min	1 h 10 min
NORM 1D	30-35	6.74	6.75	0.01	22.0	22.0	50 min	1 h 10 min
NORM 2	30	5.53	5.51	0.02	22.0	22.1	50 min	1 h 10 min
NORM 3B	10-30	6.66	6.71	0.05	21.7	21.7	55 min	1 h 20 min
NORM 3C	30-40	7.59	7.61	0.02	21.9	21.8	55 min	1 h 35 min
NORM 4B	10-20	7.30	7.31	0.01	21.8	21.8	55 min	1 h 45 min
NORM 4C	20-25	7.55	7.54	0.01	21.8	21.8	55 min	1 h 45 min
NORM 4D	25-30	7.58	7.58	0.00	21.8	21.9	55 min	2 h
NORM 5B	5-20	6.91	6.94	0.03	21.8	21.9	55 min	2 h
NORM 5A	20-30	7.57	7.55	0.02	21.8	21.8	55 min	2 h 20

Appendix 5 Table of ICP-MS results obtained in this work along with the limit of quantification (LOQ) of each element, the relative uncertainty of each element (U %) and the uncertainty of each result. Empty cells signify concentrations below LOQ.

		27 Al [ppb]	±	unc.	28 Si [ppm]	±	unc.	31 P [ppb]	±	unc.	51 V [ppb]	±	unc.	52 Cr [ppb]	±	unc.	55 Mn [ppb]	±	unc.
LOQ 10σ	-	1.5			0.003			1			0.002			0.02			0.06		
U %	-	15			7			16			6			10			15		
Sample	**Sampling Site**	265	±	40	15.5	±	1.1	129	±	21	2.87	±	0.17	1.40	±	0.14	2157	±	324
Porewater 1- 10 cm	Korsnäs	45.9	±	6.9	17.2	±	1.2	79.7	±	12.8	1.19	±	0.07	1.15	±	0.12	4134	±	620
Porewater 2- 10 cm	Korsnäs	70.4	±	10.6	39.6	±	2.8	151	±	24	1.22	±	0.07	1.28	±	0.13	11945	±	1792
Porewater 2- 20 cm	Korsnäs	49.8	±	7.5	28.7	±	2.0	119	±	19	1.02	±	0.06	1.11	±	0.11	7814	±	1172
Porewater 2- 30 cm	Korsnäs				8.56	±	0.6	66.9	±	10.7	0.024	±	0.001	0.069	±	0.007	8887	±	1333
Water 10A	Korsnäs				9.76	±	0.68	73.8	±	11.8	0.031	±	0.002	0.082	±	0.008	10672	±	1601
Water 10B	Korsnäs	11.9	±	1.8	1.74	±	0.12	18.8	±	3.0	0.120	±	0.007	0.136	±	0.014	14.8	±	2.2
Water 1A	Korsnäs	14.8	±	2.2	2.00	±	0.14	24.7	±	4.0	0.139	±	0.008	0.179	±	0.018	17.3	±	2.6
Water 1B	Korsnäs	95.2	±	14.3	2.89	±	0.2	199	±	32	0.607	±	0.036	0.900	±	0.090	99.6	±	14.9
Water 2A	Korsnäs	121	±	18	3.52	±	0.25	227	±	36	0.792	±	0.047	1.12	±	0.11	133	±	20
Water 2B	Korsnäs	575	±	86	14.5	±	1.0	254	±	41	1.54	±	0.09	1.45	±	0.15	149	±	22
Water 3A	Korsnäs	625	±	94	13.4	±	0.9	206	±	33	1.27	±	0.08	1.27	±	0.13	137	±	21
Water 3B	Korsnäs	16.6	±	2.5	18.8	±	1.3	37.0	±	5.9	1.92	±	0.12	1.16	±	0.12	11731	±	1760
Water 4 - 10 m - A	Korsnäs	15.2	±	2.3	18.2	±	1.3	40.3	±	6.5	1.89	±	0.11	1.12	±	0.11	11330	±	1700
Water 4 - 10 m - B	Korsnäs	13.6	±	2.0	2.01	±	0.14	22.9	±	3.7	0.139	±	0.008	0.150	±	0.015	18.4	±	2.8
Water 4 - 1 m - A	Korsnäs	20.8	±	3.1	2.38	±	0.17	29.8	±	4.8	0.166	±	0.010	0.205	±	0.020	20.9	±	3.1
Water 4 - 1 m - B	Korsnäs	22.7	±	3.4	19.1	±	1.3	203	±	33	2.01	±	0.12	1.15	±	0.12	10768	±	1615
Water 4 - 20 m - A	Korsnäs	16.6	±	2.5	19.7	±	1.4	192	±	31	2.02	±	0.12	1.10	±	0.11	10750	±	1612
Water 4 - 20 m - B	Korsnäs	20.7	±	3.1	19.1	±	1.3	211	±	34	2.00	±	0.12	1.20	±	0.12	10413	±	1562
Water 4 - 25 m - A	Korsnäs	19.9	±	3.0	22.4	±	1.6	173	±	28	2.37	±	0.14	1.34	±	0.13	10771	±	1616
Water 4 - 25 m - B	Korsnäs	3.4	±	0.51	13.8	±	1.0	33.7	±	5.4	0.112	±	0.007	0.227	±	0.023	9631	±	1445
Water 4 - 5 m - A	Korsnäs	5.23	±	0.79	14.0	±	1.0	34.0	±	5.4	0.110	±	0.007	0.242	±	0.024	10594	±	1589
Water 4 - 5 m - B	Korsnäs	4.98	±	0.75	0.828	±	0.058	27.9	±	4.5	0.049	±	0.003	0.100	±	0.010	83.6	±	12.5
Water 5A	Korsnäs	5.55	±	0.83	0.875	±	0.061	26.4	±	4.2	0.053	±	0.003	0.058	±	0.006	89.1	±	13.4
Water 5B	Korsnäs	46.3	±	7.0	16.3	±	1.1	154	±	25	0.947	±	0.057	0.88	±	0.088	397	±	60

Sample	Sampling Site	27 Al [ppb]	±	unc.	28 Si [ppm]	±	unc.	31 P [ppb]	±	unc.	51 V [ppb]	±	unc.	52 Cr [ppb]	±	unc.	55 Mn [ppb]	±	unc.
Water 6A	Korsnäs	50.4	±	7.6	16.9	±	1.2	173	±	28	1.01	±	0.06	0.961	±	0.096	431	±	65
Water 6B	Korsnäs	1506	±	226	22.7	±	1.6	175	±	28	3.48	±	0.21	5.29	±	0.53	216	±	32
Water 7A	Korsnäs	1215	±	182	17.1	±	1.2	139	±	22	2.61	±	0.16	3.90	±	0.39	161	±	24
Water 7B	Korsnäs	514	±	77	19.0	±	1.3	235	±	38	2.04	±	0.12	2.07	±	0.21	216	±	33
Water 8A	Korsnäs	558	±	84	17.9	±	1.3	238	±	38	2.18	±	0.13	2.05	±	0.21	207	±	31
Water 8B	Korsnäs	428	±	64	16.3	±	1.1	99.5	±	15.9	1.93	±	0.12	1.94	±	0.19	213	±	32
Water 9A	Korsnäs	398	±	60	15.9	±	1.1	100	±	16	1.80	±	0.11	1.84	±	0.18	204	±	31
Water 9B	Korsnäs	418	±	63	9.82	±	0.69	38.3	±	6.1	1.21	±	0.07	1.33	±	0.13	54.1	±	8.1
Ref. Water A	Korsnäs	401	±	60	9.95	±	0.70	39.1	±	6.3	1.28	±	0.08	1.33	±	0.13	54.1	±	8.1
Ref. Water B	Korsnäs				24.2	±	1.7	6.58	±	1.05	0.040	±	0.002	0.184	±	0.018	1397	±	209
P106A	Vihanti				25.2	±	1.8	7.76	±	1.24	0.041	±	0.002	0.182	±	0.018	1588	±	238
P106B	Vihanti				16.1	±	1.1	54.9	±	8.8	0.035	±	0.002	0.118	±	0.012	6697	±	1005
P110A	Vihanti				16.1	±	1.1	48.4	±	7.7	0.035	±	0.002	0.120	±	0.012	7742	±	1161
P110B	Vihanti				6.91	±	0.48	32.5	±	5.2	0.054	±	0.003				334	±	50
P113A	Vihanti	3.52	±	0.53	6.99	±	0.49	38.1	±	6.1	0.056	±	0.003	0.039	±	0.004	338	±	51
P113B	Vihanti	3.90	±	0.59	17.6	±	1.2	38.1	±	6.1	0.411	±	0.025	1.63	±	0.16	2041	±	306
P114A	Vihanti	252	±	38	17.4	±	1.2	35.9	±	5.8	0.387	±	0.023	1.40	±	0.14	2364	±	355
P114B	Vihanti	4422	±	663	41.2	±	2.9	34.6	±	5.5	0.098	±	0.006	1.33	±	0.13	2273	±	341
P115A	Vihanti	4227	±	634	19.0	±	1.3	16.9	±	2.7	0.039	±	0.002	0.578	±	0.058	2204	±	331
P115B	Vihanti				22.7	±	1.6	11.5	±	1.9	0.040	±	0.002	0.102	±	0.010	804	±	121
P116A	Vihanti				25.7	±	1.8	15.9	±	2.5	0.042	±	0.002	0.102	±	0.010	953	±	143
P116B	Vihanti				25.7	±	1.8	15.9	±	2.5	0.042	±	0.002	0.102	±	0.010	953	±	143
P117A	Vihanti	3.67	±	0.55	24.9	±	1.7	15.8	±	2.5	0.026	±	0.002	0.151	±	0.015	1279	±	192
P117B	Vihanti	3.88	±	0.58	25.1	±	1.8	14.2	±	2.3	0.026	±	0.002	0.171	±	0.017	1362	±	204
Porewater 1 - 9 cm	Vihanti	20.1	±	3.0	5.71	±	0.4	12.7	±	2.0	0.045	±	0.003	0.097	±	0.010	2.51	±	0.38
Porewater 1 -19 cm	Vihanti	10.2	±	1.5	13.8	±	1.0	28.9	±	4.6	0.047	±	0.003	0.653	±	0.065	1140	±	171
Porewater 1 - 29 cm	Vihanti	34.9	±	5.2	15.2	±	1.1	29.0	±	4.7	0.056	±	0.003	0.086	±	0.009	1430	±	215
Porewater 2 - 60 cm	Vihanti	33.2	±	5.0	44.6	±	3.1	176	±	28	0.132	±	0.008	0.437	±	0.044	2049	±	307
Porewater 2 - 30 cm	Vihanti	6380	±	957	28.7	±	2.0	119	±	19	0.560	±	0.034	0.360	±	0.036	6444	±	967

Sample	Sampling Site	27 Al [ppb]	±	unc.	28 Si [ppm]	±	unc.	31 P [ppb]	±	unc.	51 V [ppb]	±	unc.	52 Cr [ppb]	±	unc.	55 Mn [ppb]	±	unc.
Porewater 3 - 16 cm	Vihanti	12.4	±	1.9	14.6	±	1.0	46.6	±	7.5	0.082	±	0.005	0.071	±	0.007	1203	±	180
Porewater 3 - 26 cm	Vihanti	20.3	±	3.0	18.1	±	1.3	51.9	±	8.3	0.059	±	0.004	0.038	±	0.004	763	±	114
Porewater 3 - 36 cm	Vihanti	32.4	±	4.9	19.4	±	1.4	68.3	±	10.9	0.095	±	0.006	0.085	±	0.008	846	±	127
Porewater 4 - 15 cm	Vihanti	186000	±	28000	206	±	14	1527	±	244	403	±	24	383	±	38	11444	±	1717
Porewater 4 - 25 cm	Vihanti	603000	±	91000	196	±	14	16924	±	2708	2746	±	165	1312	±	131	23569	±	3535
Water 10A	Vihanti	3.06	±	0.46	5.38	±	0.38	27.8	±	4.5	0.029	±	0.002	0.100	±	0.01	18.8	±	2.8
Water 10B	Vihanti	2.49	±	0.37	5.17	±	0.36	16.7	±	2.7	0.027	±	0.002	0.043	±	0.004	18.9	±	2.8
Water 11A	Vihanti	10.7	±	1.6	1.64	±	0.12	19.5	±	3.1	0.049	±	0.003	1.07	±	0.11	2.51	±	0.38
Water 1 - 1 m - A	Vihanti	12.4	±	1.9	1.26	±	0.09	38.1	±	6.1	0.147	±	0.009	0.427	±	0.043	11.9	±	1.8
Water 11B	Vihanti	8.95	±	1.34	1.67	±	0.12	18.3	±	2.9	0.052	±	0.003	1.06	±	0.11	2.50	±	0.38
Water 1 - 1 m - B	Vihanti	10.9	±	1.6	1.29	±	0.09	54.5	±	8.7	0.161	±	0.010	0.447	±	0.045	12.9	±	1.9
Water 12A	Vihanti	12.8	±	1.9	6.74	±	0.47	40.7	±	6.5	0.052	±	0.003	0.460	±	0.046	169	±	25
Water 1 - 2m - A	Vihanti	11.6	±	1.7	1.31	±	0.09	42.1	±	6.7	0.158	±	0.010	0.447	±	0.045	11.7	±	1.8
Water 12B	Vihanti	14.8	±	2.2	6.27	±	0.44	38.1	±	6.1	0.050	±	0.003	0.406	±	0.041	160	±	24
Water 1 - 2m - B	Vihanti	8.56	±	1.28	1.21	±	0.09	37.5	±	6.0	0.139	±	0.008	0.391	±	0.039	10.9	±	1.6
Water 15A	Vihanti	24.6	±	3.7	11.2	±	0.8	21.8	±	3.5	0.516	±	0.031	0.818	±	0.082	857	±	129
Water 15B	Vihanti	26.0	±	3.9	11.6	±	0.8	24.0	±	3.8	0.500	±	0.030	0.801	±	0.080	732	±	110
Water 16A	Vihanti	232000	±	35000	128	±	9	5425	±	868	790	±	47	540	±	54	10768	±	1615
Water 16B	Vihanti	221000	±	33000	106	±	7	4214	±	674	643	±	39	424	±	42	8539	±	1281
Water 17A	Vihanti	3.08	±	0.46	1.34	±	0.09	28.7	±	4.6	0.081	±	0.005	0.411	±	0.041	8.86	±	1.33
Water 17B	Vihanti	4.04	±	0.61	1.33	±	0.09	30.4	±	4.9	0.083	±	0.005	0.359	±	0.036	7.77	±	1.17
Water 18A	Vihanti				6.88	±	0.48	30.0	±	4.8	0.022	±	0.001				333	±	50
Water 18B	Vihanti	3.14	±	0.47	7.20	±	0.5	24.7	±	4.0	0.028	±	0.002				350	±	53
Water 2A -A	Vihanti	21.3	±	3.2	4.40	±	0.31	28.9	±	4.6	0.083	±	0.005	0.098	±	0.010	155	±	23
Water 2A -B	Vihanti	21.9	±	3.3	3.89	±	0.27	25.1	±	4.0	0.079	±	0.005	0.103	±	0.010	143	±	21
Water 2B -A	Vihanti	8.19	±	1.23	5.86	±	0.41	37.0	±	5.9	0.016	±	0.001	0.035	±	0.004	183	±	28
Water 2B -B	Vihanti	8.27	±	1.24	6.25	±	0.44	33.6	±	5.4	0.020	±	0.001				203	±	30
Water 3A	Vihanti	16.3	±	2.5	12.3	±	0.9	21.3	±	3.4	0.277	±	0.017	0.585	±	0.059	633	±	95
Water 3B	Vihanti	11.4	±	1.7	12.2	±	0.9	24.5	±	3.9	0.220	±	0.013	0.606	±	0.061	647	±	97

Sample	Sampling Site	27 Al [ppb]	±	unc.	28 Si [ppm]	±	unc.	31 P [ppb]	±	unc.	51 V [ppb]	±	unc.	52 Cr [ppb]	±	unc.	55 Mn [ppb]	±	unc.
Water 4A	Vihanti	140	±	21	11.9	±	0.8	31.5	±	5.0	0.250	±	0.015	1.40	±	0.14	110	±	17
Water 4B	Vihanti	139	±	21	11.5	±	0.8	34.5	±	5.5	0.247	±	0.015	1.41	±	0.14	108	±	16
Water 5A	Vihanti	41.7	±	6.3	8.30	±	0.58	52.9	±	8.5	0.907	±	0.054	2.80	±	0.28	1260	±	189
Water 5B	Vihanti	45.3	±	6.8	8.26	±	0.58	53.6	±	8.6	0.898	±	0.054	2.96	±	0.30	1240	±	186
Water 6A	Vihanti	233	±	35	19.6	±	1.4	33.9	±	5.4	0.029	±	0.002	0.313	±	0.031	202	±	30
Water 6B	Vihanti	262	±	39	20.6	±	1.4	30.1	±	4.8	0.050	±	0.003	0.430	±	0.043	227	±	34
Water 7A	Vihanti	62.4	±	9.4	10.1	±	0.7	20.1	±	3.2	0.760	±	0.046	1.35	±	0.14	325	±	49
Water 7B	Vihanti	62.7	±	9.4	9.35	±	0.66	23.2	±	3.7	0.707	±	0.042	1.28	±	0.13	306	±	46
Water 8A	Vihanti	1587	±	238	15.8	±	1.1	32.2	±	5.2	0.055	±	0.003	0.527	±	0.053	1899	±	285
Water 8B	Vihanti	9383	±	1407	23.6	±	1.7	34.1	±	5.5	0.063	±	0.004	1.41	±	0.14	2244	±	337
Water 9A	Vihanti	1390	±	208	9.32	±	0.65	31.6	±	5.1	1.85	±	0.11	2.72	±	0.27	103	±	15
Water 9B	Vihanti	1331	±	200	9.16	±	0.64	30.3	±	4.8	1.82	±	0.11	2.66	±	0.27	102	±	15
Ref Water A	Vihanti	223	±	34	1.06	±	0.07	33.8	±	5.4	0.876	±	0.053	0.705	±	0.071	80.4	±	12.1
Ref Water B	Vihanti	315	±	47	1.05	±	0.07	29.4	±	4.7	0.883	±	0.053	0.793	±	0.079	81.0	±	12.2

Appendix 5 continues. Note that the elements have changed

		56 Fe [ppb]	±	unc.	59 Co [ppb]	±	unc.	60 Ni [ppb]	±	unc.	63 Cu [ppb]	±	unc.	66 Zn [ppb]	±	unc.	75 As [ppb]	±	unc.
LOQ 10σ		0.3			0.002			0.03			0.06			0.05			0.01		
U %		9			7			11			5			11			5		
Sample	**Sampling Site**																		
Porewater 1 - 10 cm	Korsnäs	4433	±	399	8.25	±	0.58	63.0	±	6.9	4.17	±	0.21	29.0	±	3.2	3.39	±	0.17
Porewater 2- 10 cm	Korsnäs	635	±	57	8.10	±	0.57	60.5	±	6.7	8.99	±	0.45	13.9	±	1.5	1.20	±	0.06
Porewater 2 -20 cm	Korsnäs	28026	±	2522	62.5	±	4.4	135	±	15	11.2	±	0.6	47.2	±	5.2	3.84	±	0.19
Porewater 2 - 30 cm	Korsnäs	78359	±	7052	35.7	±	2.5	63.2	±	7.0	3.28	±	0.16	19.2	±	2.1	3.60	±	0.18
Water 10A	Korsnäs	30104	±	2709	0.296	±	0.021	3.00	±	0.33	0.108	±	0.005	0.884	±	0.097	0.316	±	0.016
Water 10B	Korsnäs	36444	±	3280	0.341	±	0.024	3.41	±	0.38	0.141	±	0.007	1.04	±	0.11	0.365	±	0.018
Water 1A	Korsnäs	8.19	±	0.74	0.150	±	0.010	20.4	±	2.2	1.12	±	0.06	3.56	±	0.39	0.396	±	0.020

Sample	Sampling site	56 Fe [ppb]	±	unc.	59 Co [ppb]	±	unc.	60 Ni [ppb]	±	unc.	63 Cu [ppb]	±	unc.	66 Zn [ppb]	±	unc.	75 As [ppb]	±	unc.
Water 2A	Korsnäs	1338	±	120	0.722	±	0.051	21.6	±	2.4	1.63	±	0.08	3.19	±	0.35	0.646	±	0.032
Water 2B	Korsnäs	1194	±	107	0.96	±	0.067	24.0	±	2.6	1.91	±	0.10	4.57	±	0.50	0.775	±	0.039
Water 3A	Korsnäs	3009	±	271	2.88	±	0.20	21.5	±	2.4	5.90	±	0.30	14.1	±	1.6	0.870	±	0.044
Water 3B	Korsnäs	3112	±	280	2.54	±	0.18	18.8	±	2.1	5.29	±	0.26	13.8	±	1.5	0.799	±	0.040
Water 4 - 10 m - A	Korsnäs	41645	±	3748	1.00	±	0.07	3.89	±	0.43				1.27	±	0.14	0.434	±	0.022
Water 4 - 10 m - B	Korsnäs	39974	±	3598	0.961	±	0.067	3.76	±	0.41	0.289	±	0.014	1.41	±	0.16	0.421	±	0.021
Water 4 - 1 m - A	Korsnäs	7.23	±	0.65	0.186	±	0.013	23.5	±	2.6	2.71	±	0.14	2.73	±	0.30	0.483	±	0.024
Water 4 - 1 m - B	Korsnäs	12.5	±	1.1	0.216	±	0.015	24.2	±	2.7	3.06	±	0.15	3.00	±	0.33	0.527	±	0.026
Water 4 - 20 m - A	Korsnäs	28766	±	2589	0.381	±	0.027	3.19	±	0.35				0.797	±	0.088	0.468	±	0.023
Water 4 - 20 m - B	Korsnäs	36096	±	3249	0.389	±	0.027	3.24	±	0.36				1.05	±	0.12	0.453	±	0.023
Water 4 - 25 m - A	Korsnäs	31350	±	2821	0.423	±	0.03	3.36	±	0.37				1.83	±	0.20	0.461	±	0.023
Water 4 - 25 m - B	Korsnäs	37356	±	3362	0.498	±	0.035	3.83	±	0.42				0.725	±	0.08	0.528	±	0.026
Water 4 - 5 m - A	Korsnäs	12.4	±	1.1	3.36	±	0.24	40.4	±	4.4	1.12	±	0.06	8.94	±	0.98	0.386	±	0.019
Water 4 - 5 m - B	Korsnäs	12.6	±	1.1	3.41	±	0.24	37.9	±	4.2	1.06	±	0.05	8.67	±	0.95	0.361	±	0.018
Water 5A	Korsnäs	42.1	±	3.8	0.059	±	0.004	2.85	±	0.31	0.376	±	0.019	4.18	±	0.46	0.157	±	0.008
Water 5B	Korsnäs	43.5	±	3.9	0.061	±	0.004	2.97	±	0.33	0.356	±	0.018	4.28	±	0.47	0.166	±	0.008
Water 6A	Korsnäs	342	±	31	1.55	±	0.11	16.0	±	1.8	1.33	±	0.07	3.40	±	0.37	1.99	±	0.10
Water 6B	Korsnäs	378	±	34	1.66	±	0.12	17.1	±	1.9	1.35	±	0.07	3.35	±	0.37	2.09	±	0.11
Water 7A	Korsnäs	4403	±	396	24.2	±	1.7	98.8	±	10.9	8.40	±	0.42	5.09	±	0.56	1.84	±	0.09
Water 7B	Korsnäs	3552	±	320	20.7	±	1.5	85.4	±	9.4	6.05	±	0.30	4.00	±	0.44	1.39	±	0.07
Water 8A	Korsnäs	2407	±	217	4.23	±	0.3	28.4	±	3.1	7.43	±	0.37	17.9	±	2.0	1.09	±	0.05
Water 8B	Korsnäs	2522	±	227	4.04	±	0.28	27.1	±	3.0	7.13	±	0.36	17.3	±	1.9	1.11	±	0.06
Water 9A	Korsnäs	3806	±	343	3.16	±	0.22	27.2	±	3.0	105	±	5	8.26	±	0.91	1.24	±	0.06
Water 9B	Korsnäs	3617	±	325	2.97	±	0.21	26.0	±	2.9	5.57	±	0.28	6.22	±	0.69	1.22	±	0.06
Ref. Water A	Korsnäs	1505	±	135	1.27	±	0.09	13.8	±	1.5	7.53	±	0.38	3.28	±	0.36	1.16	±	0.06
Ref. Water B	Korsnäs	1477	±	133	1.28	±	0.09	13.8	±	1.5	7.48	±	0.37	2.55	±	0.28	1.15	±	0.06
P106A	Vihanti	571	±	51	0.188	±	0.013	0.488	±	0.054	0.147	±	0.007	4.83	±	0.53	0.065	±	0.003
P106B	Vihanti	592	±	53	0.200	±	0.014	0.503	±	0.055	0.149	±	0.007	4.83	±	0.53	0.073	±	0.004
P110A	Vihanti	22271	±	2004	0.595	±	0.042	3.80	±	0.42				114	±	13	0.151	±	0.008

Sample	Sampling site	56 Fe [ppb]	±	unc.	59 Co [ppb]	±	unc.	60 Ni [ppb]	±	unc.	63 Cu [ppb]	±	unc.	66 Zn [ppb]	±	unc.	75 As [ppb]	±	unc.
P113A	Vihanti	3.80	±	0.34	0.424	±	0.03	6.46	±	0.71	1.00	±	0.05	261	±	29	0.973	±	0.049
P113B	Vihanti	4.18	±	0.38	0.412	±	0.029	6.22	±	0.68	0.852	±	0.043	236	±	26	0.981	±	0.049
P114A	Vihanti	29.9	±	2.7	20.1	±	1.4	245	±	27	0.899	±	0.045	350	±	39	0.684	±	0.034
P114B	Vihanti	32.7	±	3	23.5	±	1.6	257	±	28	0.827	±	0.041	379	±	42	0.669	±	0.033
P115A	Vihanti	318	±	29	102	±	7	470	±	52	2656	±	133	54233	±	5966	0.645	±	0.032
P115B	Vihanti	135	±	12	99.1	±	6.9	456	±	50	2498	±	125	51729	±	5690	0.299	±	0.015
P116A	Vihanti	4.89	±	0.44	0.256	±	0.018	0.714	±	0.079	0.799	±	0.040	23.0	±	2.5	0.077	±	0.004
P116B	Vihanti	3.34	±	0.30	0.290	±	0.02	0.811	±	0.089	0.903	±	0.045	25.8	±	2.8	0.095	±	0.005
P117A	Vihanti	420	±	38	0.230	±	0.016	0.562	±	0.062	0.136	±	0.007	9.19	±	1.01	0.208	±	0.01
P117B	Vihanti	374	±	34	0.236	±	0.017	0.626	±	0.069	0.215	±	0.011	10.1	±	1.1	0.204	±	0.01
Porewater 1 - 9 cm	Vihanti	30.2	±	2.7	0.037	±	0.003	5.24	±	0.58	20.3	±	1.0	658	±	72	0.115	±	0.006
Porewater 1 -19 cm	Vihanti	17469	±	1572	0.042	±	0.003	0.797	±	0.088	0.245	±	0.012	3.50	±	0.39	0.944	±	0.047
Porewater 1 - 29 cm	Vihanti	26513	±	2386	0.032	±	0.002	1.12	±	0.12	0.814	±	0.041	11.6	±	1.3	1.54	±	0.08
Porewater 2 - 60 cm	Vihanti	131000	±	11800	0.357	±	0.025	4.79	±	0.53	8.35	±	0.42	78.4	±	8.6	45.0	±	2.3
Porewater 2 - 30 cm	Vihanti	7970	±	717	28.8	±	2.0	172	±	19	6.86	±	0.34	5077	±	558	5.75	±	0.29
Porewater 3 - 16 cm	Vihanti	23560	±	2120	0.078	±	0.005	0.652	±	0.072	1.24	±	0.06	21.5	±	2.4	2.70	±	0.14
Porewater 3 - 26 cm	Vihanti	34753	±	3128	0.037	±	0.003	0.405	±	0.045	0.955	±	0.048	7.92	±	0.87	1.69	±	0.08
Porewater 3 - 36 cm	Vihanti	26908	±	2422	0.151	±	0.011	1.18	±	0.13	0.545	±	0.027	13.2	±	1.5	10.2	±	0.5
Porewater 4 - 15 cm	Vihanti	4615000	±	415000	927	±	65	1841	±	203	19177	±	959	517000	±	57000	21.3	±	1.1
Porewater 4 - 25 cm	Vihanti	32987000	±	2969000	4275	±	299	9027	±	993	39621	±	1981	437000	±	48000	219	±	11
Water 10A	Vihanti	17.6	±	1.6	0.402	±	0.028	16.1	±	1.8	2.20	±	0.11	9454	±	1040	0.134	±	0.007
Water 10B	Vihanti	14.1	±	1.3	0.388	±	0.027	15.7	±	1.7	2.06	±	0.10	9314	±	1025	0.124	±	0.006
Water 11A	Vihanti	155	±	14	0.039	±	0.003	1.64	±	0.18	9.91	±	0.50	107	±	12	0.604	±	0.030
Water 1 - 1 m - A	Vihanti	18.4	±	1.7	0.092	±	0.006	0.486	±	0.053	2.04	±	0.10	17.2	±	1.9	0.280	±	0.014
Water 11B	Vihanti	154	±	14	0.040	±	0.003	1.65	±	0.18	9.94	±	0.50	107	±	12	0.608	±	0.030
Water 1 - 1 m - B	Vihanti	12.7	±	1.2	0.106	±	0.007	0.697	±	0.077	2.63	±	0.13	23.5	±	2.6	0.315	±	0.016
Water 12A	Vihanti	644	±	58	0.534	±	0.037	7.15	±	0.79	1.77	±	0.09	326	±	36	0.194	±	0.010
Water 1 - 2m - A	Vihanti	12.7	±	1.1	0.103	±	0.007	0.474	±	0.052	1.21	±	0.06	12.3	±	1.4	0.294	±	0.015
Water 12B	Vihanti	623	±	56	0.495	±	0.035	6.74	±	0.74	1.90	±	0.10	286	±	32	0.176	±	0.009

Sample	Sampling site	56 Fe [ppb]	±	unc.	59 Co [ppb]	±	unc.	60 Ni [ppb]	±	unc.	63 Cu [ppb]	±	unc.	66 Zn [ppb]	±	unc.	75 As [ppb]	±	unc.
Water 15A	Vihanti	6646	±	598	1.04	±	0.07	4.94	±	0.54	1.38	±	0.07	468	±	52	0.271	±	0.014
Water 15B	Vihanti	7188	±	647	1.09	±	0.08	5.08	±	0.56	1.47	±	0.07	408	±	45	0.286	±	0.014
Water 16A	Vihanti	13121000	±	1181000	1094	±	77	2104	±	231	14089	±	704	346000	±	38000	84.2	±	4.2
Water 16B	Vihanti	13235000	±	1191000	1070	±	75	2086	±	230	14239	±	712	340000	±	37000	68.6	±	3.4
Water 17A	Vihanti	159	±	14	0.080	±	0.006	0.437	±	0.048	0.515	±	0.026	9.84	±	1.08	0.253	±	0.013
Water 17B	Vihanti	139	±	13	0.084	±	0.006	0.437	±	0.048	0.493	±	0.025	9.47	±	1.04	0.251	±	0.013
Water 18A	Vihanti	10.2	±	0.9	1.76	±	0.12	31.5	±	3.5	2.55	±	0.13	3011	±	331	0.203	±	0.010
Water 18B	Vihanti	14.5	±	1.3	1.85	±	0.13	31.3	±	3.4	2.56	±	0.13	2991	±	329	0.216	±	0.011
Water 2A -A	Vihanti	79.7	±	7.2	0.496	±	0.035	9.25	±	1.02	4.90	±	0.25	1250	±	137	0.411	±	0.021
Water 2A -B	Vihanti	75.2	±	6.8	0.457	±	0.032	8.35	±	0.92	4.47	±	0.22	1176	±	129	0.368	±	0.018
Water 2B -A	Vihanti	11.1	±	1.0	1.03	±	0.07	14.3	±	1.6	6.57	±	0.33	2601	±	286	0.140	±	0.007
Water 2B -B	Vihanti	10.8	±	1.0	1.18	±	0.08	16.5	±	1.8	7.63	±	0.38	2899	±	319	0.155	±	0.008
Water 3A	Vihanti	492	±	44	1.15	±	0.08	5.39	±	0.59	2.19	±	0.11	318	±	35	0.278	±	0.014
Water 3B	Vihanti	464	±	42	1.15	±	0.08	5.43	±	0.60	2.22	±	0.11	323	±	36	0.258	±	0.013
Water 4A	Vihanti	1468	±	132	0.645	±	0.045	2.70	±	0.30	7.31	±	0.37	96.5	±	10.6	0.972	±	0.049
Water 4B	Vihanti	1601	±	144	0.617	±	0.043	2.72	±	0.30	7.37	±	0.37	96.1	±	10.6	0.937	±	0.047
Water 5A	Vihanti	295	±	27	2.90	±	0.20	11.5	±	1.3	5.64	±	0.28	445	±	49	0.889	±	0.044
Water 5B	Vihanti	284	±	26	2.87	±	0.20	11.5	±	1.3	5.57	±	0.28	453	±	50	0.904	±	0.045
Water 6A	Vihanti	28.2	±	2.5	24.1	±	1.7	573	±	63	918	±	46	34726	±	3820	0.159	±	0.008
Water 6B	Vihanti	34.3	±	3.1	17.7	±	1.2	357	±	39	584	±	29	45256	±	4978	0.174	±	0.009
Water 7A	Vihanti	5317	±	479	0.501	±	0.035	2.33	±	0.26	1.80	±	0.09	74.8	±	8.2	0.431	±	0.022
Water 7B	Vihanti	6165	±	555	0.468	±	0.033	2.19	±	0.24	1.70	±	0.09	68.3	±	7.5	0.399	±	0.020
Water 8A	Vihanti	34227	±	3080	35.3	±	2.5	146	±	16	1554	±	78	85986	±	9458	0.269	±	0.013
Water 8B	Vihanti	16088	±	1448	45.9	±	3.2	174	±	19	7574	±	379	105000	±	12000	0.535	±	0.027
Water 9A	Vihanti	1635	±	147	1.23	±	0.09	4.73	±	0.52	12.9	±	0.6	234	±	26	0.861	±	0.043
Water 9B	Vihanti	1590	±	143	1.19	±	0.08	4.75	±	0.52	12.7	±	0.6	230	±	25	0.887	±	0.044
Ref Water A	Vihanti	4193	±	377	0.531	±	0.037	2.10	±	0.23	3.98	±	0.20	124	±	14	1.72	±	0.09
Ref Water B	Vihanti	5835	±	525	0.581	±	0.041	2.18	±	0.24	4.36	±	0.22	128	±	14	1.82	±	0.09

Appendix 5 continues. Note that the elements have changed

		78 Se [ppb]	±	unc.	95 Mo [ppb]	±	unc.	111 Cd [ppb]	±	unc.	208 Pb [ppb]	±	unc.	238 U [ppb]	±	unc.
LOQ 10σ		0.01			0.005			0.002			0.003			0.001		
U %		14			4			17			16			6		
Sample	**Sampling Site**															
Porewater 1 - 10 cm	Korsnäs	1.25	±	0.18	1.46	±	0.06	2.33	±	0.40	50.3	±	8.1	418	±	25
Porewater 2- 10 cm	Korsnäs	1.35	±	0.19	3.40	±	0.14	3.73	±	0.63	514	±	82	180	±	11
Porewater 2 -20 cm	Korsnäs	2.83	±	0.40	9.16	±	0.37	7.53	±	1.28	654	±	105	1139	±	68
Porewater 2 - 30 cm	Korsnäs	1.45	±	0.20	2.64	±	0.11	0.316	±	0.054	48.7	±	7.8	721	±	43
Water 10A	Korsnäs	0.073	±	0.010	0.125	±	0.005	0.009	±	0.002	1.28	±	0.20	2.11	±	0.13
Water 10B	Korsnäs	0.091	±	0.013	0.145	±	0.006	0.009	±	0.002	1.47	±	0.24	2.43	±	0.15
Water 1A	Korsnäs	0.081	±	0.011	0.295	±	0.012	0.029	±	0.005	0.045	±	0.007	74.9	±	4.5
Water 1B	Korsnäs	0.108	±	0.015	0.340	±	0.014	0.031	±	0.005	0.020	±	0.003	86.1	±	5.2
Water 2A	Korsnäs	0.212	±	0.030	0.249	±	0.010	0.032	±	0.005	1.47	±	0.24	12.9	±	0.8
Water 2B	Korsnäs	0.259	±	0.036	0.299	±	0.012	0.038	±	0.006	1.68	±	0.27	15.4	±	0.9
Water 3A	Korsnäs	0.152	±	0.021	0.692	±	0.028	0.079	±	0.013	0.452	±	0.072	0.673	±	0.04
Water 3B	Korsnäs	0.152	±	0.021	0.675	±	0.027	0.079	±	0.013	0.498	±	0.080	0.720	±	0.043
Water 4 - 10 m - A	Korsnäs	0.256	±	0.036	0.321	±	0.013	0.011	±	0.002	0.381	±	0.061	723	±	43
Water 4 - 10 m - B	Korsnäs	0.245	±	0.034	0.317	±	0.013	0.011	±	0.002	0.849	±	0.136	673	±	40
Water 4 - 1 m - A	Korsnäs	0.083	±	0.012	0.321	±	0.013	0.032	±	0.005	5.02	±	0.80	80.7	±	4.8
Water 4 - 1 m - B	Korsnäs	0.121	±	0.017	0.403	±	0.016	0.041	±	0.007	0.269	±	0.043	100	±	6
Water 4 - 20 m - A	Korsnäs	0.252	±	0.035	0.515	±	0.021	0.009	±	0.002	0.213	±	0.034	709	±	43
Water 4 - 20 m - B	Korsnäs	0.250	±	0.035	0.541	±	0.022	0.011	±	0.002	0.220	±	0.035	682	±	41
Water 4 - 25 m - A	Korsnäs	0.274	±	0.038	0.501	±	0.020	0.010	±	0.002	0.126	±	0.020	673	±	40
Water 4 - 25 m - B	Korsnäs	0.316	±	0.044	0.589	±	0.024	0.013	±	0.002	0.072	±	0.012	816	±	49
Water 4 - 5 m - A	Korsnäs	0.209	±	0.029	0.371	±	0.015	0.085	±	0.014	0.237	±	0.038	472	±	28
Water 4 - 5 m - B	Korsnäs	0.205	±	0.029	0.366	±	0.015	0.085	±	0.014	0.193	±	0.031	441	±	26
Water 5A	Korsnäs	0.055	±	0.008	0.016	±	0.001	0.031	±	0.005	3.48	±	0.56	0.117	±	0.007

Sample	Sampling Site	78 Se [ppb]	±	unc.	95 Mo [ppb]	±	unc.	111 Cd [ppb]	±	unc.	208 Pb [ppb]	±	unc.	238 U [ppb]	±	unc.
Water 6A	Korsnäs	1.12	±	0.16	1.34	±	0.05	0.048	±	0.008	6.41	±	1.03	139	±	8
Water 6B	Korsnäs	1.19	±	0.17	1.37	±	0.06	0.050	±	0.009	6.50	±	1.04	150	±	9
Water 7A	Korsnäs	0.641	±	0.09	0.121	±	0.005	0.055	±	0.009	3.16	±	0.51	2.91	±	0.18
Water 7B	Korsnäs	0.502	±	0.07	0.081	±	0.003	0.034	±	0.006	2.15	±	0.34	2.10	±	0.13
Water 8A	Korsnäs	0.189	±	0.026	0.627	±	0.025	0.100	±	0.017	0.326	±	0.052	0.728	±	0.044
Water 8B	Korsnäs	0.188	±	0.026	0.585	±	0.023	0.098	±	0.017	0.488	±	0.078	0.705	±	0.042
Water 9A	Korsnäs	0.236	±	0.033	0.539	±	0.022	0.048	±	0.008	6.31	±	1.01	10.6	±	0.6
Water 9B	Korsnäs	0.246	±	0.034	0.514	±	0.021	0.051	±	0.009	6.24	±	1.00	10.2	±	0.6
Ref. Water A	Korsnäs	0.199	±	0.028	0.428	±	0.017	0.042	±	0.007	0.448	±	0.072	0.576	±	0.035
Ref. Water B	Korsnäs	0.206	±	0.029	0.420	±	0.017	0.039	±	0.007	0.381	±	0.061	0.546	±	0.033
P106A	Vihanti	0.018	±	0.003	0.062	±	0.002	0.064	±	0.011				0.025	±	0.001
P106B	Vihanti	0.019	±	0.003	0.066	±	0.003	0.066	±	0.011				0.023	±	0.001
P110A	Vihanti	0.093	±	0.013	0.064	±	0.003	0.246	±	0.042				0.156	±	0.009
P110B	Vihanti	0.088	±	0.012	0.067	±	0.003	0.244	±	0.041				0.155	±	0.009
P113A	Vihanti	0.219	±	0.031	33.2	±	1.3	0.432	±	0.073	1.82	±	0.29	7.89	±	0.47
P113B	Vihanti	0.207	±	0.029	33.0	±	1.3	0.417	±	0.071	1.63	±	0.26	8.32	±	0.50
P114A	Vihanti	0.339	±	0.047	95.2	±	3.8	0.085	±	0.014	0.130	±	0.021	52.0	±	3.1
P114B	Vihanti	0.348	±	0.049	108	±	4	0.100	±	0.017	0.130	±	0.021	54.1	±	3.2
P115A	Vihanti	0.585	±	0.082	0.041	±	0.002	174	±	30	23.6	±	3.8	0.346	±	0.021
P115B	Vihanti	0.246	±	0.034	0.044	±	0.002	161	±	27	12.6	±	2.0	0.175	±	0.011
P116A	Vihanti				0.013	±	0.001	1.64	±	0.28				0.037	±	0.002
P116B	Vihanti				0.011	±	0.0005	1.98	±	0.34				0.0033	±	0.0002
P117A	Vihanti	0.032	±	0.004	0.010	±	0.0004	0.118	±	0.020				0.0025	±	0.0001
P117B	Vihanti	0.026	±	0.004	0.021	±	0.001	0.121	±	0.021	0.015	±	0.002	0.003	±	0.0002
Porewater 1 - 9 cm	Vihanti	0.451	±	0.063	9.80	±	0.39	0.591	±	0.100	6.62	±	1.06	33.7	±	2.0
Porewater 1 -19 cm	Vihanti	0.069	±	0.010	0.527	±	0.021				0.311	±	0.050	44.2	±	2.7
Porewater 1 - 29 cm	Vihanti	0.054	±	0.008	0.554	±	0.022	0.014	±	0.002	0.517	±	0.083	35.9	±	2.2
Porewater 2 - 60 cm	Vihanti	0.356	±	0.050	4.56	±	0.18	0.308	±	0.052	0.313	±	0.050	984	±	59
Porewater 2 - 30 cm	Vihanti	0.728	±	0.102	5.37	±	0.22	12.1	±	2.1	86.7	±	13.9	673	±	40

Sample	Sampling Site	78 Se [ppb]	±	unc.	95 Mo [ppb]	±	unc.	111 Cd [ppb]	±	unc.	208 Pb [ppb]	±	unc.	238 U [ppb]	±	unc.
Porewater 3 - 26 cm	Vihanti	0.099	±	0.014	5.67	±	0.23	0.013	±	0.002	0.617	±	0.099	54.4	±	3.3
Porewater 3 - 36 cm	Vihanti	0.104	±	0.015	13.1	±	0.5	0.021	±	0.004	0.684	±	0.109	53.3	±	3.2
Porewater 4 - 15 cm	Vihanti	29.2	±	4.1	0.267	±	0.011	809	±	137	9.49	±	1.52	109	±	7
Porewater 4 - 25 cm	Vihanti	91.0	±	12.7	2.95	±	0.12	831	±	141	90.8	±	14.5	489	±	29
Water 10A	Vihanti	0.264	±	0.037	12.3	±	0.5	7.94	±	1.35				55.7	±	3.3
Water 10B	Vihanti	0.265	±	0.037	11.6	±	0.5	7.76	±	1.32				54.7	±	3.3
Water 11A	Vihanti	0.123	±	0.017	1.03	±	0.04	0.245	±	0.042	1.21	±	0.19	1.28	±	0.08
Water 1 - 1 m - A	Vihanti	0.051	±	0.007	0.925	±	0.037	0.010	±	0.002	0.518	±	0.083	11.6	±	0.7
Water 11B	Vihanti	0.139	±	0.019	1.03	±	0.04	0.242	±	0.041	1.14	±	0.18	1.30	±	0.08
Water 1 - 1 m - B	Vihanti	0.068	±	0.009	0.928	±	0.037	0.015	±	0.003	1.55	±	0.25	12.0	±	0.7
Water 12A	Vihanti	0.107	±	0.015	1.73	±	0.07	0.051	±	0.009	0.067	±	0.011	44.5	±	2.7
Water 1 - 2m - A	Vihanti	0.048	±	0.007	0.922	±	0.037	0.007	±	0.001	0.168	±	0.027	11.4	±	0.7
Water 12B	Vihanti	0.087	±	0.012	1.59	±	0.06	0.053	±	0.009	0.563	±	0.090	43.3	±	2.6
Water 1 - 2m - B	Vihanti	0.056	±	0.008	0.883	±	0.035	0.005	±	0.001	0.123	±	0.020	10.9	±	0.7
Water 15A	Vihanti	0.057	±	0.008	0.288	±	0.012	0.584	±	0.099	0.102	±	0.016	3.65	±	0.22
Water 15B	Vihanti	0.066	±	0.009	0.302	±	0.012	0.598	±	0.102	0.851	±	0.136	3.91	±	0.24
Water 16A	Vihanti	36.5	±	5.1	0.527	±	0.021	499	±	85	871	±	139	142	±	9
Water 16B	Vihanti	27.8	±	3.9	0.573	±	0.023	484	±	82	742	±	119	117	±	7
Water 17A	Vihanti	0.062	±	0.009	0.892	±	0.036	0.004	±	0.001				10.5	±	0.6
Water 17B	Vihanti	0.066	±	0.009	0.895	±	0.036							11.0	±	0.7
Water 18A	Vihanti	0.203	±	0.028	1.50	±	0.06	1.93	±	0.33	0.057	±	0.009	12.6	±	0.8
Water 18B	Vihanti	0.219	±	0.031	1.54	±	0.06	2.00	±	0.34	0.073	±	0.012	13.6	±	0.8
Water 2A -A	Vihanti	0.098	±	0.014	0.518	±	0.021	0.261	±	0.044	0.367	±	0.059	5.20	±	0.31
Water 2A -B	Vihanti	0.088	±	0.012	0.460	±	0.018	0.26	±	0.044	0.063	±	0.010	4.42	±	0.27
Water 2B -A	Vihanti	0.076	±	0.011	0.133	±	0.005	2.60	±	0.44	0.034	±	0.005	8.05	±	0.48
Water 2B -B	Vihanti	0.088	±	0.012	0.146	±	0.006	2.83	±	0.48	0.031	±	0.005	8.49	±	0.51
Water 3A	Vihanti	0.055	±	0.008	0.282	±	0.011	0.552	±	0.094				3.26	±	0.20
Water 3B	Vihanti	0.060	±	0.008	0.276	±	0.011	0.550	±	0.094				3.13	±	0.19
Water 4A	Vihanti	0.152	±	0.021	0.100	±	0.004	0.043	±	0.007	2.46	±	0.39	1.36	±	0.08

Sample	Sampling Site	78 Se [ppb]	±	unc.	95 Mo [ppb]	±	unc.	111 Cd [ppb]	±	unc.	208 Pb [ppb]	±	unc.	238 U [ppb]	±	unc.
Water 5A	Vihanti	0.354	±	0.050	8.16	±	0.33	0.443	±	0.075	0.068	±	0.011	69.7	±	4.2
Water 5B	Vihanti	0.354	±	0.049	7.91	±	0.32	0.438	±	0.074				68.8	±	4.1
Water 6A	Vihanti	0.982	±	0.137	0.125	±	0.005	238	±	41				0.878	±	0.053
Water 6B	Vihanti	1.03	±	0.14	0.138	±	0.006	161	±	27				0.938	±	0.056
Water 7A	Vihanti	0.078	±	0.011	0.458	±	0.018	0.039	±	0.007	0.290	±	0.046	7.38	±	0.44
Water 7B	Vihanti	0.070	±	0.01	0.417	±	0.017	0.034	±	0.006	0.249	±	0.040	6.92	±	0.42
Water 8A	Vihanti	0.545	±	0.076	0.030	±	0.001	143	±	24	2.21	±	0.35	11.1	±	0.7
Water 8B	Vihanti	0.734	±	0.103	0.029	±	0.001	201	±	34	19.0	±	3.0	74.4	±	4.5
Water 9A	Vihanti	0.135	±	0.019	0.124	±	0.005	0.342	±	0.058	0.882	±	0.141	0.824	±	0.049
Water 9B	Vihanti	0.135	±	0.019	0.119	±	0.005	0.336	±	0.057	0.808	±	0.129	0.814	±	0.049
Ref Water A	Vihanti	0.183	±	0.026	0.026	±	0.001	0.095	±	0.016	9.78	±	1.56	0.102	±	0.006
Ref Water B	Vihanti	0.187	±	0.026	0.027	±	0.001	0.096	±	0.016	10.4	±	1.7	0.111	±	0.007

Appendix 6 Table of all gamma spectroscopic results obtained in this work, activity concentrations for all nuclides are presented as Bq/kg of dry weight and uncertainties are expressed as relative uncertainties (1 σ). Empty cells signify results below the relevant detection limit.

Vihanti																	
Sample	Depth (cm)	^{40}K	^{40}K; Unc. 1σ	^{228}Ra	^{228}Ra; Unc. 1σ	^{228}Th	^{228}Th; Unc. 1σ	^{232}Th	^{232}Th; Unc. 1σ	^{210}Pb	^{210}Pb; Unc. 1σ	^{226}Ra	^{226}Ra; Unc. 1σ	^{238}U	^{238}U; Unc. 1σ	^{235}U	^{235}U; Unc. 1σ
Core 1B	0	158	8%	10	10%	8.1	7%	8.0	8%	456	10%	468	8%	333	10%	14	10%
Core 1B	0-1	169	7%	9.4	10%	8.1	7%	8.5	8%	162	9%	336	10%	189	15%	10	10%
Core 1B	1-2	189	8%	10	13%	9.5	8%	9.4	9%	184	5%	349	8%	195	15%	12	10%
Core 1B	2-3	197	8%	10	9%	9.7	7%	9.5	7%	164	5%	306	6%	233	8%	9.7	8%
Core 1B	3-4	206	14%	9.7	9%	8.5	8%	8.3	8%	202	10%	289	7%	297	10%	12	12%
Core 1B	4-5	215	7%	12	7%	10	7%	10	7%	201	10%	347	8%	302	7%	12	10%
Core 1B	5-6	181	8%	11	9%	11	7%	9.6	7%	187	10%	264	8%	263	11%	14	10%
Core 1B	6-7	184	7%	12	8%	11	7%	11	7%	191	8%	267	10%	272	8%	15	11%
Core 1B	7-8	166	9%	11	13%	10	8%	9.9	10%	189	6%	276	8%	237	16%	14	10%
Core 1B	8-9	145	14%	9.3	8%	8.8	7%	8.6	7%	244	10%	310	12%	235	9%	13	14%
Core 1B	9-10	162	9%	8.9	9%	8.5	7%	8.5	7%	199	10%	356	9%	232	10%	11	11%
Core 1B	10-11	145	9%	8.3	11%	7.2	8%	7.0	9%	164	18%	400	0%	175	14%	8.5	7%
Core 1B	11-12	145	9%	7.6	11%	8.0	7%	7.1	8%	169	18%	319	9%	276	8%	14	11%
Core 1B	12-14	122	9%	6.6	8%	5.7	7%	5.7	7%	108	18%	221	9%	328	7%	16	11%
Core 1B	14-16	139	10%	4.3	16%	5.8	8%	4.9	11%	109	10%	230	9%	306	11%	13	11%
Core 1B	16-18	134	9%	7.0	12%	7.2	8%	6.5	9%	176	18%	358	9%	404	9%	22	11%
Core 1B	18-20	131	8%	8.6	12%	6.9	8%	7.1	9%	137	6%	341	8%	403	9%	17	10%
Core 1B	20-22	129	9%	6.4	9%	5.6	7%	5.6	7%	125	8%	254	9%	272	8%	15	11%
Core 1B	22-24	140	8%	6.5	13%	5.9	9%	6.4	10%	94	6%	238	8%	270	11%	12	10%
Core 1B	24-26	152	9%	6.4	11%	6.0	7%	5.7	8%	133	18%	245	9%	284	9%	17	11%
Core 1B	26-28	147	7%	6.4	11%	5.9	7%	5.8	9%	124	9%	254	10%	264	9%	13	11%
Core 1B	28-30	161	8%	6.1	13%	6.0	9%	5.7	10%	121	6%	261	8%	262	11%	12	10%
Core 1B	30-32	176	7%	6.5	11%	5.6	8%	5.4	10%	115	9%	244	10%	203	12%	12	11%
Core 1B	32-34	145	13%	5.7	9%	5.1	7%	5.0	7%	125	10%	223	12%	208	8%	11	14%
Core 1B	34-36	139	14%	5.7	11%	4.9	8%	4.8	10%	122	10%	223	12%	243	10%	12	14%
Core 1B	36-38	129	10%	4.6	10%	5.0	8%	4.5	9%	109	8%	220	10%	195	12%	12	11%

Sample	Depth (cm)	^{40}K	^{40}K; Unc. 1σ	^{228}Ra	^{228}Ra; Unc. 1σ	^{228}Th	^{228}Th; Unc. 1σ	^{232}Th	^{232}Th; Unc. 1σ	^{210}Pb	^{210}Pb; Unc. 1σ	^{226}Ra	^{226}Ra; Unc. 1σ	^{238}U	^{238}U; Unc. 1σ	^{235}U	^{235}U; Unc. 1σ
Core 2B	0	196	9%	9.2	11%	9.5	7%	8.4	8%	190	18%	207	9%	198	12%	13	11%
Core 2B	0-1	240	7%	12	9%	11	7%	11	7%	189	9%	241	10%	213	12%	9.8	11%
Core 2B	1-2	210	9%	13	9%	12	7%	11	7%	194	18%	248	9%	176	13%	13	11%
Core 2B	2-3	182	8%	11	10%	11	8%	10	8%	167	5%	278	8%	355	10%	14	10%
Core 2B	3-4	182	14%	9.8	9%	9.5	7%	9.0	7%	181	10%	239	12%	288	10%	13	14%
Core 2B	4-5	214	9%	10	9%	9.3	7%	8.7	7%	179	18%	253	9%	262	9%	17	11%
Core 2B	5-6	230	7%	9.2	9%	8.5	7%	8.7	8%	148	9%	238	10%	225	11%	11	11%
Core 2B	6-7	197	13%	7.4	9%	8	7%	7.0	7%	156	10%	210	12%	198	10%	9.1	14%
Core 2B	7-8	223	7%	8.6	9%	7.9	7%	8.1	7%	130	9%	224	10%	189	10%	7.6	11%
Core 2B	8-9	204	8%	8.4	11%	8.5	8%	7.6	9%	139	5%	239	8%	227	12%	10	10%
Core 2B	9-10	230	8%	10	9%	9.2	7%	9.2	7%	155	10%	295	9%	344	10%	15	10%
Core 2B	10-12	195	8%	9.0	10%	9.3	7%	8.9	8%	140	5%	258	8%	339	8%	15	10%
Core 2B	12-14	181	11%	9.2	8%	8.7	7%	8.5	7%	136	10%	267	10%	354	7%	15	12%
Core 2B	14-16	180	13%	8.7	7%	7.8	7%	7.6	7%	151	10%	221	12%	203	8%	10	14%
Core 2B	16-18	226	7%	9.6	8%	9.3	7%	9.3	7%	137	5%	257	8%	237	8%	9.3	10%
Core 2B	18-20	223	9%	9.9	8%	9.9	7%	9.0	7%	153	8%	264	9%	274	9%	14	11%
Core 2B	20-22	202	7%	9.6	8%	9.1	7%	8.5	7%	117	5%	266	8%	315	6%	14	10%
Core 2B	22-24	192	9%	9.8	8%	9.3	7%	9.1	7%	182	8%	317	10%	335	8%	17	11%
Core 2B	24-26	210	9%	9.6	9%	9.5	7%	8.9	7%	186	18%	294	9%	313	8%	20	11%
Core 2B	26-28	231	9%	11	9%	11	7%	10	7%	165	18%	250	9%	278	8%	16	11%
Core 2B	28-30	257	6%	13	7%	13	6%	13	6%	154	9%	235	10%	243	8%	11	11%
Core 3B	0-1	361	8%	7.6	9%	5.9	8%	5.9	8%	47	6%	51	9%			0.59	11%
Core 3B	1-2	449	8%	8.9	10%	8.3	8%	8.6	8%	51	6%	68	9%			0.39	10%
Core 3B	2-3	372	7%	9.0	8%	8.2	7%	8.3	7%	36	6%	63	8%			0.73	10%
Core 3B	3-4	408	8%	9.1	9%	10	7%	9.0	7%	48	6%	61	9%			1.2	11%
Core 3B	4-5	467	8%	11	8%	12	7%	11	7%	70	6%	67	8%			1.0	10%
Core 3B	5-6	512	6%	12	7%	12	6%	12	6%	42	9%	49	10%			0.93	12%
Core 3B	6-7	506	9%	12	8%	12	7%	12	7%	55	18%	50	9%			1.1	11%
Core 3B	7-8	481	8%	9.0	12%	12	8%	11	9%	48	8%	44	10%			0.82	12%

Sample	Depth (cm)	^{40}K	^{40}K; Unc. 1σ	^{228}Ra	^{228}Ra; Unc. 1σ	^{228}Th	^{228}Th; Unc. 1σ	^{232}Th	^{232}Th; Unc. 1σ	^{210}Pb	^{210}Pb; Unc. 1σ	^{226}Ra	^{226}Ra; Unc. 1σ	^{238}U	^{238}U; Unc. 1σ	^{235}U	^{235}U; Unc. 1σ
Core 3B	8-9	518	7%	12	9%	12	7%	12	7%	34	10%	47	11%			0.57	13%
Core 3B	9-10	614	9%	12	7%	12	7%	12	7%	40	10%	44	9%			0.57	11%
Core 3B	10-12	466	8%	11	10%	11	7%	9.9	8%	135	5%	185	8%			1.6	10%
Core 3B	12-14	156	13%	3.7	9%	3.9	7%	3.5	8%	86	10%	161	12%			2.0	14%
Core 3B	14-16	145	9%	2.9	9%	2.7	8%	2.8	8%	34	15%	92	23%	34	23%	1.6	23%
Core 3B	16-18	196	9%	4.1	16%	3.5	8%	3.0	9%	124	18%	249	9%			3.5	11%
Core 3B	18-20	170	8%	4.5	21%	2.3	14%	1.9	17%	151	5%	314	8%			1.6	10%
Core 3B	20-22	151	10%	4.5	15%	2.7	9%	2.4	13%	155	10%	305	9%			1.5	11%
Core 3B	22-24	145	10%	4.5	18%	3.9	9%	4.1	12%	142	10%	316	9%			1.9	11%
Core 3B	24-26	177	9%	4.2	13%	3.7	8%	3.5	9%	164	10%	270	9%			2.4	11%
Core 3B	26-28	198	7%	6.3	10%	4.6	8%	4.8	8%	142	9%	279	10%			1.6	11%
Core 3B	28-29	379	8%	9.0	8%	8.2	7%	8.2	7%	90	5%	141	8%			1.6	10%
NORM 1	25	111	7%	7.2	7%	7.2	7%	6.9	7%	278	12%	293	8%	60	13%	2.9	10%
NORM 3	60	207	8%	12	7%	11	6%	11	6%	171	14%	318	8%	199	6%	10	10%
Ref. Soil	0-10	30	21%							159	15%	3.2	26%			0.57	29%
Ref. Soil	10-20	18	15%							85	15%	4.4	15%			0.38	17%
Soil 1	0-3	225	11%	6.1	11%	6.9	8%	6.3	9%	283	10%	20	15%			0.79	16%
Soil 1	3-8	424	8%	11	7%	9.6	7%	11	6%	40	6%	24	11%			1.2	12%
Soil 1	8-15	406	8%	12	8%	12	6%	12	7%	45	14%	53	8%	60	17%	2.7	10%
Soil 1	15-20	274	7%	13	7%	13	7%	12	7%	104	6%	206	9%	191	9%	8.3	11%
Soil 2	0-2	97	13%	3.7	45%	3.1	19%	4.9	38%	535	5%	84	9%			3.4	11%
Soil 2	2-8	399	8%	11	9%	8.4	7%	8.8	8%	103	6%	119	8%	95	18%	4.4	10%
Soil 2	8-17	538	8%	11	8%	12	7%	11	7%	11	9%	13	7%			0.67	9%
Soil 2	17-22	544	8%	13	7%	13	6%	13	6%	8.5	16%	15	9%			0.68	11%
Soil 3	0-3	24	12%	1.6	26%	0.96	11%	1.3	20%	217	10%	14	10%			0.95	12%
Soil 3	3-9	71	7%	4.8	10%	3.7	7%	4.2	8%	205	6%	105	9%	162	10%	6.0	11%
Soil 3	9-15	21	13%	3.0	13%	2.8	8%	2.6	11%	99	15%	51	9%	218	9%	11	11%
Soil 3	15-20	43	12%			1.5	11%	2.4	52%	39	8%	11	13%			1.7	15%
Soil 4	0-2	44	15%			1.8	16%			441	5%	7.7	18%			0.38	20%

Sample	Depth (cm)	^{40}K	^{40}K; Unc. 1σ	^{228}Ra	^{228}Ra; Unc. 1σ	^{228}Th	^{228}Th; Unc. 1σ	^{232}Th	^{232}Th; Unc. 1σ	^{210}Pb	^{210}Pb; Unc. 1σ	^{226}Ra	^{226}Ra; Unc. 1σ	^{238}U	^{238}U; Unc. 1σ	^{235}U	^{235}U; Unc. 1σ
Soil 4	2-6	409	8%	10	7%	9.8	6%	9.6	6%	109	14%	30	8%	28	25%	1.3	10%
Soil 4	6-12	217	8%	5.3	10%	4.8	10%	4.4	10%	108	6%	35	9%	43	25%	2.2	11%
Soil 4	12-16	493	7%	6.4	9%	6.2	7%	6.3	7%	5.1	14%	6.4	12%			0.38	14%
Soil 4	16-21	497	11%	8.2	8%	3.3	8%	3.2	8%	6.2	11%	7.1	15%			0.31	16%
Vih Sedi 1	0-10	655	6%	20	7%	20	6%	20	6%	18	7%	23	9%	34	23%	1.2	11%
Vih Sedi 2	0-10	671	9%	20	7%	21	6%	20	6%	22	15%	25	9%	33	16%	1.3	11%
Vih Sedi 3	0-10	603	8%	19	7%	19	6%	18	6%	19	15%	22	9%	34	20%	1.7	11%
Vih Sedi 4	0-10	146	8%	6.1	9%	5.6	8%	6.0	7%	19	11%	6.4	10%	46	27%	2.2	27%
Vih Sedi 5	0-10	9.7	36%							34	11%	4.9	14%	91	26%	4.3	26%
Korsnäs																	
Sample	**Depth (cm)**	**^{40}K**	**^{40}K; Unc. 1σ**	**^{228}Ra**	**^{228}Ra; Unc. 1σ**	**^{228}Th**	**^{228}Th; Unc. 1σ**	**^{232}Th**	**^{232}Th; Unc. 1σ**	**^{210}Pb**	**^{210}Pb; Unc. 1σ**	**^{226}Ra**	**^{226}Ra; Unc. 1σ**	**^{238}U**	**^{238}U; Unc. 1σ**	**^{235}U**	**^{235}U; Unc. 1σ**
Core 1A	2-3	146	12%	75	8%	72	7%	73	7%	657	18%	180	9%	610	13%	29	11%
Core 1A	3-4	672	9%	265	7%	267	6%	255	6%	893	18%	560	9%	682	11%	41	11%
Core 1A	6-7	1219	9%	429	7%	429	6%	418	6%	368	10%	712	9%	690	9%	28	10%
Core 1A	7-8	992	13%	297	7%	304	6%	287	6%	343	10%	496	12%	513	7%	25	14%
Core 1A	8-9	998	13%	275	7%	280	6%	266	6%	329	10%	435	12%	495	7%	26	14%
Core 1A	15-16	1019	13%	253	7%	253	6%	243	6%	348	10%	469	12%	518	8%	29	14%
Core 1A	20-22	892	13%	308	7%	316	6%	300	6%	457	10%	720	12%	749	8%	35	13%
Core 1A	22-24	989	9%	408	7%	402	6%	385	6%	549	18%	963	9%	950	7%	49	10%
Core 1A	24-26	1013	7%	298	7%	293	6%	283	6%	342	5%	594	8%	684	7%	32	10%
Core 1A	26-28	1106	8%	252	7%	254	6%	242	6%	306	5%	449	8%	623	7%	26	10%
Core 1A	28-30	989	13%	276	7%	282	6%	267	6%	389	10%	553	12%	680	7%	32	14%
Core 1A	30-32	1089	6%	308	6%	308	6%	300	6%	382	8%	669	10%	843	6%	37	11%
Core 1A	0-2	320	9%	62	8%	65	7%	65	7%	715	9%	173	10%	543	19%	22	12%
Core 1A	4-6	1142	9%	378	7%	379	6%	366	6%	339	10%	629	9%	521	9%	25	11%
Core 1A	9-11	1084	9%	351	7%	353	6%	342	6%	267	10%	501	9%	574	8%	26	11%
Core 1A	11-13	1139	6%	312	6%	308	6%	301	6%	269	8%	488	10%	503	6%	21	11%
Core 1A	13-15	1032	7%	382	7%	379	6%	365	6%	266	5%	565	8%	665	6%	27	10%

Sample	Depth (cm)	^{40}K	^{40}K; Unc. 1σ	^{228}Ra	^{228}Ra; Unc. 1σ	^{228}Th	^{228}Th; Unc. 1σ	^{232}Th	^{232}Th; Unc. 1σ	^{210}Pb	^{210}Pb; Unc. 1σ	^{226}Ra	^{226}Ra; Unc. 1σ	^{238}U	^{238}U; Unc. 1σ	^{235}U	^{235}U; Unc. 1σ
Core 1A	16-18	1127	6%	247	6%	247	6%	242	6%	262	9%	453	10%	533	8%	23	11%
Core 1A	18-20	1029	9%	272	7%	271	6%	257	6%	374	18%	585	9%	746	8%	38	11%
Core 2A	5-6	685	7%	298	7%	287	6%	280	6%	380	5%	659	8%	376	12%	17	10%
Core 2A	6-7	546	8%	274	7%	274	6%	260	6%	501	5%	800	8%	478	11%	19	10%
Core 2A	7-8	512	9%	297	7%	297	6%	282	6%	501	8%	1105	9%	472	10%	25	11%
Core 2A	8-9	564	7%	281	7%	295	6%	268	6%	671	5%	1392	8%	690	6%	31	10%
Core 2A	9-10	548	13%	196	7%	207	6%	190	6%	683	10%	1011	12%	689	9%	40	13%
Core 2A	12-13	597	9%	182	7%	184	6%	173	6%	633	18%	843	9%	671	9%	34	11%
Core 2A	22-24	142	9%	7.9	16%	5.2	8%	7.7	13%	43	10%	10	12%	137	28%	6.2	14%
Core 2A	24-26	36	15%	4.2	24%	6.2	9%	5.2	14%	41	19%	9.5	11%	150	20%	7.2	14%
Core 2A	26-28	84	16%	12	18%	7.0	13%	8.9	19%	39	11%	9.6	11%			6.0	15%
Core 2A	28-30	150	11%	14	13%	17	8%	14	10%	38	10%	15	12%			4.0	15%
Core 2A	30-32	417	9%	28	9%	27	7%	27	8%	32	10%	25	11%	70	16%	3.0	13%
Core 2A	32-34	595	9%	40	8%	39	7%	38	7%	38	19%	34	10%	84	29%	2.9	12%
Core 2A	0-3	458	8%	46	7%	45	7%	43	7%	221	6%	91	8%	309	12%	15	10%
Core 2A	3-5	561	8%	400	7%	403	6%	387	6%	463	5%	810	8%	556	8%	23	10%
Core 2A	10-12	657	8%	186	7%	185	6%	179	6%	397	5%	839	8%	959	8%	38	10%
Core 2A	13-15	247	10%	81	8%	75	7%	75	7%	684	5%	360	8%	1415	9%	62	10%
Core 2A	15-17	65	29%	20	18%	20	10%	21	14%	267	9%	83	11%	1083	14%	43	13%
Core 2A	17-19	32	17%	10	14%	8.3	10%	9.7	11%	161	6%	34	10%	771	10%	47	12%
Core 2A	19-22	59	14%	9.0	16%	6.3	9%	8.2	12%	48	9%	19	10%	424	14%	15	13%
Kors Ref Sedi	0-10	992	8%	83	7%	82	6%	76	6%	78	9%	101	9%	76	15%	4.5	11%
Kors Sedi 1	0-10	971	7%	76	7%	73	6%	72	6%	65	5%	88	8%	80	11%	3.1	10%
Kors Sedi 2	0-10	717	9%	116	7%	116	6%	110	6%	225	18%	250	9%	403	8%	19	11%
Kors Sedi 3	0-10	912	11%	72	7%	73	6%	71	6%	65	10%	84	11%	63	15%	2.2	12%
Kors Sedi 4 B1	0-10	475	13%	41	7%	47	6%	42	6%	716	10%	74	12%	848	7%	36	14%
Kors Sedi 4 B2	0-10	646	11%	53	7%	55	6%	52	6%	97	10%	97	11%	316	8%	14	12%
Kors Sedi 4A	0-10	721	7%	71	6%	67	6%	67	6%	144	10%	120	8%	673	6%	30	10%

Sample	Depth (cm)	^{40}K	^{40}K; Unc. 1σ	^{228}Ra	^{228}Ra; Unc. 1σ	^{228}Th	^{228}Th; Unc. 1σ	^{232}Th	^{232}Th; Unc. 1σ	^{210}Pb	^{210}Pb; Unc. 1σ	^{226}Ra	^{226}Ra; Unc. 1σ	^{238}U	^{238}U; Unc. 1σ	^{235}U	^{235}U; Unc. 1σ
NORM 1A	0-10	306	7%	229	7%	230	6%	226	6%	480	6%	445	9%	819	6%	34	10%
NORM 1B	10-20	484	7%	1079	6%	1057	6%	1043	6%	743	4%	2805	8%	2056	5%	77	9%
NORM 1C	20-30	677	7%	2241	6%	2210	6%	2187	6%	2238	10%	7779	8%	4098	5%	154	10%
NORM 1D	30-35	664	11%	148	7%	151	6%	144	6%	384	10%	370	10%	735	7%	32	12%
NORM 2	30	692	8%	39	7%	39	6%	37	6%	38	14%	52	8%	53	8%	3.4	10%
NORM 3A	0-10	347	8%	136	7%	141	6%	134	6%	519	5%	325	8%	302	10%	13	10%
NORM 3B	10-30	1114	6%	312	7%	309	6%	304	6%	268	6%	626	8%	456	6%	19	10%
NORM 3C	30-40	901	7%	283	7%	283	6%	270	6%	346	4%	781	8%	728	6%	32	9%
NORM 4A	0-10	956	8%	257	6%	119	7%	119	7%	236	14%	489	8%	345	6%	17	11%
NORM 4B	10-20	1032	7%	257	6%	257	6%	253	6%	213	10%	440	8%	317	6%	13	10%
NORM 4C	20-25	890	11%	283	7%	290	6%	277	6%	246	10%	512	10%	516	7%	20	12%
NORM 4D	25-30	976	7%	259	7%	262	6%	248	6%	287	5%	545	8%	551	6%	26	10%
NORM 5A	20-30	946	8%	370	6%	377	6%	363	6%	190	14%	479	8%	603	6%	26	10%
NORM 5B	5-20	1206	7%	215	7%	213	6%	205	6%	193	5%	436	8%	286	7%	13	10%
NORM 5C	0-5	243	11%	93	7%	97	6%	92	6%	639	10%	215	11%	347	9%	16	12%
Ref. Soil	0-3	52	14%	6.0	16%	6.9	9%	7.1	11%	333	5%	12	15%			0.8	17%
Ref. Soil	3-8	75	9%	11	9%	12	7%	11	7%	194	14%	15	11%			1.3	12%
Ref. Soil	8-15	544	7%	41	7%	42	6%	41	6%	39	10%	30	9%	42	18%	1.4	6%
Ref. Soil	15-20	670	7%	54	7%	52	6%	52	6%	26	6%	37	9%	50	16%	1.5	11%
Soil 1	0-2	260	7%	55	7%	56	6%	54	6%	316	6%	106	9%	107	23%	4.4	11%
Soil 1	2-7	867	6%	283	7%	286	6%	280	6%	375	6%	530	9%	546	8%	19	10%
Soil 1	7-13	674	8%	232	7%	232	6%	226	6%	348	6%	420	8%	534	9%	24	10%
Soil 1	13-20	546	6%	35	7%	17	7%	17	7%	28	7%	33	9%	62	11%	2.9	11%
Soil 3	0-2	915	7%	197	7%	196	6%	191	6%	316	5%	532	8%	401	9%	14	10%
Soil 3	2-7	1090	6%	232	7%	233	6%	230	6%	230	6%	565	8%	451	7%	17	10%
Soil 3	7-12	956	8%	244	6%	254	6%	240	6%	240	14%	574	8%	509	7%	25	10%
Soil 3	12-20	992	8%	245	6%	251	6%	239	6%	228	14%	546	8%	492	5%	22	10%
Soil 4	0-6	441	9%	361	7%	155	7%	156	7%	261	15%	419	9%	847	7%	34	10%
Soil 4	6-10	118	8%	972	6%	428	7%	428	7%	259	14%	1117	8%	1410	6%	58	10%

Sample	Depth (cm)	^{40}K	^{40}K; Unc. 1σ	^{228}Ra	^{228}Ra; Unc. 1σ	^{228}Th	^{228}Th; Unc. 1σ	^{232}Th	^{232}Th; Unc. 1σ	^{210}Pb	^{210}Pb; Unc. 1σ	^{226}Ra	^{226}Ra; Unc. 1σ	^{238}U	^{238}U; Unc. 1σ	^{235}U	^{235}U; Unc. 1σ
Soil 4	10-15	108	7%	1074	7%	1054	6%	1049	6%	251	6%	1296	8%	1641	5%	50	10%
Soil 4	15-20	86	8%	1047	6%	1034	6%	1013	6%	266	5%	1249	8%	1379	6%	58	9%